

Chemistry–A European Journal

Supporting Information

Double Chalcogen Bonding Recognition Arrays in Solution

Deborah Romito, Hanspeter Kählig, Paolo Tecilla, Gabriele C. Sosso, and Davide Bonifazi*

Supporting Information materials

Table of Contents

1. General remarks

- 1.1 Instrumentation
- 1.2 Materials and methods

2. Synthetic procedures

- 2.1 Synthesis of *tert*-butyl 2-chloronicotinate **3**
- 2.2 Synthesis of di-*tert*-butyl 2,2'-diselanediyldinicotinate **4**
- 2.3 Synthesis of 2,2'-diselanediyldinicotinic acid **5**
- 2.4 Synthesis of 2-phenyl-[1,2]selenazolo[5,4- β]pyridin-3(2H)-one **1_{Ph}**
- 2.5 Synthesis of 2-pentyl-[1,2]selenazolo[5,4- β]pyridin-3(2H)-one **1_{Alk}**
- 2.6 Synthesis of 2-(anthracen-9-yl)-[1,2]selenazolo[5,4- β]pyridin-3(2H)-one **1_{Anthr}**
- 2.7 Synthesis of 2-(4-fluorophenyl)-[1,2]selenazolo[5,4- β]pyridin-3(2H)-one **1_F**
- 2.8 Synthesis of 2-(4-methoxyphenyl)-[1,2]selenazolo[5,4- β]pyridine-3(2H)-one **1_{Met}**
- 2.9 Synthesis of 2-(3,4,5-trifluorophenyl)-[1,2]selenazolo[5,4- β]pyridin-3(2H)-one **1_{3F}**
- 2.10 Synthesis of 2-(3,4,5-trimethoxyphenyl)-[1,2]selenazolo[5,4- β]pyridin-3(2H)-one **1_{3Met}**

3. NMR-HRMS Spectroscopic characterization (¹H, ¹³C, ¹⁹F, HRMS)

- 3.1 Characterization of **3**
- 3.2 Characterization of **4**
- 3.3 Characterization of **5**
- 3.4 Characterization of **1_{Ph}**
- 3.5 Characterization of **1_{Alk}**
- 3.6 Characterization of **1_{Anthr}**
- 3.7 Characterization of **1_F**
- 3.8 Characterization of **1_{Met}**
- 3.9 Characterization of **1_{3F}**
- 3.10 Characterization of **1_{3Met}**

4. Crystallographic data

5. ¹H and ⁷⁷Se NMR measurements

- 5.1 Dilution experiments
- 5.2 Variable Temperature (VT) experiments

6. Computational studies

1. General remarks

1.1 Instrumentation

Thin layer chromatography (TLC) was conducted on pre-coated aluminum sheets with 0.20 mm *Merck Millipore* Silica gel 60 with fluorescent indicator F254. **Column chromatography** was carried out using *Merck Gerduran* silica gel 60 (particle size 40-63 μ m). **Melting points** (mp) were measured on a *Gallenkamp* apparatus in open capillary tubes and have not been corrected. **Nuclear magnetic resonance**: (NMR) spectra were recorded on a Bruker Fourier 300 MHz spectrometer equipped with a dual (¹³C, ¹H) probe, a Bruker AVANCE III HD 400 MHz NMR spectrometer equipped with a Broadband multinuclear (BBFO) SmartProbe™, a

Bruker AVANCE III HD 500 MHz Spectrometer equipped with Broadband multinuclear (BBO) Prodigy CryoProbe or a Bruker AV III HDX 700 MHz NMR spectrometer (Bruker BioSpin, Rheinstetten, Germany) with a quadruple (^1H , ^{13}C , ^{15}N , ^{19}F) inverse helium cooled cryo probe. ^1H spectra were obtained at 300, 400, 500, 600 or 700 MHz, $^{13}\text{C}\{^1\text{H}\}$ spectra were obtained at 75, 100, 125, 150 or 175 MHz NMR and ^{19}F spectra were obtained at 376, 470 and 659 MHz. ^{125}Te NMR experiments were done on a Bruker AV III 600 MHz NMR spectrometer using a nitrogen cooled broad band observe cryo probe at a resonance frequency of 189.38 MHz. All spectra were obtained at r.t. Chemical shifts were reported in ppm relative to tetramethylsilane using the residual solvent signal for ^1H or the solvent signal for ^{13}C as an internal reference (CDCl_3 : $\delta_{\text{H}} = 7.26$ ppm, $\delta_{\text{C}} = 77.16$ ppm; C_6D_6 : $\delta_{\text{H}} = 7.16$ ppm, $\delta_{\text{C}} = 128.06$ ppm). Chemical shifts for ^{19}F and ^{125}Te are reported on a unified scale relative to ^1H using the Ξ value for CDCl_3 .^[28] Coupling constants (J) were given in Hz. Resonance multiplicity was described as *s* (singlet), *d* (doublet), *t* (triplet), *dd* (doublet of doublets), *ddd* (doublet of doublets of doublets), *dm* (doublet of multiplets), *q* (quartet), *m* (multiplet) and *bs* (broad signal). Carbon spectra were acquired with ^1H decoupling. ^{77}Se NMR experiments were either recorded on a Bruker AV III HDX 700 NMR spectrometer (Bruker BioSpin, Rheinstetten, Germany) equipped with a broad band observe probe, or on a Bruker AV III 600 NMR spectrometer using a nitrogen cooled broad band observe cryo probe. The resonance frequency for ^{77}Se was 133.58 MHz or 114.48 MHz, respectively. **Infrared spectra** (IR) were recorded on a Shimadzu IR Affinity 1S FTIR spectrometer in ATR mode with a diamond monocrystal. **Mass spectrometry**: (i) High-resolution ESI mass spectra (HRMS) were performed on a Waters LCT HR TOF mass spectrometer in the positive or negative ion mode. **X-ray measurements**: The X-ray intensity data of **1_{Ph}**, **1_{Alk}**, **1_{Anthr}**, **1_{Met}** and **1_{3Met}** were measured on Bruker D8 Venture diffractometer equipped with multilayer monochromator, Mo and Cu K α INCOATEC micro focus sealed tubes and Oxford cooling system. The structures were solved by Direct Methods and Intrinsic Phasing. Non-hydrogen atoms were refined with anisotropic displacement parameters. Hydrogen atoms were inserted at calculated positions and refined with riding model. The following software was used: Bruker SAINT software package^[29] using a narrow-frame algorithm for frame integration, SADABS^[30] for absorption correction, OLEX2^[31] for structure solution, refinement, molecular diagrams and graphical user-interface, Shelxle^[32] for refinement and graphical user-interface SHELXS-2015^[32] for structure solution, SHELXL-2015^[33] for refinement, Platon^[34] for symmetry check. Data collections of **1_{3F}** were performed at the X-ray diffraction beamline (XRD1) of the Elettra Synchrotron (Trieste, Italy).^[35] The crystals were dipped in NHV oil (Jena Bioscience, Jena, Germany) and mounted on the goniometer head with nylon loops (MiTeGen, Ithaca, USA). Complete datasets were collected at 100 K (nitrogen stream supplied through an Oxford Cryostream 700). Data were acquired using a monochromatic wavelength of 0.70 Å through the rotating crystal method on a Pilatus 2M hybrid-pixel area detector (DECTRIS Ltd., Baden-Daettwil, Switzerland). The

diffraction data were indexed and integrated using XDS.^[36] The structure was solved with Olex2^[37] by using ShelXT^[38] structure solution program by Intrinsic Phasing and refined with the ShelXL^[39] refinement package using least-squares minimization. In the last cycles of refinement, non-hydrogen atoms were refined anisotropically. Hydrogen atoms were included in calculated positions, and a riding model was used for their refinement. Crystal data, data collection parameters, and structure refinement details are given in Tables S1 to S6.

1.2 Materials and methods

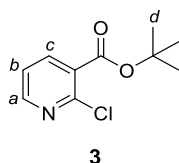
Chemicals were purchased from *Sigma Aldrich*, *Acros Organics*, *TCl*, *Apollo Scientific*, *ABCR*, *Alfa Aesar*, *Carbosynth* and *Fluorochem* and were used as received. Solvents were purchased from *Fluorochem*, *Fisher Chemical* and *Sigma Aldrich*, while deuterated solvents from *Eurisotop* and *Sigma Aldrich*. THF, Et₂O and CH₂Cl₂ were dried on a Braun MB SPS-800 solvent purification system. MeOH, CHCl₃ and acetone were purchased as reagent-grade and used without further purification. Et₃N was distilled from CaH₂ and then stored over KOH. Anhydrous dioxane and pyridine were purchased from *Sigma Aldrich*. Solutions of *i*-PrMgCl in THF were freshly prepared according to a procedure of Lin et al.^[40] and titrated with the Paquette method,^[41] or directly purchased from *Sigma Aldrich*. Low temperature baths were prepared using different solvent mixtures depending on the desired temperature: 0 °C with ice/H₂O. Anhydrous conditions were achieved by flaming two necked flasks with a heat gun under vacuum and purging with N₂. The inert atmosphere was maintained using Nitrogen-filled balloons equipped with a syringe and needle that was used to penetrate the silicon stoppers closing the flask's necks. Additions of liquid reagents were performed using dried plastic or glass syringes. All reactions were performed in dry conditions and under inert atmosphere unless otherwise stated.

2. Synthetic procedures

General comments for the preparation of the Pyrselen derivatives:

To improve the yield of **3**, *t*-BuOK needs to be activated by flame-drying it under vacuum for 20 minutes. Similarly, to freshly prepare Li_2Se_2 , the activation of Li^0 consists of pressing elemental lithium chunks with a test tube, then the resulting plates are washed with degassed petr. ether, dried under a flow of Ar and added to a solution of dry THF. For the synthesis of **1_F** and **1_{3F}**, 2.5 equivalents of corresponding primary amine were used (rather than 1.2), which were added to the acyl chloride within 30 minutes at $-40\text{ }^\circ\text{C}$.

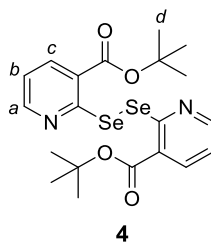
2.1 Synthesis of *tert*-butyl 2-chloronicotinate **3**



To a two-necked 50 mL round-bottomed flask with a suspension of 2-chloronicotinic acid **2** (5 g, 31.7 mmol) in SOCl_2 (25 mL) under anhydrous condition, dry DMF (2 drops) was added dropwise, then the reaction heated up to reflux, stirred for 4 h and the solvents distilled off. To a two-necked 50 mL round-bottomed flask with a solution of activated *t*-BuOK (3.56 g, 31.7 mmol) in dry THF (10 mL) under anhydrous condition, a solution of the resulting acyl chloride derivative in dry THF (8 mL) was added at $-15\text{ }^\circ\text{C}$ over 1 h. The reaction was slowly allowed to warm up to room temperature, stirred for 16 h, then poured in cold water (30 mL) and extracted with CH_2Cl_2 ($3 \times 50\text{ mL}$). The combined organic extracts were washed with brine (30 mL), dried over Na_2SO_4 , filtered and the solvents evaporated *in vacuo*. The crude was purified by silica gel chromatography (CH_2Cl_2) to give pure **3** as an orange oil (4.1 g, 61% yield).

^1H NMR (700 MHz, CDCl_3) δ : 8.45 (*d*, $J_{\text{H,H}} = 4.5\text{ Hz}$, 1H, H_a), 8.04 (*d*, $J_{\text{H,H}} = 7.6\text{ Hz}$, 1H, H_c), 7.28 (*d*, $J_{\text{H,H}} = 7.6, 4.5\text{ Hz}$, 1H, H_b), 1.59 (*s*, 9H, H_d); ^{13}C NMR (175 MHz, CDCl_3) δ : 163.9, 151.2, 149.4, 139.7, 128.8, 122.0, 28.0; FTIR (ATR): ν (cm^{-1}): 2980, 2936, 1723, 15778, 1561, 1479, 1457, 1400, 1369, 1312, 1285, 1252, 1172, 1139, 1063, 1055, 1036, 865, 847, 819, 765, 718, 647, 543, 476, 432; HRMS (ESI): m/z calcd for $\text{C}_{10}\text{H}_{12}\text{NOCl} + \text{Na}^+$: 236.0449 [$M + \text{Na}$] $^+$; found: 236.0445.

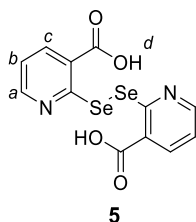
2.2 Synthesis of di-*tert*-butyl 2,2'-diselanediyldinicotinate **4**



To a flame-dried Schlenk tube loaded with a suspension of activated lithium (120 mg, 17.3 mmol) and 4,4'-di-*tert*-butylbiphenyl (100 mg, 0.38 mmol) in dry THF (25 mL) under anhydrous condition, a gentle vacuum was applied and the reaction sonicated for 15 minutes (colorless turned into dark green). Freshly grounded elemental selenium (4 g, 50.7 mmol) was added while a brisk flux of N₂ was passed through the flask, then the reaction sonicated at 50 °C for 4 h. To a suspension of the resulting dilithium diselenide derivative, a solution of *t*-butyl 2-chloroquinoline-3-carboxylate **3** (720 mg, 2.74 mmol) in dry THF (8 mL) was added dropwise at -15 °C. The reaction was slowly allowed to warm up to room temperature, stirred for 72 h, then quenched with MeOH (30 mL) and filtered over celite. The filtrate was concentrated under reduced pressure, then MeOH (30 mL) added, and the resulting suspension centrifugated for 15 minutes (5000 rpm). The system was filtered and the solid washed with MeOH (2 × 10 mL) to give pure **4** as an orange solid (340 mg, 33% yield).

mp: 208-210 °C; ¹H NMR (600 MHz, CDCl₃) δ: 8.47 (*dd*, *J*_{H,H} = 4.7, 1.8 Hz, 2H, *H_a*), 8.13 (*dd*, *J*_{H,H} = 7.7, 1.8 Hz, 2H, *H_c*), 7.09 (*dd*, *J*_{H,H} = 7.7, 4.7 Hz, 2H, *H_b*), 1.64 (*s*, 18H, *H_d*); ¹³C NMR (150 MHz, CDCl₃) δ: 165.4, 161.1, 152.5, 138.2, 126.4, 119.4, 28.3; FTIR (ATR): ν (cm⁻¹): 29707, 2931, 1682, 1567, 1552, 1392, 1366, 1302, 1256, 1235, 1171, 1116, 1062, 866, 847, 821, 804, 758, 714, 648, 515, 488, 471, 418; HRMS (ESI): *m/z* calcd for C₂₀H₂₄O₄N₂Se₂+H⁺: 517.0139 [*M*+H]⁺; found: 517.0146.

2.3 Synthesis of 2,2'-diselanediyldinicotinic acid **5**

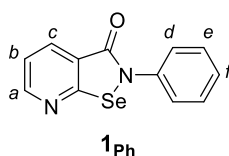


To a sealed vial loaded with a solution of di-*tert*-butyl 2,2'-diselanediyldinicotinate **4** (100 mg, 0.2 mmol) in CH₂Cl₂ (8 mL), CH₃SO₃H (148 mg, 0.1 mL, 1.6 mmol) was added dropwise at room temperature. The reaction was stirred for 16 h, then quenched by MeOH (10 mL).

The resulting insoluble solid was filtered and washed with MeOH (2 × 20 mL) and water (3 × 20 mL) to give pure **5** as a yellow solid (79 mg, 96% yield).

mp: 192-194 °C; ¹H NMR (600 MHz, DMSO-*d*₆) δ: 8.55 (*dd*, *J*_{H,H} = 4.8, 1.7 Hz, 2H, *H*_a), 8.22 (*dd*, *J*_{H,H} = 7.7, 1.7 Hz, 2H, *H*_c), 7.31 (*dd*, *J*_{H,H} = 7.7, 4.8 Hz, 2H, *H*_b); ¹³C NMR (150 MHz, DMSO-*d*₆) δ: 167.8, 161.6, 153.0, 138.7, 125.7, 120.4; FTIR (ATR): ν (cm⁻¹): 3140, 2855, 1663, 1569, 1548, 1445, 1421, 1383, 1300, 1238, 1225, 1150, 1120, 1064, 889, 818, 758, 705, 644, 553, 523, 476, 450, 437, 420; HRMS (ESI): *m/z* calcd for C₁₂H₈O₄N₂Se₂+H⁺: 404.8890 [*M*+H]⁺; found: 404.8873.

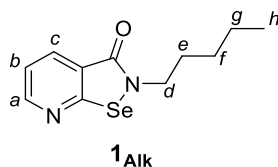
2.4 Synthesis of 2-phenyl-[1,2]selenazolo[5,4-β]pyridin-3(2H)-one **1_{Ph}**



To a two-necked 25 mL round-bottomed flask with a suspension of 2,2'-diselanediyldinicotic acid **5** (80 mg, 0.2 mmol) in SOCl₂ (0.6 mL) under anhydrous condition, dry DMF (2 drops) was added dropwise, then the reaction heated up to reflux and stirred for 6 h. The reaction was cooled down to room temperature and a second portion of SOCl₂ (0.6 mL) and dry DMF (2 drops) added. The solution was heated up to reflux and stirred for 16 h, then the solvents distilled off. To a solution of the resulting acyl chloride derivative in dry CH₂Cl₂ (5 mL), a solution of aniline (20 mg, 0.22 mmol) and NEt₃ (44 mg, 0.06 mL, 0.44 mmol) in dry CH₂Cl₂ (0.4 mL) was added dropwise at -15 °C. The reaction was slowly allowed to warm up to room temperature and stirred for 16 hours, then poured in cold water (30 mL) and extracted with CH₂Cl₂ (3 × 30 mL). The combined organic extracts were washed with brine (20 mL), dried over Na₂SO₄, filtered and the solvents evaporated *in vacuo*. The crude was purified by silica gel chromatography (CHCl₃/EtOAc 3:1) to give pure **1_{Ph}** as a white solid (25 mg, 45% yield).

mp: 180-182 °C; ¹H NMR (600 MHz, CDCl₃) δ: 8.84 (*d*, *J*_{H,H} = 4.5 Hz, 1H, *H*_a), 8.39 (*dd*, *J*_{H,H} = 7.7, 1.7 Hz, 1H, *H*_c), 7.65 (*dm*, *J*_{H,H} = 8.5 Hz, 2H, *H*_d), 7.49 (*d*, *J*_{H,H} = 7.7, 4.5 Hz, 1H, *H*_b), 7.46 (*dd*, *J*_{H,H} = 8.5, 7.5 Hz, 2H, *H*_e), 7.31 (*t*, *J*_{H,H} = 7.5 Hz, 1H, *H*_f); ¹³C NMR (150 MHz, CDCl₃) δ: 163.8, 161.7, 152.7, 138.8, 137.6, 129.6, 127.1, 125.7, 124.5, 122.1; ⁷⁷Se NMR (114 MHz, CDCl₃) δ: 953.8 (*s*); FTIR (ATR): ν (cm⁻¹): 3070, 2921, 2852, 1655, 1638, 1584, 1486, 1452, 1391, 1336, 1262, 1205, 1181, 1141, 1108, 1085, 943, 815, 751, 692, 672, 600, 528, 481; HRMS (ESI): *m/z* calcd for C₁₂H₈ON₂Se+H⁺: 276.9875 [*M*+H]⁺; found: 276.9873. Single crystals suitable for X-ray diffraction analysis were grown from slow evaporation of solvent from a CHCl₃/toluene 1:1 solution.

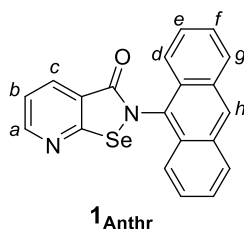
2.5 Synthesis of 2-pentyl-[1,2]selenazolo[5,4-β]pyridin-3(2H)-one **1_{Alk}**



To a two-necked 25 mL round-bottomed flask with a suspension of 2,2'-diselanediyldnicotinic acid **5** (80 mg, 0.2 mmol) in SOCl₂ (0.6 mL) under anhydrous condition, dry DMF (2 drops) was added dropwise, then the reaction heated up to reflux and stirred for 6 h. The reaction was cooled down to room temperature and a second portion of SOCl₂ (0.6 mL) and dry DMF (2 drops) added. The solution was heated up to reflux and stirred for 16 h, then the solvents distilled off. To a solution of the resulting acyl chloride derivative in dry CH₂Cl₂ (5 mL), a solution of amylamine (19 mg, 0.03 mL, 0.22 mmol) and NEt₃ (44 mg, 0.06 mL, 0.44 mmol) in dry CH₂Cl₂ (0.4 mL) was added dropwise at -15 °C. The reaction was slowly allowed to warm up to room temperature and stirred for 16 h, then poured in cold water (30 mL) and extracted with CH₂Cl₂ (3 × 30 mL). The combined organic extracts were washed with brine (20 mL), dried over Na₂SO₄, filtered and the solvents evaporated *in vacuo*. The crude was purified by silica gel chromatography (CHCl₃/EtOAc 4:1) to give pure **1_{Alk}** as a white solid (38 mg, 72% yield).

mp: 138-140 °C; ¹H NMR (600 MHz, CDCl₃) δ: 8.74 (*dd*, *J*_{H,H} = 4.9, 1.7 Hz, 1H, *H_a*), 8.25 (*dd*, *J*_{H,H} = 7.8, 1.7 Hz, 1H, *H_c*), 7.39 (*dd*, *J*_{H,H} = 7.8, 4.9 Hz, 1H, *H_b*), 3.87 (*t*, *J*_{H,H} = 7.2 Hz, 2H, *H_d*), 1.78 – 1.73 (*m*, 2H, *H_e*), 1.42 – 1.36 (*m*, 4H, *H_{f,g}*), 0.91 (*t*, *J*_{H,H} = 7.2 Hz, 3H, *H_h*); ¹³C NMR (150 MHz, CDCl₃) δ: 165.2, 161.8, 152.7, 136.5, 123.5, 121.5, 44.6, 30.2, 28.8, 22.3, 13.9; ⁷⁷Se NMR (114 MHz, CDCl₃) δ: 897.6 (s); FTIR (ATR): ν (cm⁻¹): 2950, 2923, 2854, 1641, 1624, 1581, 1562, 1465, 1385, 1308, 1251, 1217, 1167, 1105, 1082, 1051, 820, 755, 698, 666, 519, 490, 443; HRMS (ESI): *m/z* calcd for C₁₁H₁₄ON₂Se+Na⁺: 293.0164 [*M*+Na]⁺; found: 293.0167. Single crystals suitable for X-ray diffraction analysis were grown from slow evaporation of solvent from a toluene solution.

2.6 Synthesis of 2-(anthracen-9-yl)-[1,2]selenazolo[5,4-β]pyridin-3(2H)-one **1_{Anthr}**

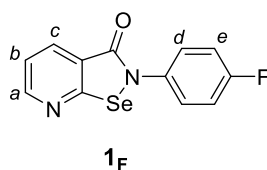


To a two-necked 25 mL round-bottomed flask with a suspension of 2,2'-diselanediyldnicotinic acid **5** (80 mg, 0.2 mmol) in SOCl₂ (0.6 mL) under anhydrous condition, dry DMF (2 drops) was added dropwise, then the reaction heated up to reflux and stirred for 6 h. The reaction was cooled down to room temperature and a second portion of

SOCl₂ (0.6 mL) and dry DMF (2 drops) added. The solution was heated up to reflux and stirred for 16 h, then the solvents were distilled off. To a solution of the resulting acyl chloride derivative in dry CH₂Cl₂ (5 mL), a solution of anthracen-9-amine (43 mg, 0.22 mmol) and NEt₃ (44 mg, 0.06 mL, 0.44 mmol) in dry CH₂Cl₂ (0.4 mL) was added dropwise at -15 °C. The reaction was stirred at 50 °C for 16 h, then poured in cold water (30 mL) and extracted with CH₂Cl₂ (3 × 30 mL). The combined organic extracts were washed with brine (20 mL), dried over Na₂SO₄, filtered and the solvents evaporated *in vacuo*. The crude was purified by silica gel chromatography (CHCl₃/EtOAc 3:1) to give pure **1_{Anthr}** as a pale-yellow solid (30 mg, 41% yield).

mp: > 230 °C; ¹H NMR (600 MHz, CDCl₃) δ: 8.89 (*dd*, *J*_{H,H} = 4.9, 1.7 Hz, 1H, *H_a*), 8.63 (*s*, 1H, *H_h*), 8.46 (*dd*, *J*_{H,H} = 7.8, 1.7 Hz, 1H, *H_c*), 8.18 (*d*, *J*_{H,H} = 8.6 Hz, 2H, *H_d*), 7.89 (*d*, *J*_{H,H} = 8.6 Hz, 2H, *H_g*), 7.57 – 7.49 (*m*, 5H, *H_{b,e,f}*); ¹³C NMR (150 MHz, CDCl₃) δ: 165.6, 163.2, 153.8, 137.6, 131.9, 129.7, 129.1, 128.9, 128.6, 127.4, 125.8, 123.0, 122.1, 121.8; FTIR (ATR): ν (cm⁻¹): 2979, 2363, 1639, 1579, 1560, 1463, 1409, 1391, 1366, 1233, 1083, 912, 843, 820, 782, 757, 731, 697, 671, 596, 551, 512, 476, 446, 435; HRMS (LD): *m/z* calcd for C₂₀H₁₂ON₂Se⁺: 376.0110 [*M*]⁺; found: 376.0103. Single crystals suitable for X-ray diffraction analysis were grown from slow evaporation of solvent from a CHCl₃/toluene solution.

2.7 Synthesis of 2-(4-fluorophenyl)-[1,2]selenazolo[5,4-β]pyridin-3(2H)-one **1_F**

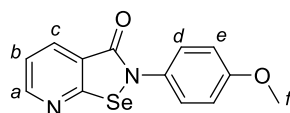


To a two-necked 25 mL round-bottomed flask with a suspension of 2,2'-diselanediyldinicotic acid **5** (80 mg, 0.2 mmol) in SOCl₂ (0.6 mL) under anhydrous condition, dry DMF (2 drops) was added dropwise, then the reaction heated up to reflux and stirred for 6 h. The reaction was cooled down to room temperature and a second portion of SOCl₂ (0.6 mL) and dry DMF (2 drops) added. The solution was heated up to reflux and stirred for 16 h, then the solvents were distilled off. To a solution of the resulting acyl chloride derivative in dry CH₂Cl₂ (5 mL), a solution of 4-fluoroaniline (61 mg, 52 μL, 0.55 mmol) and NEt₃ (67 mg, 0.08 mL, 0.6 mmol) in dry CH₂Cl₂ (0.4 mL) was added dropwise at -40 °C. The reaction was stirred at room temperature for 8 h, then poured in cold water (30 mL) and extracted with CH₂Cl₂ (3 × 30 mL). The combined organic extracts were washed with brine (20 mL), dried over Na₂SO₄, filtered and the solvents evaporated *in vacuo*. The crude was purified by silica gel chromatography (CHCl₃/EtOAc 5:1) to give pure **1_F** as a pale-yellow solid (13 mg, 23% yield).

mp: 158-160 °C; ^1H NMR (400 MHz, CDCl_3) δ : 8.83 (*d*, $J_{\text{H,H}} = 4.5$ Hz, 1H, H_a), 8.36 (*d*, $J_{\text{H,H}} = 7.7$ Hz, 1H, H_c), 7.59 (*dd*, $J_{\text{H,H}} = 8.4, 4.8$ Hz, 2H, H_d), 7.48 (*dd*, $J_{\text{H,H}} = 7.7, 4.5$ Hz, 1H, H_b), 7.15 (*d*, $J_{\text{H,H}} = 8.8, 8.4$ Hz, 2H, H_e); ^{19}F NMR (376 MHz, CDCl_3) δ : -113.80 (s, 1F); ^{13}C NMR (100 MHz, CDCl_3) δ : 161.6, 153.1, 137.3, 127.7, 127.6, 123.6, 122.0, 116.4, 116.2, 110.3 (*d*, $J_{\text{C,F}} = 250.1$ Hz); FTIR (ATR): ν (cm^{-1}): 3052, 2989, 1687, 1644, 1523, 1491, 1463, 1343, 1290, 1223, 1199, 1156, 1111, 1063, 943, 889, 823, 778, 699, 616; HRMS (ESI): m/z calcd for $\text{C}_{12}\text{H}_7\text{ON}_2\text{FSe}+\text{Na}^+$: 316.9600 [$M+\text{Na}$] $^+$; found: 316.9599.

2.8 Synthesis of 2-(4-methoxyphenyl)-[1,2]selenazolo[5,4- β]pyridin-3(2H)-one

1_{Met}

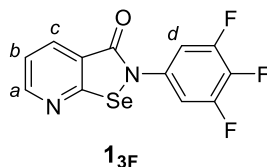


1_{Met}

To a two-necked 25 mL round-bottomed flask with a suspension of 2,2'-diselanediyldinicotinic acid **5** (80 mg, 0.2 mmol) in SOCl_2 (0.6 mL) under anhydrous condition, dry DMF (2 drops) was added dropwise, then the reaction heated up to reflux and stirred for 6 h. The reaction was cooled down to room temperature and a second portion of SOCl_2 (0.6 mL) and dry DMF (2 drops) added. The solution was heated up to reflux and stirred for 16 h, then the solvents were distilled off. To a solution of the resulting acyl chloride derivative in dry CH_2Cl_2 (5 mL), a solution of 4-methoxyaniline (28 mg, 0.22 mmol) and NEt_3 (44 mg, 0.06 mL, 0.44 mmol) in dry CH_2Cl_2 (0.4 mL) was added dropwise at -15 °C. The reaction was stirred at room temperature for 16 h, then poured in cold water (30 mL) and extracted with CH_2Cl_2 (3 \times 30 mL). The combined organic extracts were washed with brine (20 mL), dried over Na_2SO_4 , filtered and the solvents evaporated *in vacuo*. The crude was purified by silica gel chromatography ($\text{CHCl}_3/\text{EtOAc}$ 4:1) to give pure **1_{Met}** as a white solid (52 mg, 85% yield).

mp: 133-136 °C; ^1H NMR (400 MHz, CDCl_3) δ : 8.81 (*dd*, $J_{\text{H,H}} = 5.0, 1.6$ Hz, 1H, H_a), 8.34 (*dd*, $J_{\text{H,H}} = 7.9, 1.6$ Hz, 1H, H_c), 7.51 (*d*, $J_{\text{H,H}} = 8.8$ Hz, 2H, H_d), 7.45 (*dd*, $J_{\text{H,H}} = 7.9, 5.0$ Hz, 1H, H_b), 6.97 (*d*, $J_{\text{H,H}} = 8.8$ Hz, 2H, H_e), 3.85 (s, 3H, H_f); ^{13}C NMR (100 MHz, CDCl_3) δ : 163.9, 161.8, 158.5, 152.7, 137.2, 131.1, 127.4, 123.9, 121.8, 114.6, 55.6; FTIR (ATR): ν (cm^{-1}): 3051, 2989, 2913, 1623, 1599, 1467, 1421, 1387, 1350, 1321, 1284, 1222, 1190, 1136, 1110, 993, 867, 801, 745, 721, 654, 572; HRMS (ESI): m/z calcd for $\text{C}_{13}\text{H}_{10}\text{O}_2\text{N}_2\text{Se}+\text{H}^+$: 306.9981 [$M+\text{H}$] $^+$; found: 306.9982. Single crystals suitable for X-ray diffraction analysis were grown from slow evaporation of solvent from a CHCl_3 /toluene solution.

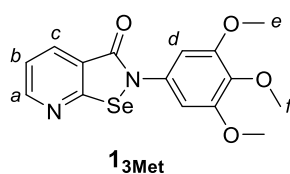
2.9 Synthesis of 2-(3,4,5-trifluorophenyl)-[1,2]selenazolo[5,4- β]pyridin-3(2H)-one **1_{3F}**



To a two-necked 25 mL round-bottomed flask with a suspension of 2,2'-diselanediyldinicotic acid **5** (80 mg, 0.2 mmol) in SOCl_2 (0.6 mL) under anhydrous condition, dry DMF (2 drops) was added dropwise, then the reaction heated up to reflux and stirred for 6 h. The reaction was cooled down to room temperature and a second portion of SOCl_2 (0.6 mL) and dry DMF (2 drops) added. The solution was heated up to reflux and stirred for 16 h, then the solvents were distilled off. To a solution of the resulting acyl chloride derivative in dry CH_2Cl_2 (5 mL), a solution of 3,4,5-trifluoroaniline (81 mg, 0.55 mmol) and NEt_3 (67 mg, 0.6 mmol) in dry CH_2Cl_2 (0.4 mL) was added dropwise at $-40\text{ }^\circ\text{C}$. The reaction was stirred at room temperature for 10 h, then poured in cold water (30 mL) and extracted with CH_2Cl_2 ($3 \times 30\text{ mL}$). The combined organic extracts were washed with brine (20 mL), dried over Na_2SO_4 , filtered and the solvents evaporated *in vacuo*. The crude was purified by silica gel chromatography ($\text{CHCl}_3/\text{EtOAc}$ 3:1) to give pure **1_{3F}** as a white solid (14 mg, 21% yield).

mp: $176\text{--}178\text{ }^\circ\text{C}$; $^1\text{H NMR}$ (400 MHz, CDCl_3) δ : 8.83 – 8.82 (*m*, 1H, H_a), 8.34 – 8.32 (*m*, 1H, H_c), 7.52 – 7.49 (*m*, 1H, H_b), 7.39 – 7.36 (*m*, 2H, H_d); $^{19}\text{F NMR}$ (659 MHz, $\text{DMSO-}d_6$) δ : -134.28 (*d*, $J_{\text{F,F}} = 22.08\text{ Hz}$, 2F), -164.45 (*t*, $J_{\text{F,F}} = 22.08\text{ Hz}$, 1 F); ^{13}C analysis is missing due to the poor solubility of the targeted molecule in several solvents screened; FTIR (ATR): ν (cm^{-1}): 3098, 2923, 2887, 1710, 1643, 1552, 1491, 1413, 1392, 1337, 1289, 1238, 1154, 1113, 1062, 983, 907, 826, 796, 701, 592, 478, 452; HRMS (ESI): m/z calcd for $\text{C}_{12}\text{H}_5\text{ON}_2\text{F}_3\text{Se}+\text{H}^+$: 330.9592 [$M+\text{H}$] $^+$; found: 330.9594.

2.10 Synthesis of 2-(3,4,5-trimethoxyphenyl)-[1,2]selenazolo[5,4- β]pyridin-3(2H)-one **1**_{3Met}



To a two-necked 25 mL round-bottomed flask with a suspension of 2,2'-diselanediyldinicotinic acid **5** (80 mg, 0.2 mmol) in SOCl₂ (0.6 mL) under anhydrous condition, dry DMF (2 drops) was added dropwise, then the reaction heated up to reflux and stirred for 6 h. The reaction was cooled down to room temperature and a second portion of SOCl₂ (0.6 mL) and dry DMF (2 drops) added. The solution was heated up to reflux and stirred for 16 h, then the solvents were distilled off. To a solution of the resulting acyl chloride derivative in dry CH₂Cl₂ (5 mL), a solution of 3,4,5-trimethoxyaniline (40 mg, 0.22 mmol) and NEt₃ (44 mg, 0.06 mL, 0.44 mmol) in dry CH₂Cl₂ (0.4 mL) was added dropwise at -15 °C. The reaction was stirred at room temperature for 16 h, then poured in cold water (30 mL) and extracted with CH₂Cl₂ (3 × 30 mL). The combined organic extracts were washed with brine (20 mL), dried over Na₂SO₄, filtered and the solvents evaporated *in vacuo*. The crude was purified by silica gel chromatography (CHCl₃/EtOAc 4:1) to give pure **1**_{3Met} as a white solid (64 mg, 88% yield).

mp: 141-143 °C; ¹H NMR (400 MHz, CDCl₃) δ: 8.83 (*d*, *J*_{H,H} = 4.7 Hz, 1H, *H*_a), 8.36 (*d*, *J*_{H,H} = 7.8 Hz, 1H, *H*_c), 7.49 (*dd*, *J*_{H,H} = 7.8, 4.7 Hz, 1H, *H*_b), 6.85 (*s*, 2H, *H*_d), 3.89 (*s*, 6H, *H*_e), 3.87 (*s*, 3H, *H*_f); ¹³C NMR (100 MHz, CDCl₃) δ: 163.9, 161.8, 153.6, 152.9, 137.3, 137.2, 134.0, 123.9, 122.0, 103.7, 60.9, 56.3; FTIR (ATR): ν (cm⁻¹): 3030, 2984, 2916, 1621, 1589, 1515, 1438, 1367, 1329, 1251, 1222, 1167, 1098, 1003, 965, 891, 744, 639, 588; HRMS (ESI): *m/z* calcd for C₁₅H₁₄O₄N₂Se+H⁺: 367.0192 [*M*+H]⁺; found: 367.0197. Single crystals suitable for X-ray diffraction analysis were grown from slow evaporation of solvent from a CHCl₃/toluene solution.

3. NMR-HRMS Spectroscopic characterization (^1H , ^{13}C , ^{19}F , ^{77}Se , HRMS)

3.1 Characterization of 3

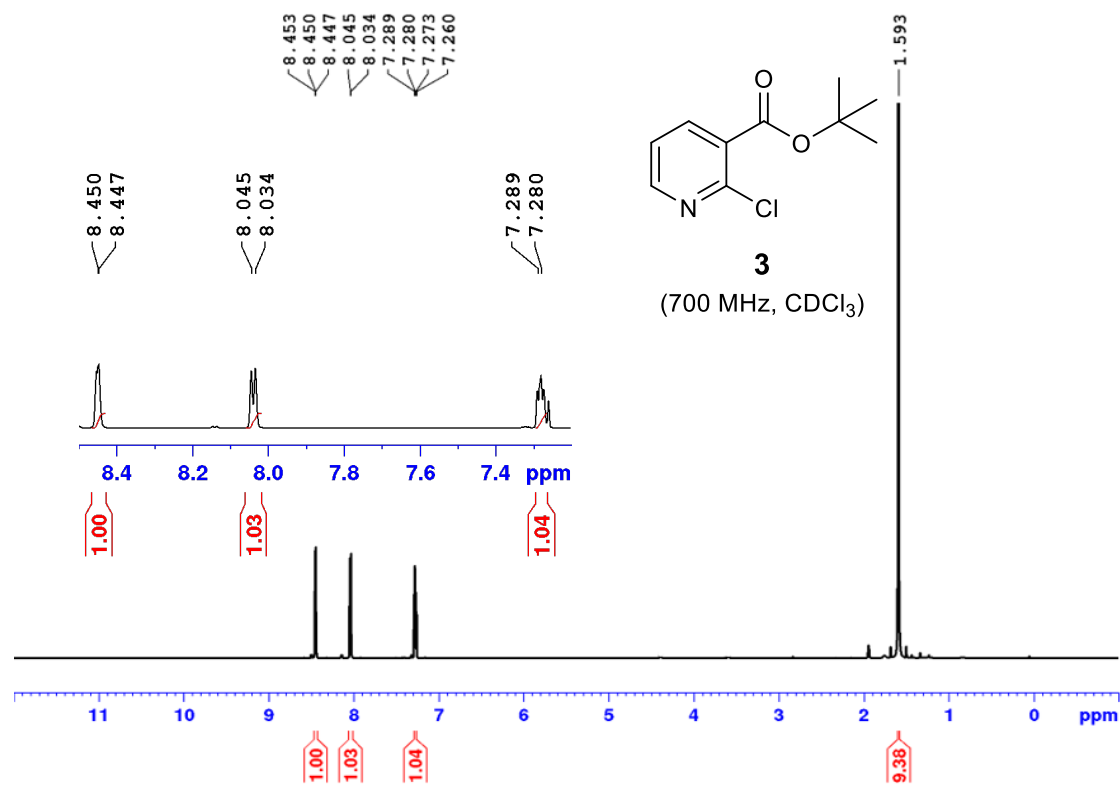


Figure S1: 700 MHz ^1H NMR in CDCl_3 of molecule 3.

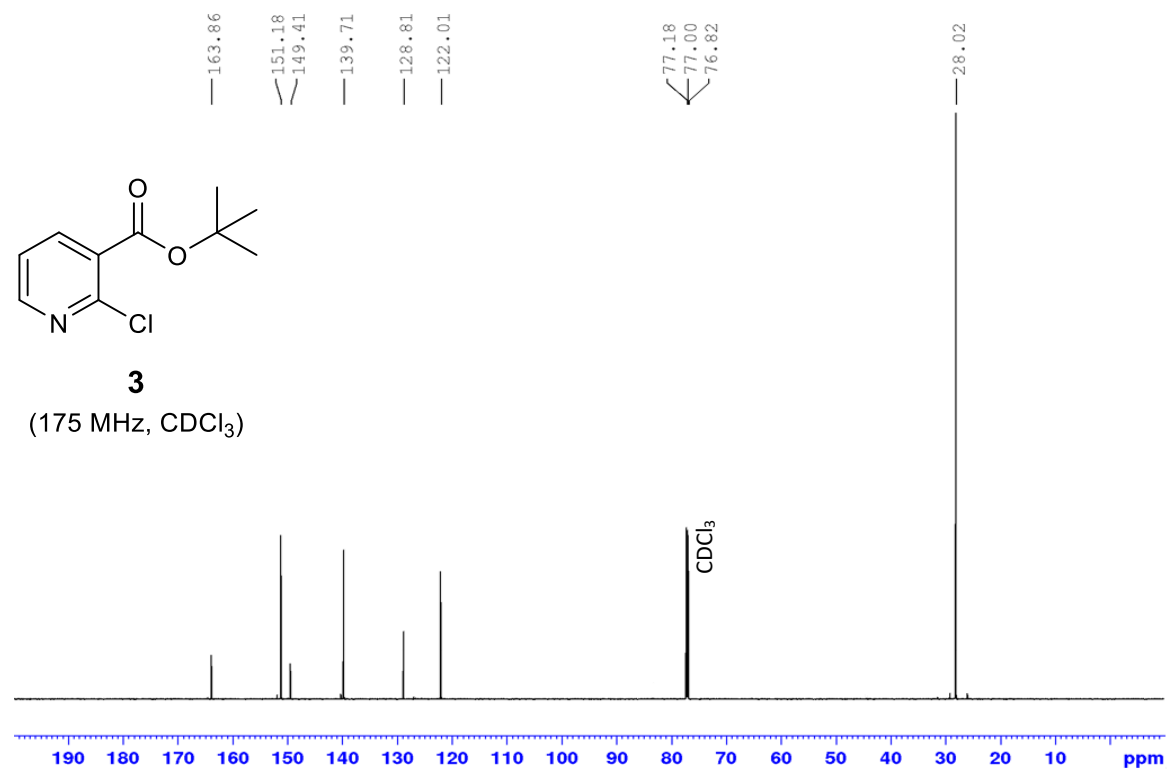


Figure S2: 175 MHz ^{13}C NMR in CDCl_3 of molecule 3.

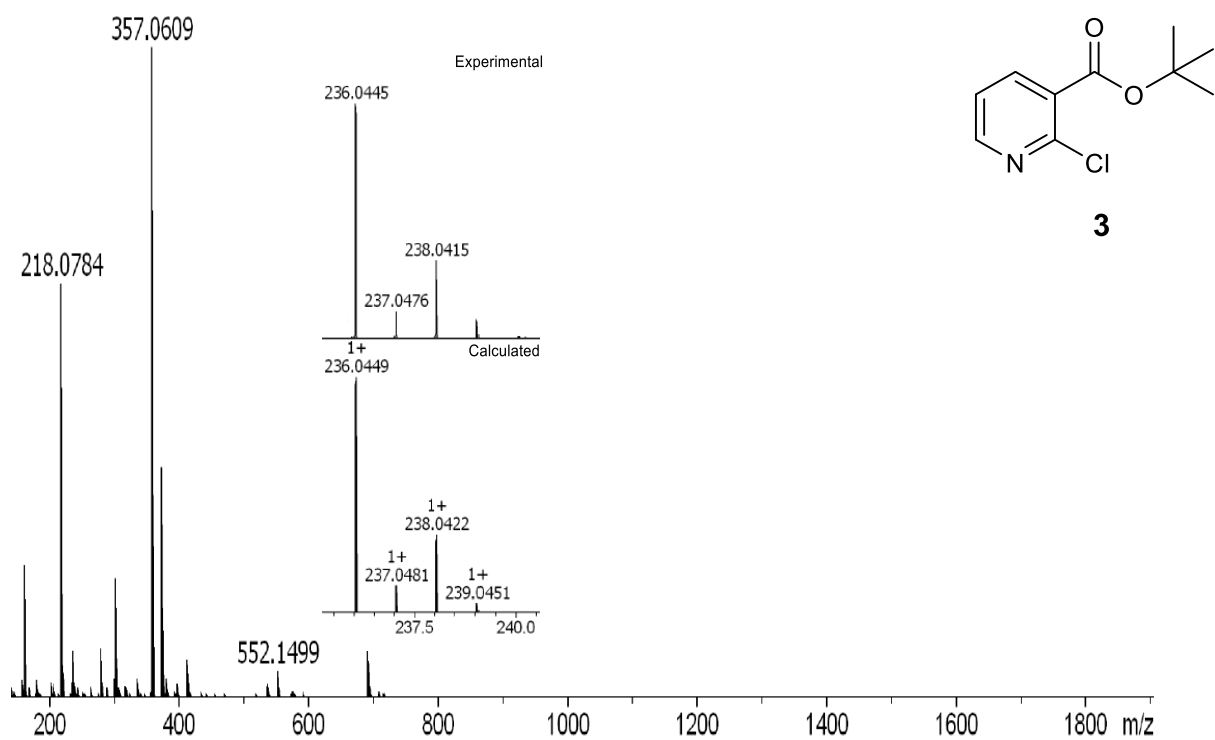


Figure S3: HRMS-ESI mass spectrum of molecule **3** in the positive ion mode.

3.2 Characterization of **4**

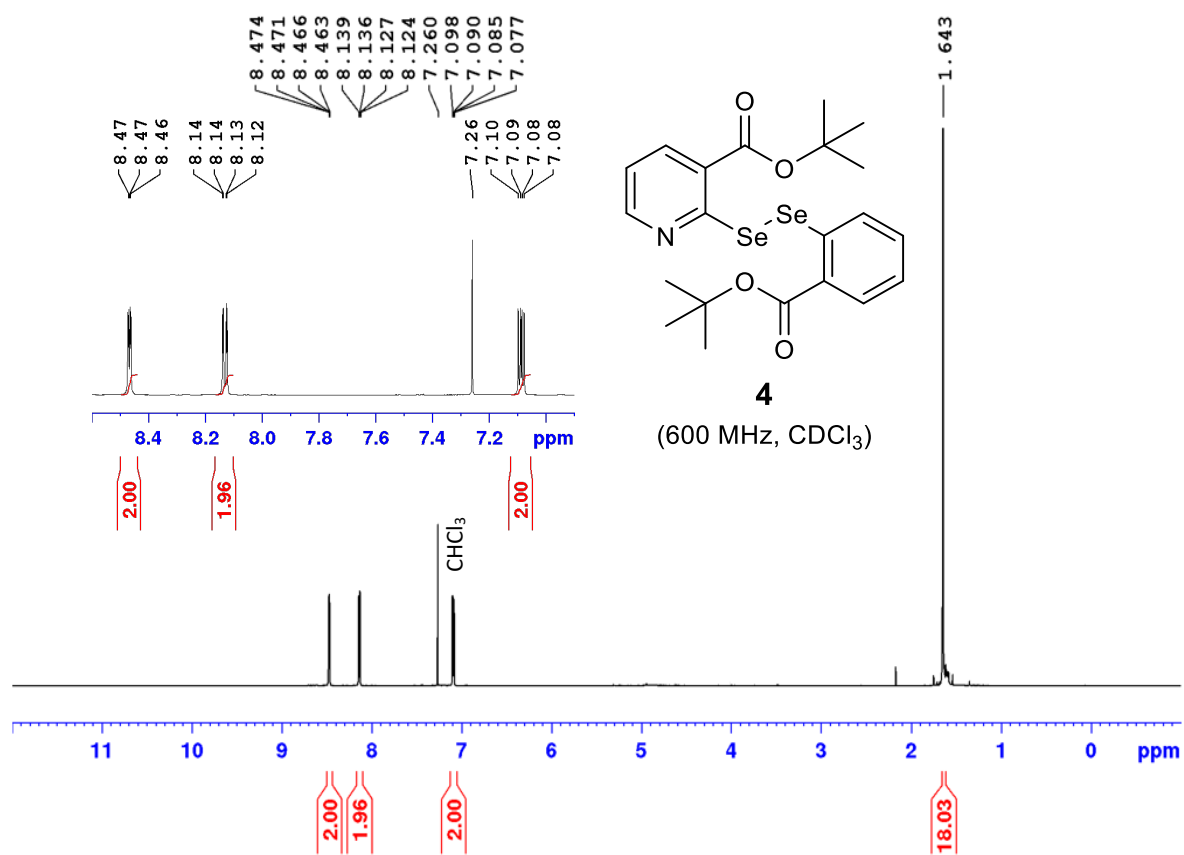


Figure S4: 600 MHz ¹H NMR in CDCl₃ of molecule **4**.

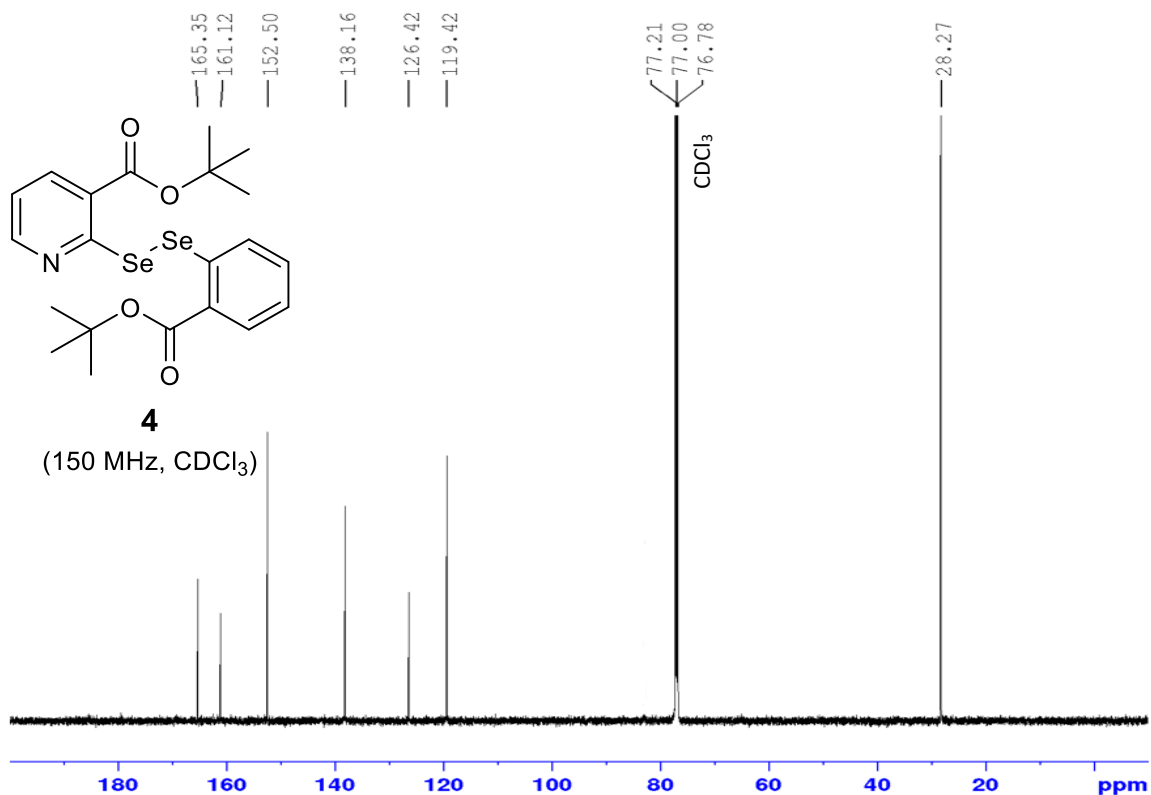


Figure S5: 150 MHz ¹³C NMR in CDCl₃ of molecule **4**.

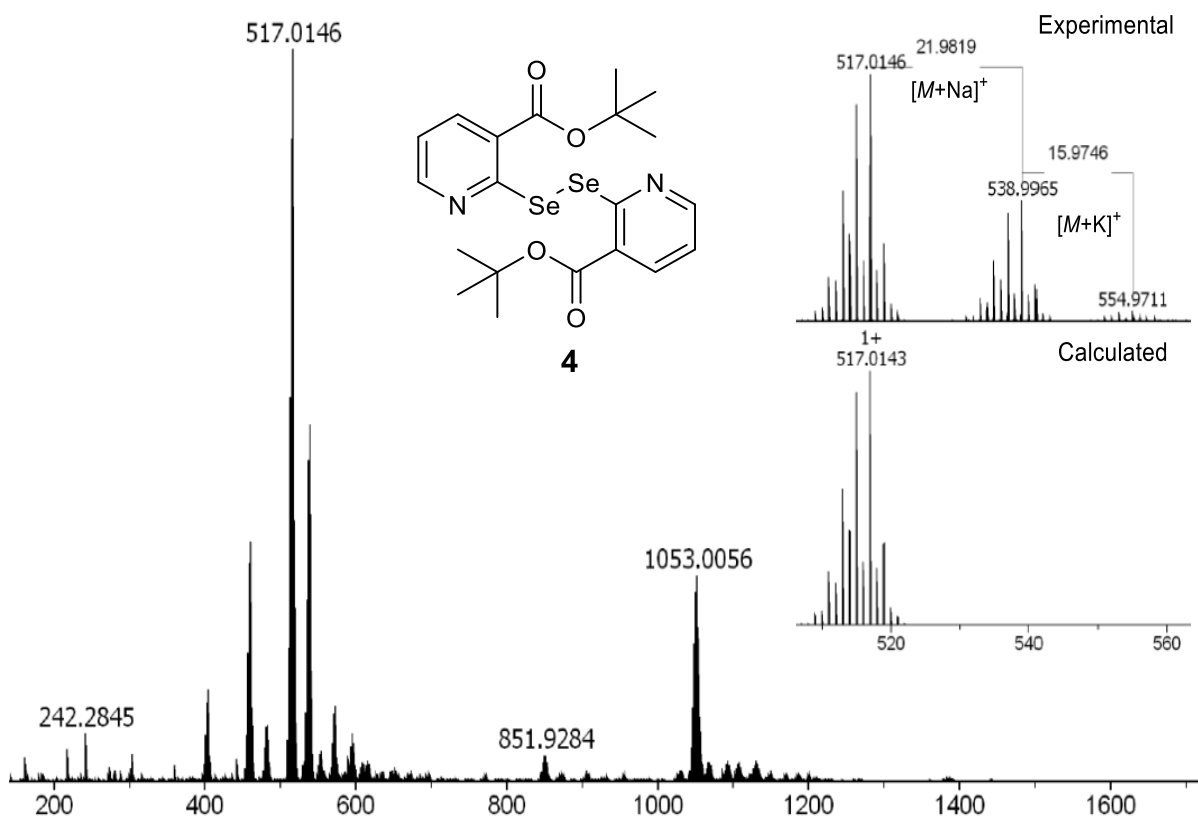


Figure S6: HRMS-ESI mass spectrum of molecule **4** in the positive ion mode. The peak at 1053 corresponds to the dimeric species.

3.3 Characterization of 5

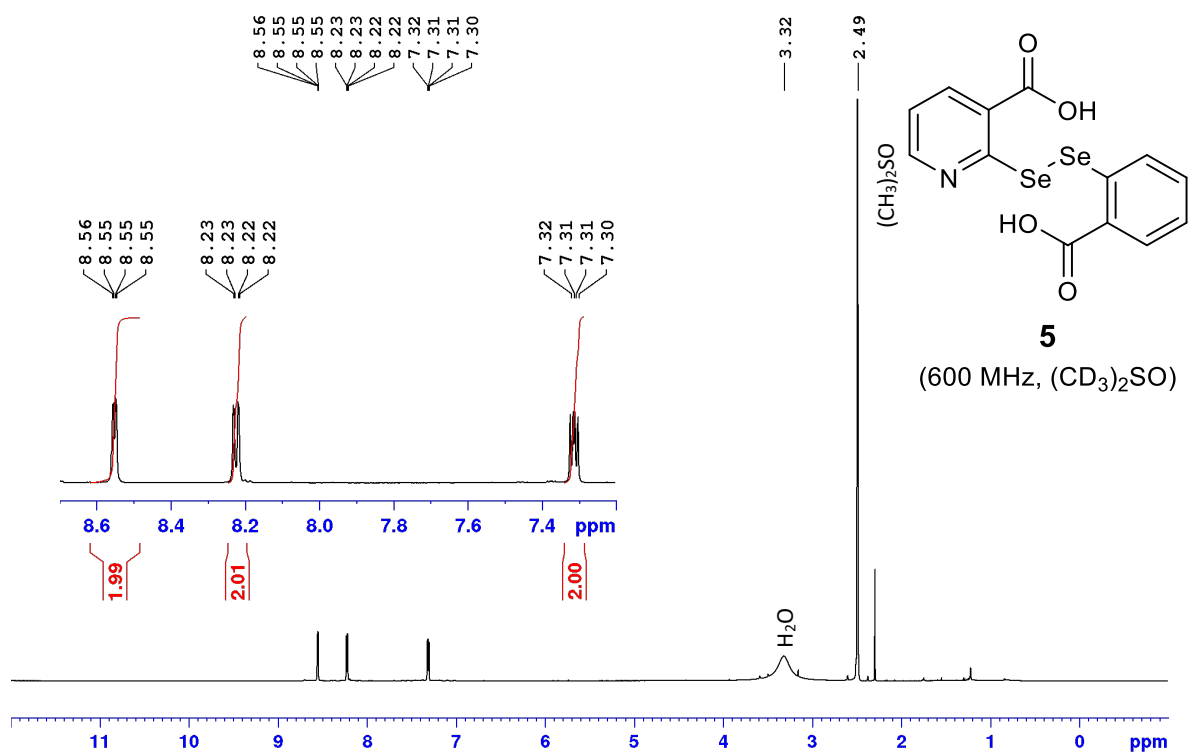


Figure S7: 600 MHz ^1H NMR in $(\text{CD}_3)_2\text{SO}$ of molecule **5**.

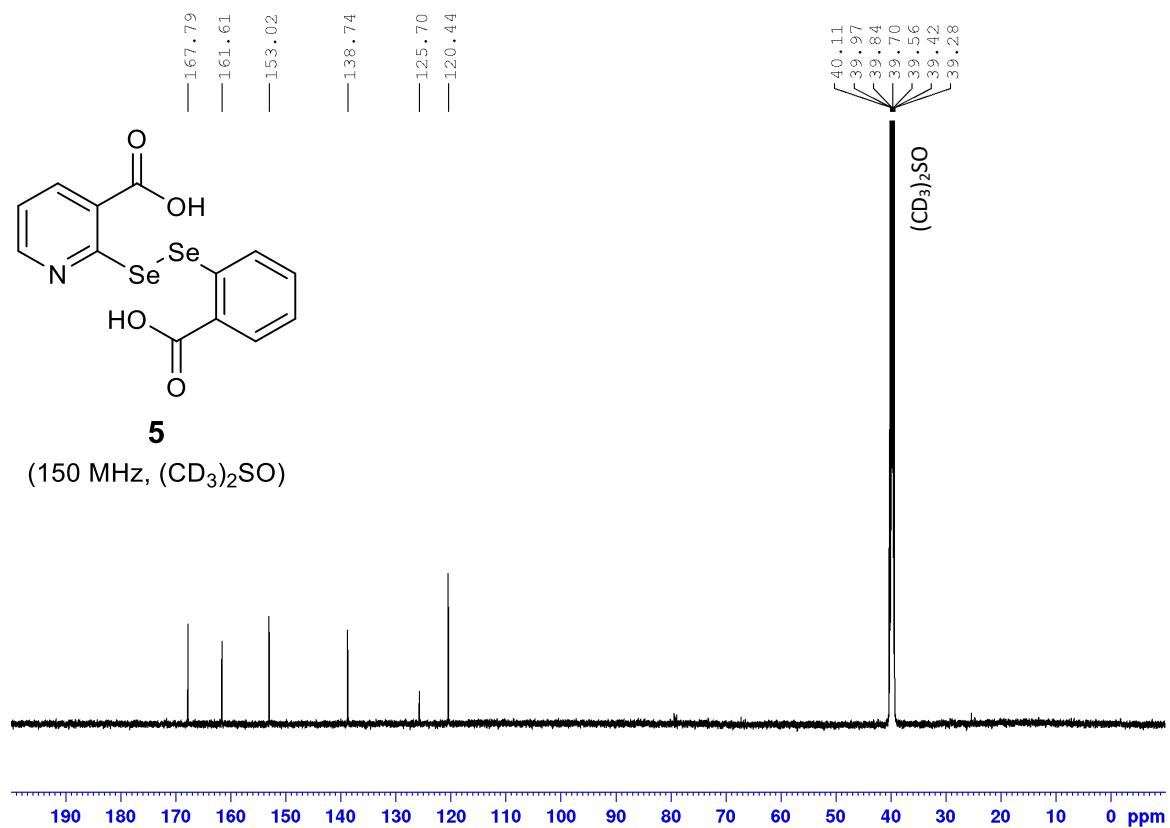


Figure S8: 150 MHz ^{13}C NMR in $(\text{CD}_3)_2\text{SO}$ of molecule **5**.

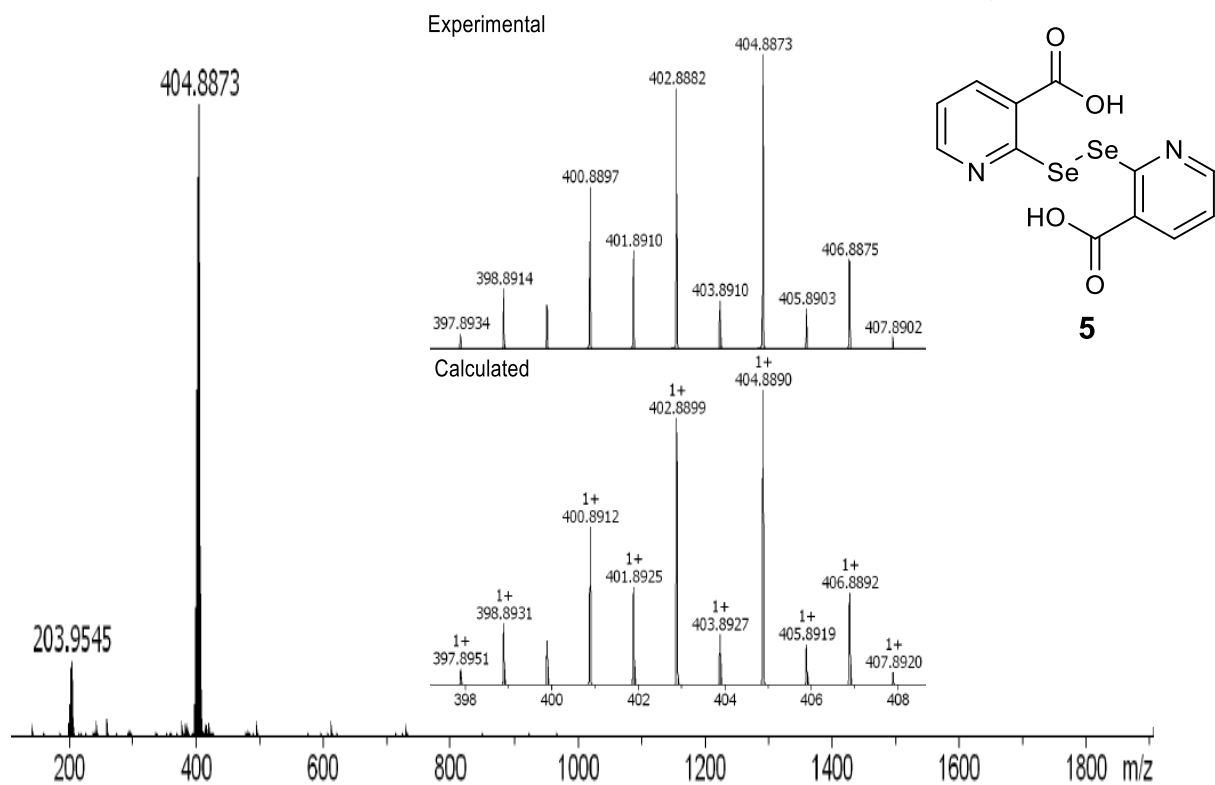


Figure S9: HRMS-ESI mass spectrum of molecule **5** in the positive ion mode.

3.4 Characterization of **1_{Ph}**

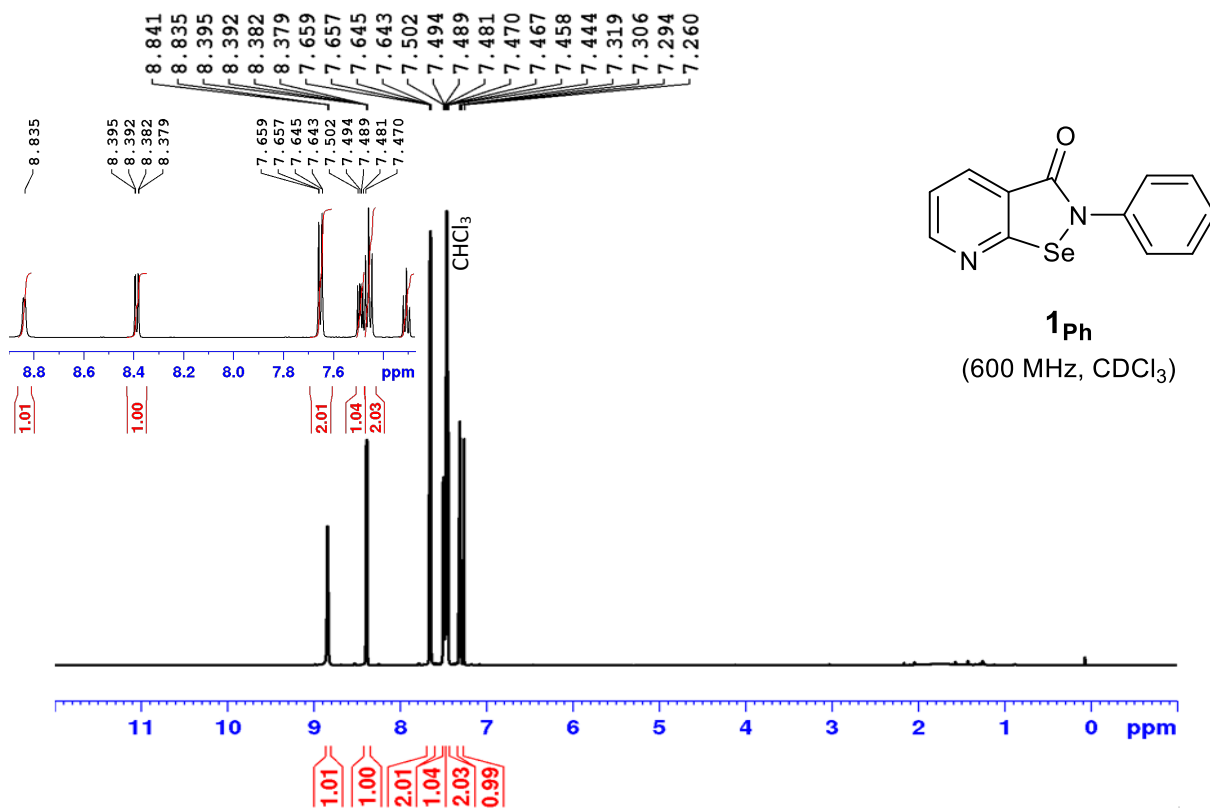


Figure S10: 600 MHz ¹H NMR in CDCl₃ of molecule **1_{Ph}**.

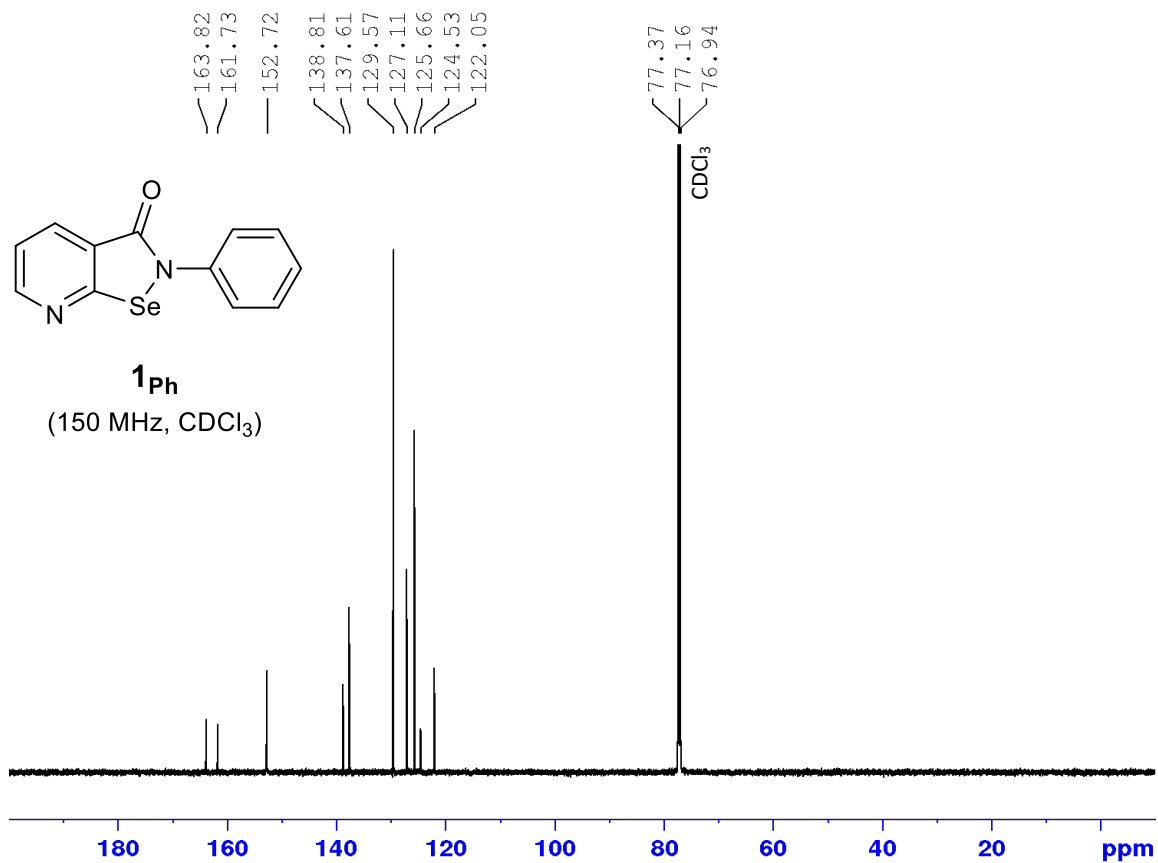


Figure S11: 150 MHz ¹³C NMR in CDCl₃ of molecule **1_{Ph}**.

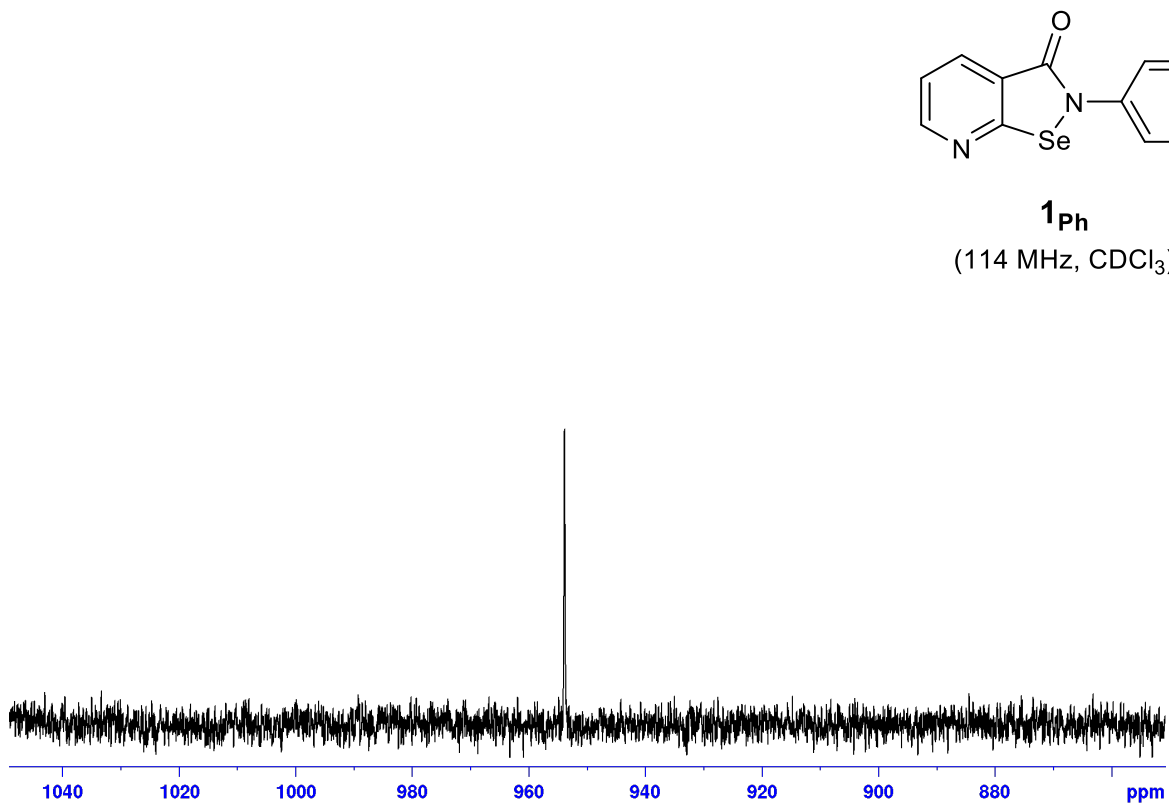


Figure S12: 114 MHz ⁷⁷Se NMR in CDCl₃ of molecule **1_{Ph}**.

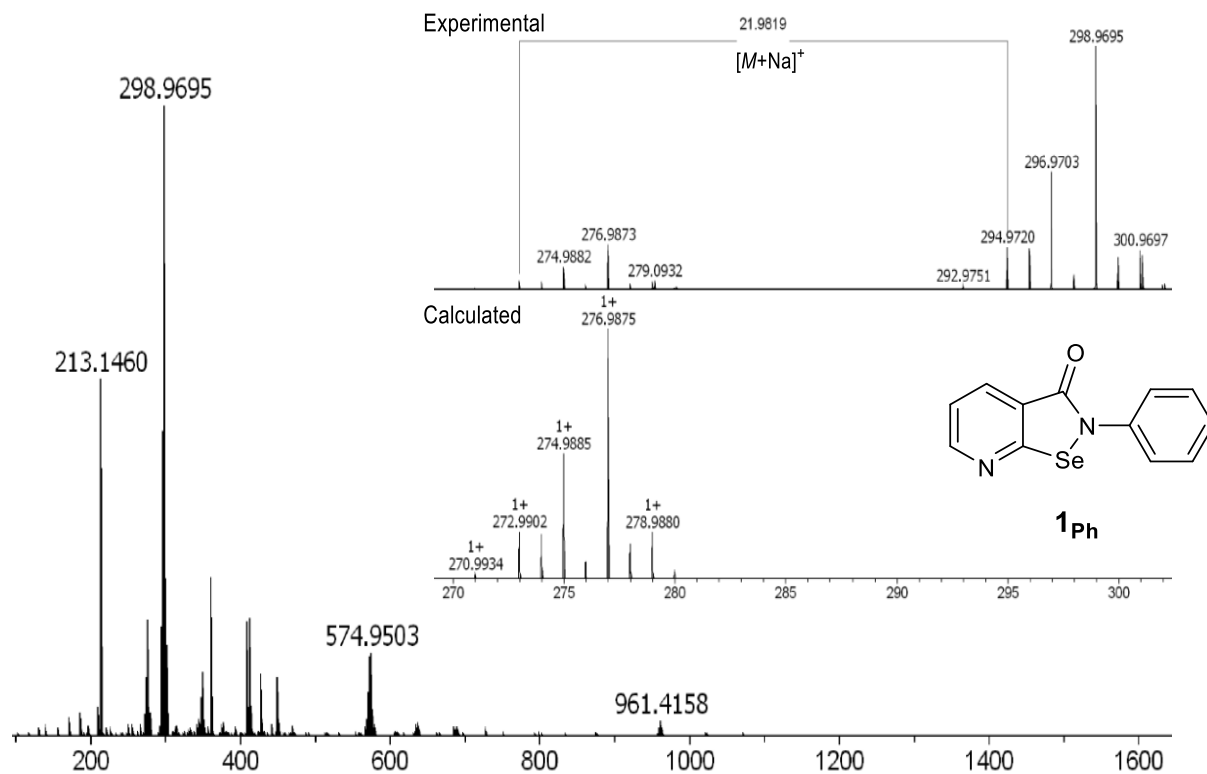


Figure S13: HRMS-ESI mass spectrum of molecule **1_{Ph}** in the positive ion mode. The peak at 574 corresponds to the dimeric species.

3.5 Characterization of **1_{Alk}**

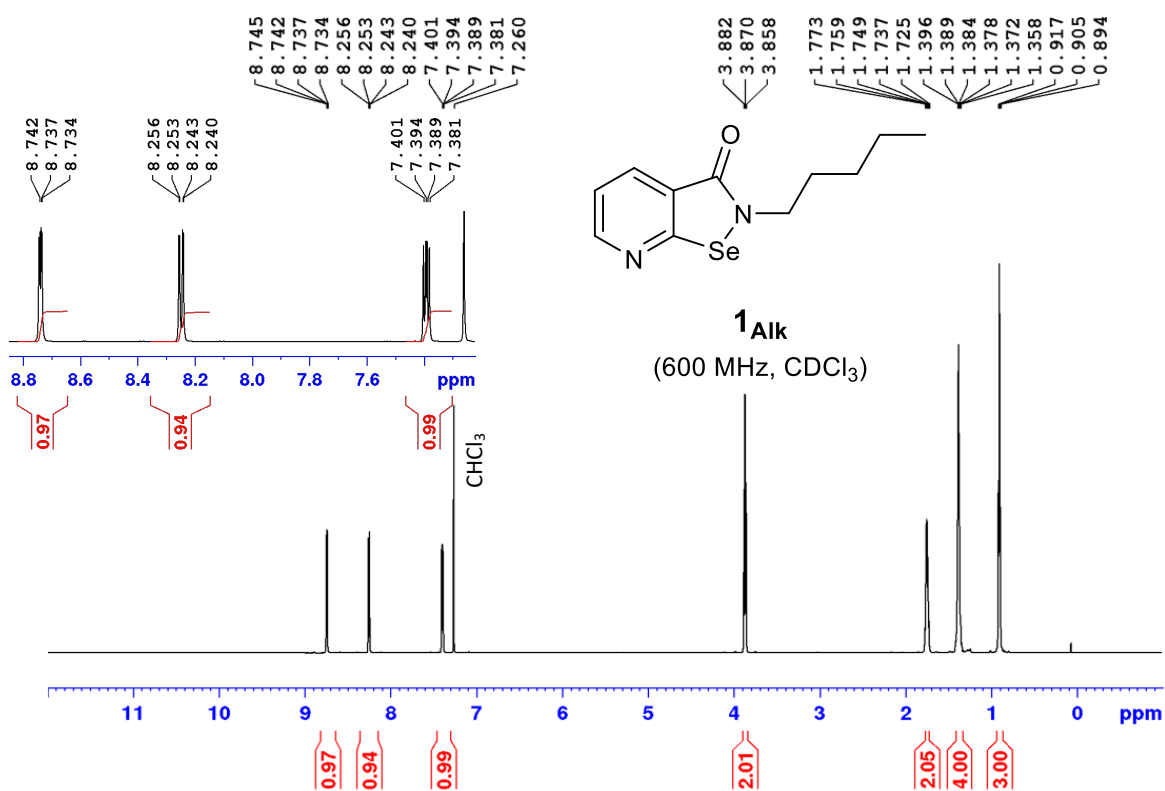


Figure S14: 600 MHz ¹H NMR in CDCl₃ of molecule **1_{Alk}**.

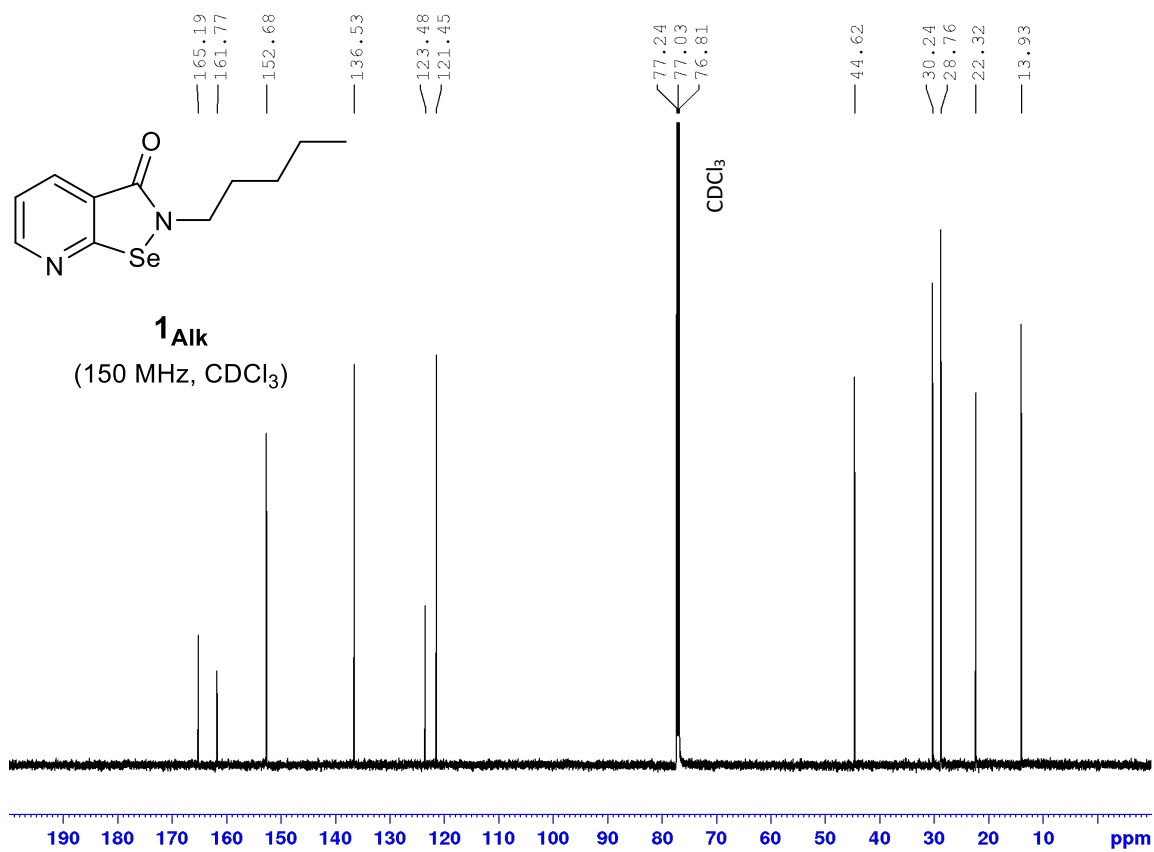


Figure S15: 150 MHz ¹³C NMR in CDCl₃ of molecule **1_{Alk}**.

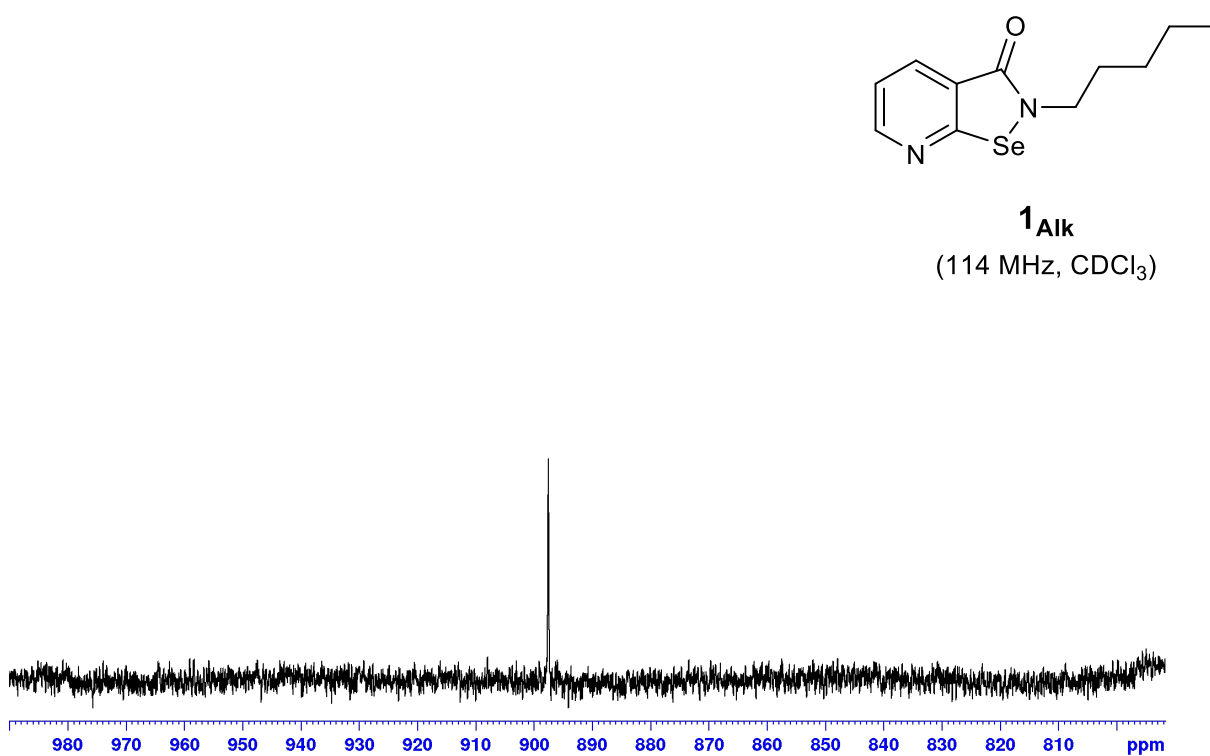


Figure S16: 114 MHz ⁷⁷Se NMR in CDCl₃ of molecule **1_{Alk}**.

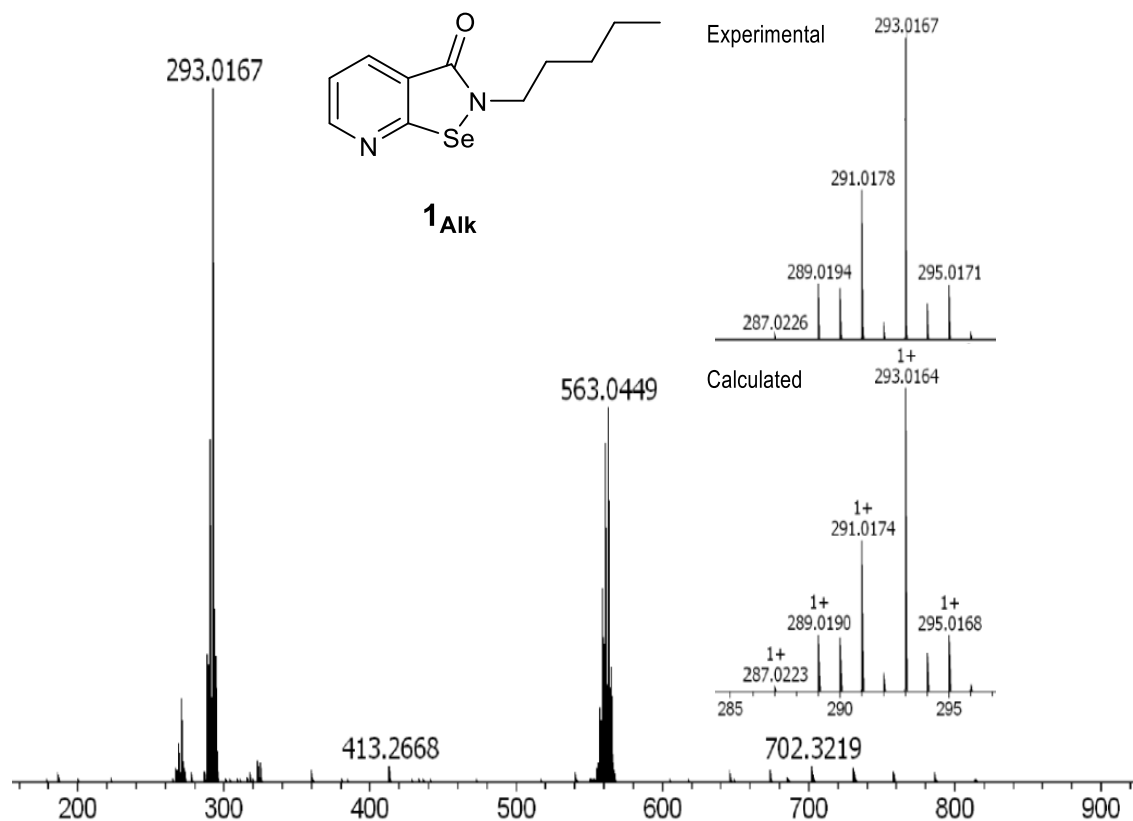


Figure S17: HRMS-ESI mass spectrum of molecule **1_{Alk}** in the positive ion mode. The peak at 563 corresponds to the dimeric species.

3.6 Characterization of **1_{Anthr}**

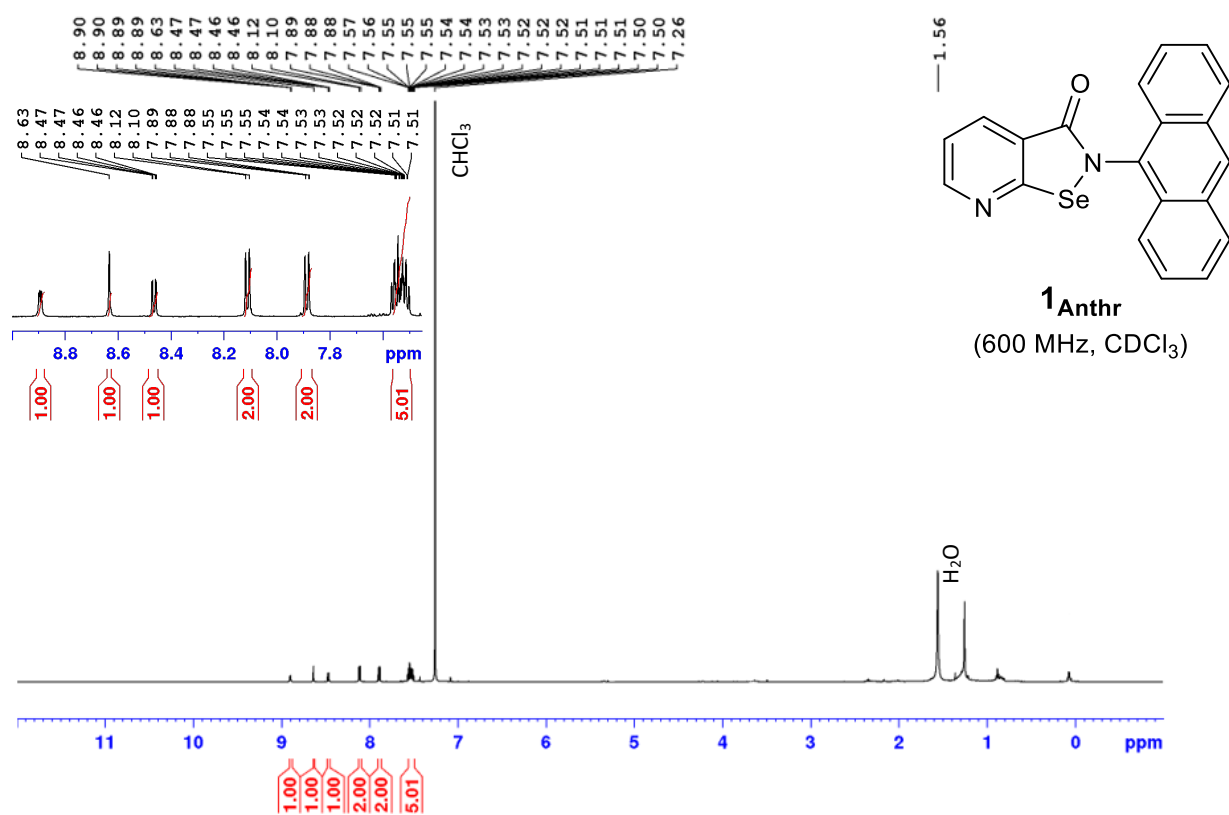


Figure S18: 600 MHz ¹H NMR in CDCl₃ of molecule **1_{Anthr}**.

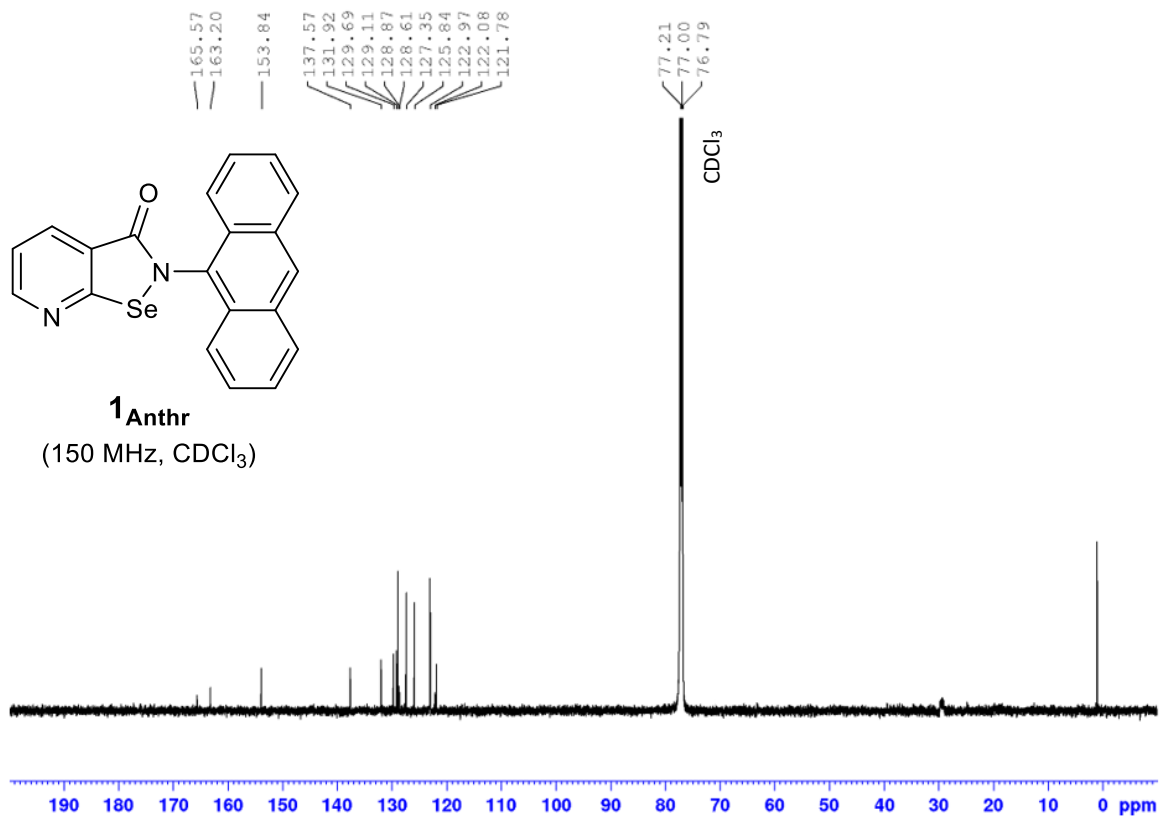


Figure S19: 150 MHz ¹³C NMR in CDCl₃ of molecule **1Anthr**.

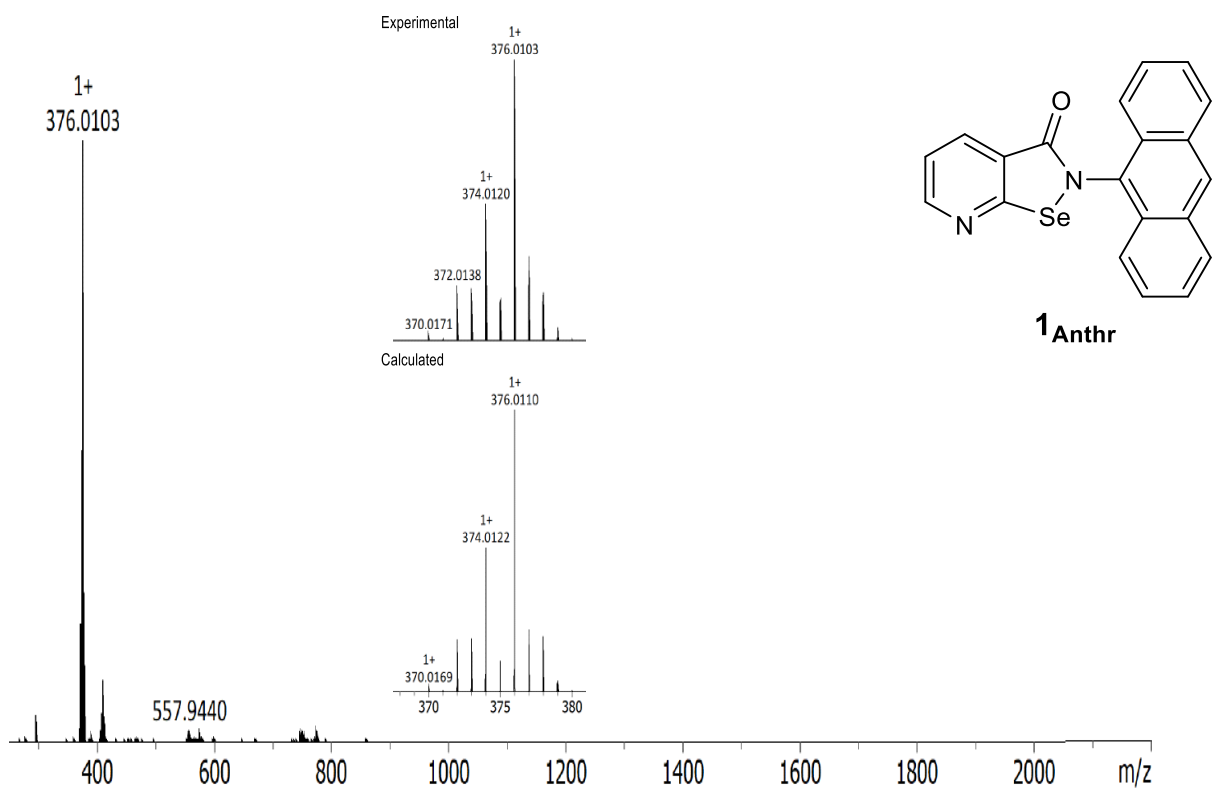


Figure S20: HRMS-LD mass spectrum of molecule **1Anthr** in the positive ion mode.

3.7 Characterization of **1_F**

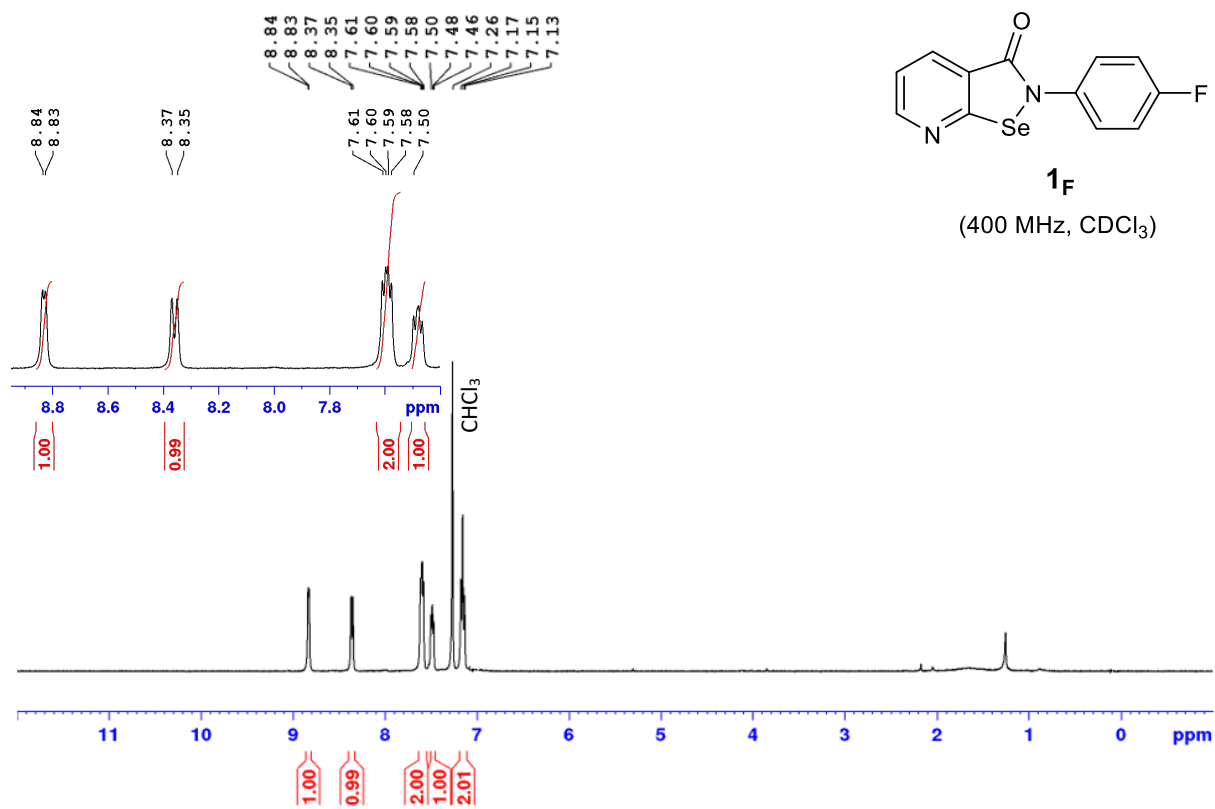


Figure S21: 400 MHz ¹H NMR in CDCl₃ of molecule **1_F**.

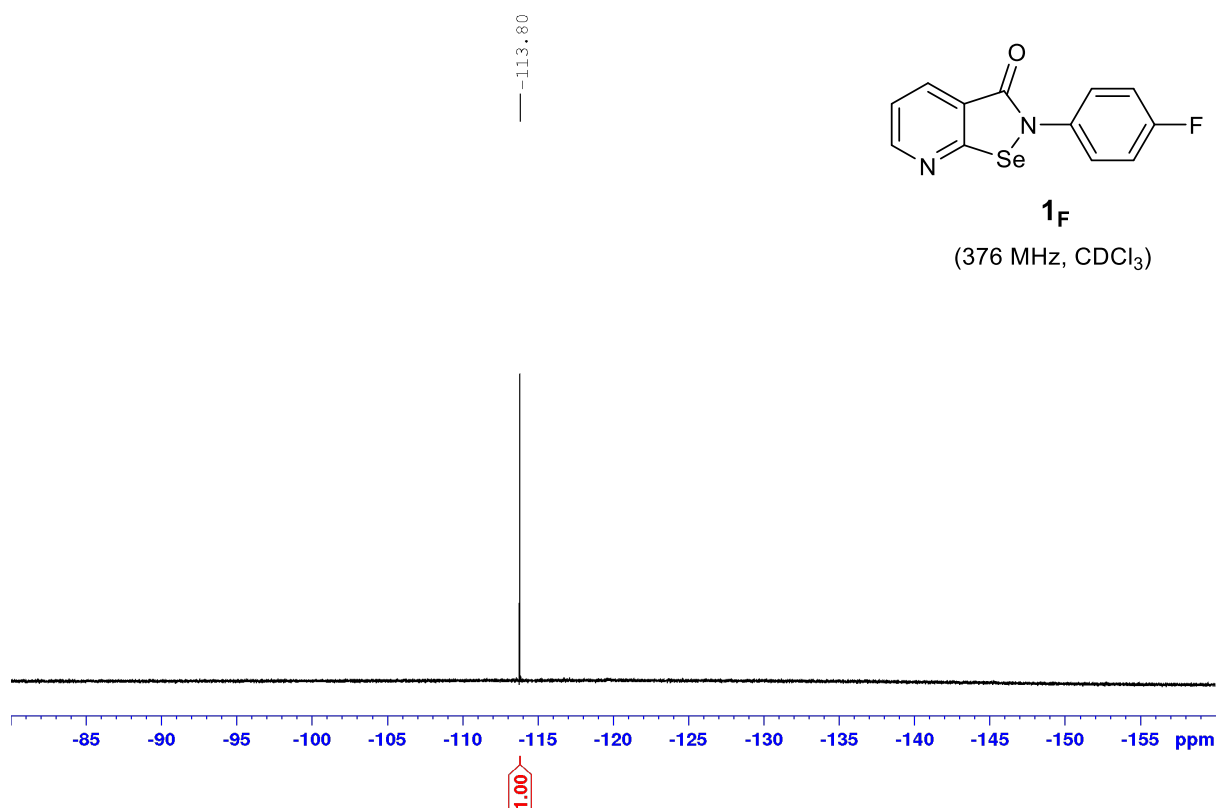


Figure S22: 376 MHz ¹⁹F NMR in CDCl₃ of molecule **1_F**.

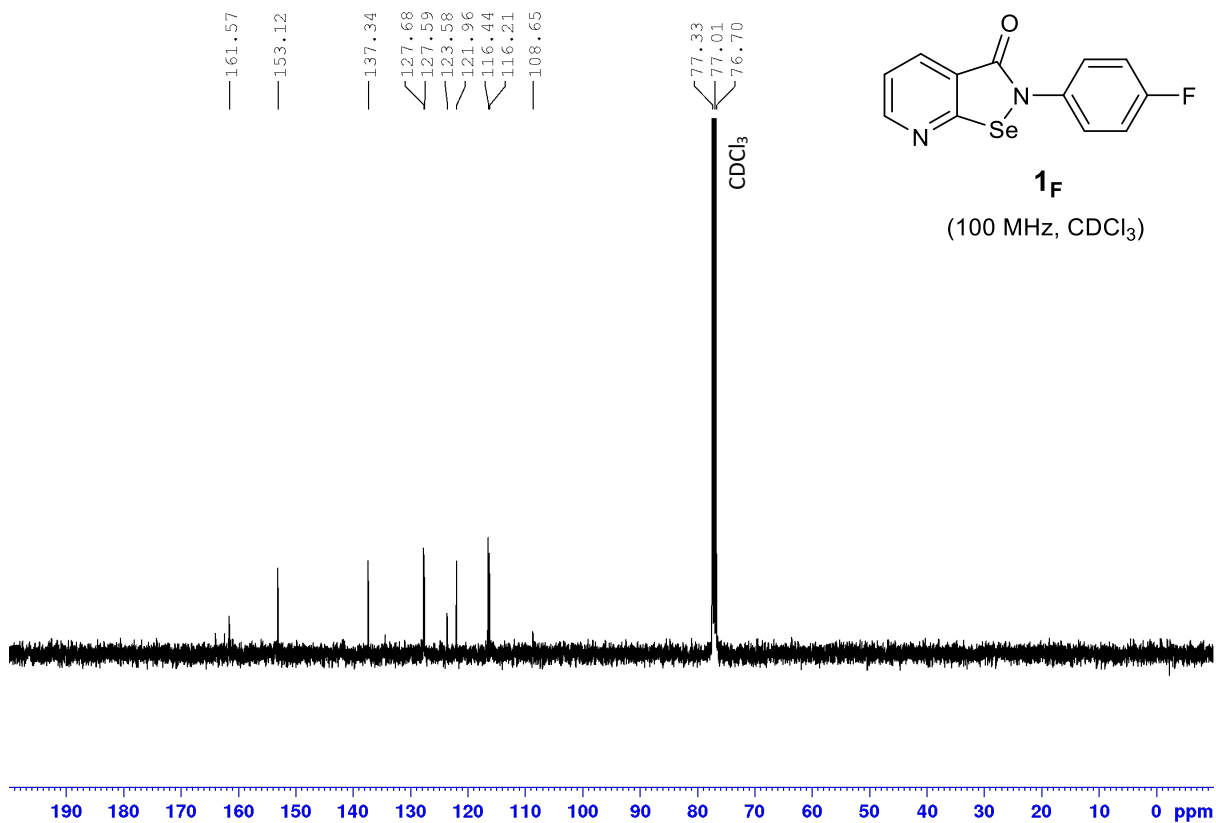


Figure S23: 100 MHz ¹³C NMR in CDCl₃ of molecule **1_F**.

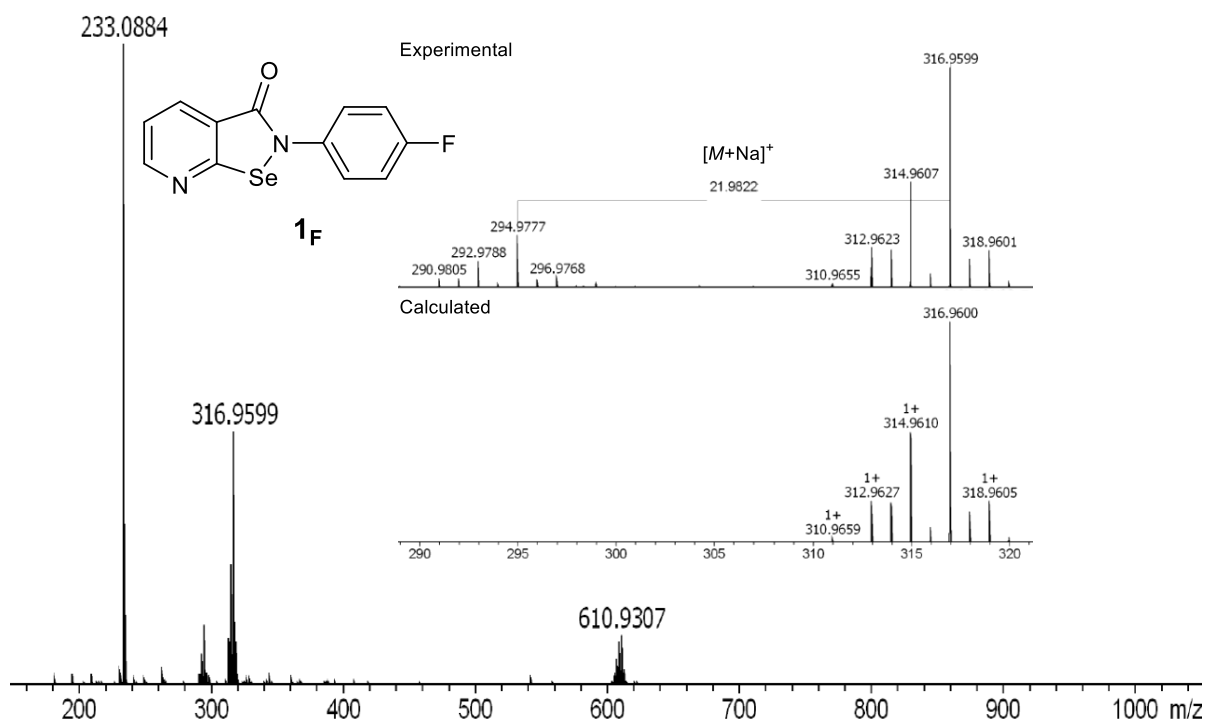


Figure S24: HRMS-ESI mass spectrum of molecule **1_F** in the positive ion mode. The peak at 610 corresponds to the dimeric species.

3.8 Characterization of **1_{Met}**

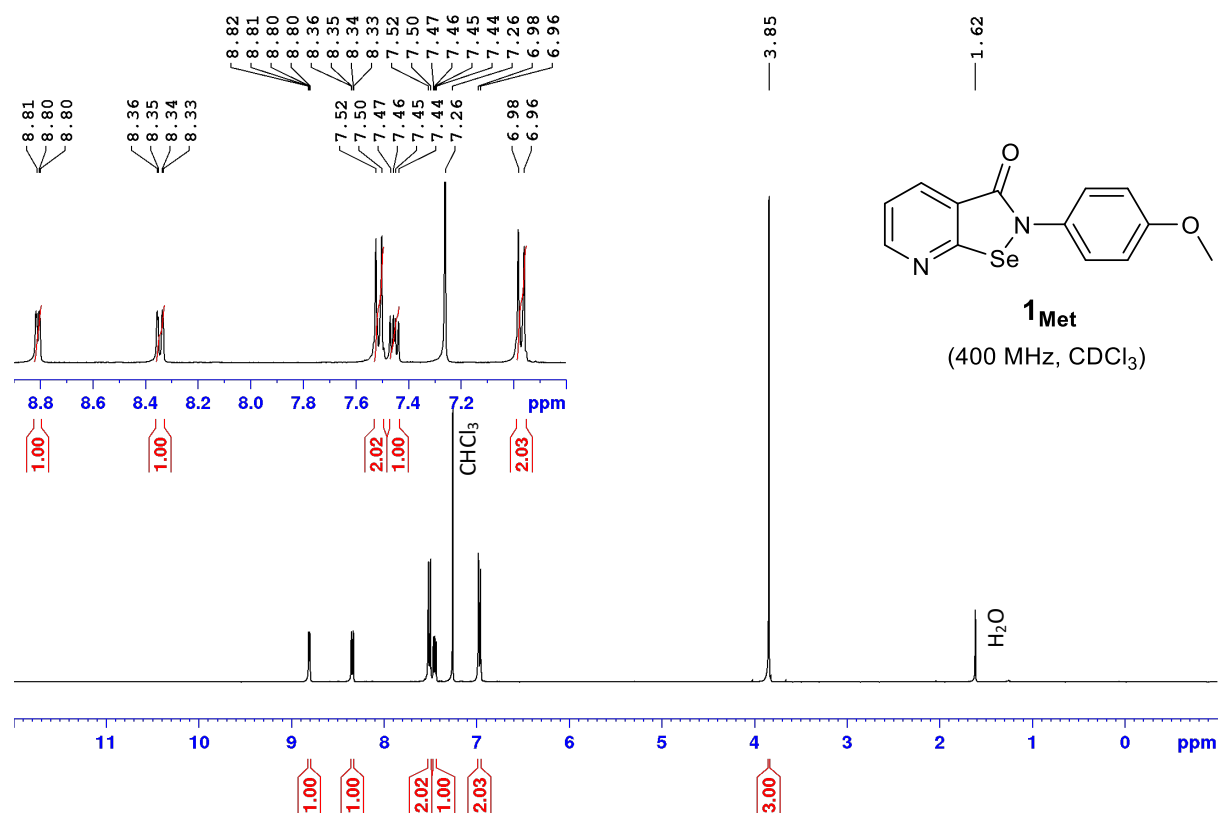


Figure S25: 400 MHz ¹H NMR in CDCl₃ of molecule **1_{Met}**.

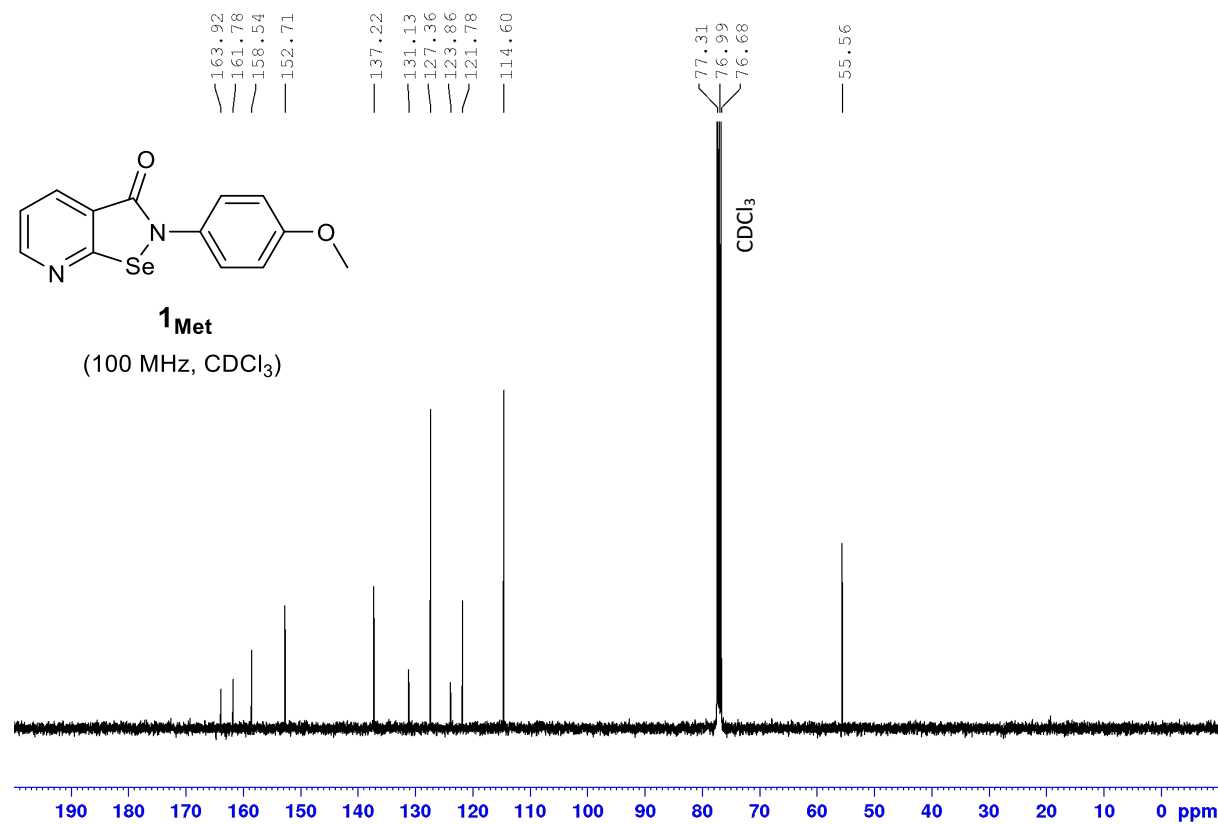


Figure S26: 100 MHz ¹³C NMR in CDCl₃ of molecule **1_{Met}**.

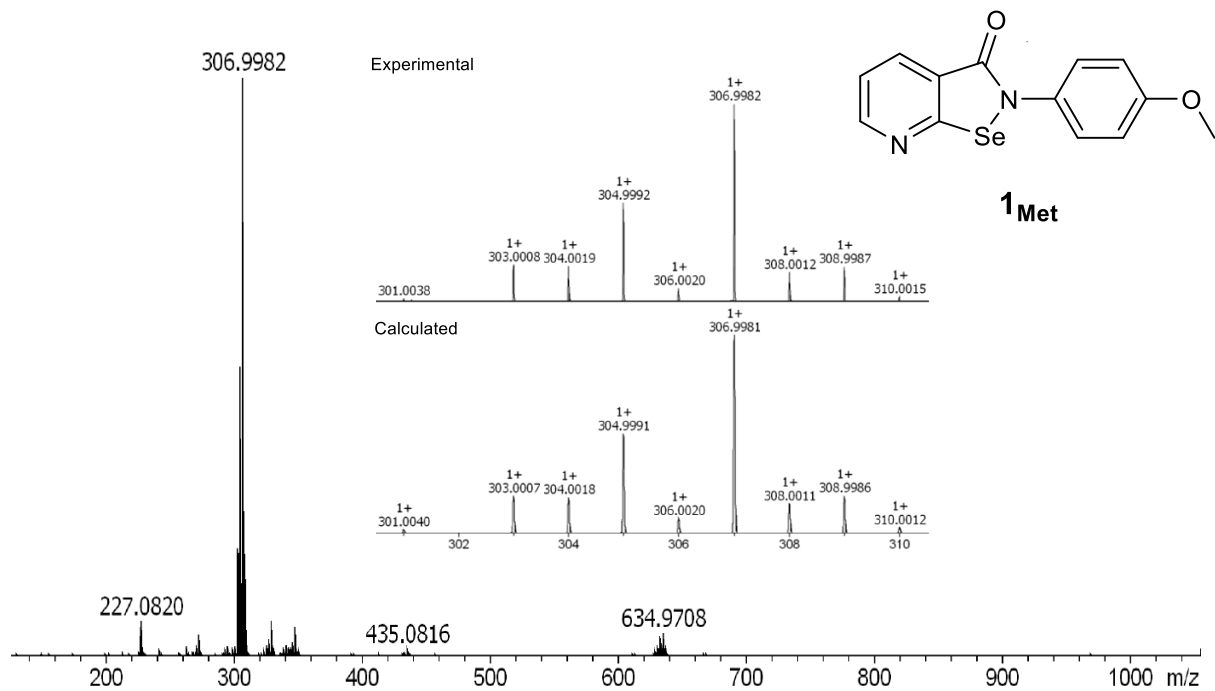


Figure S27: HRMS-ESI mass spectrum of molecule **1_{Met}** in the positive ion mode. The peak at 635 corresponds to the dimeric species.

3.9 Characterization of **1_{3F}**

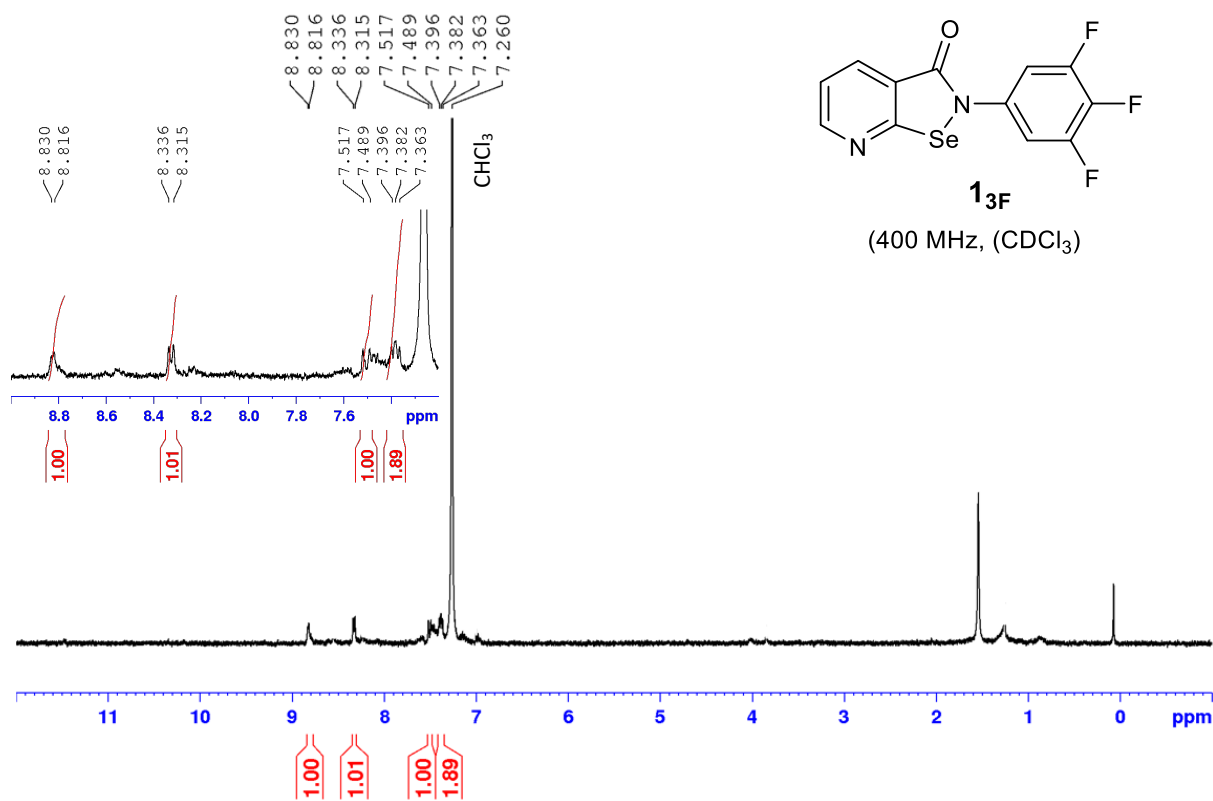


Figure S28: 400 MHz ¹H NMR in CDCl₃ of molecule **1_{3F}**.

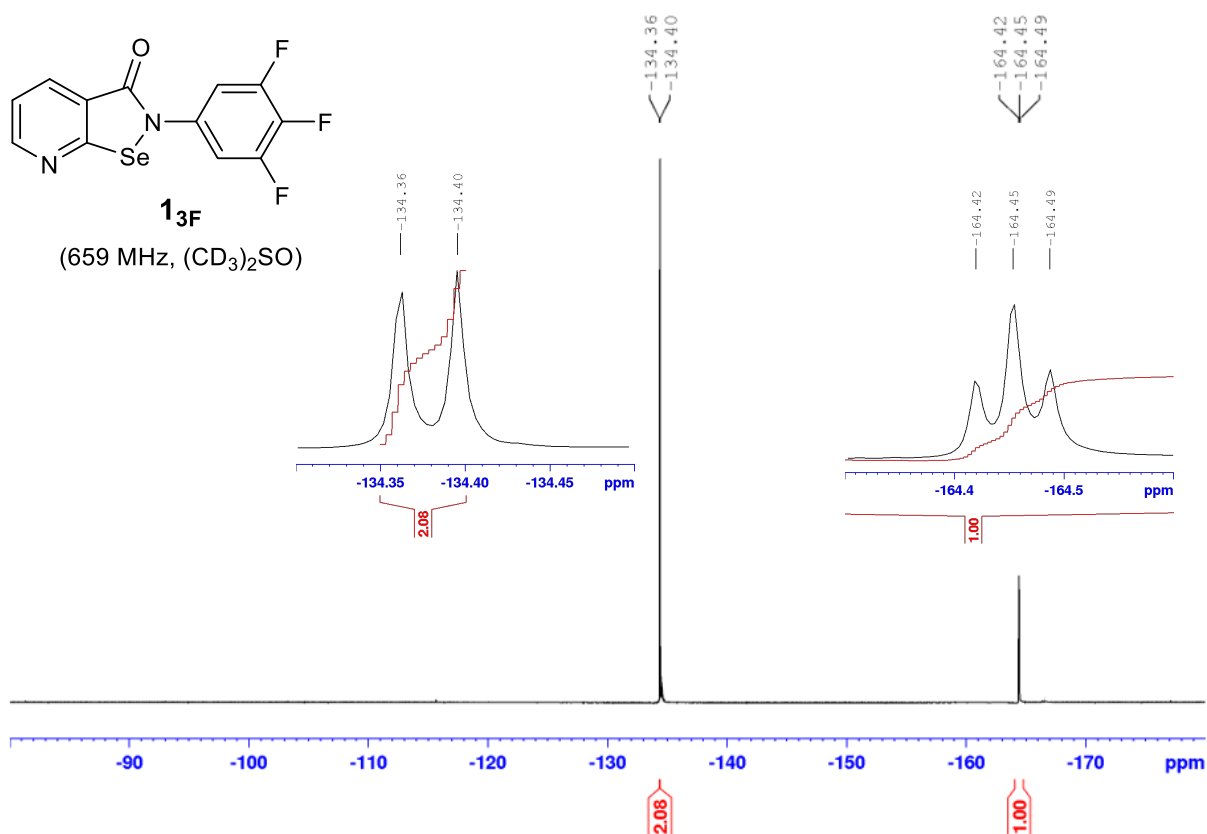


Figure S29: 659 MHz ¹⁹F NMR in (CD₃)₂SO of molecule **1₃F**.

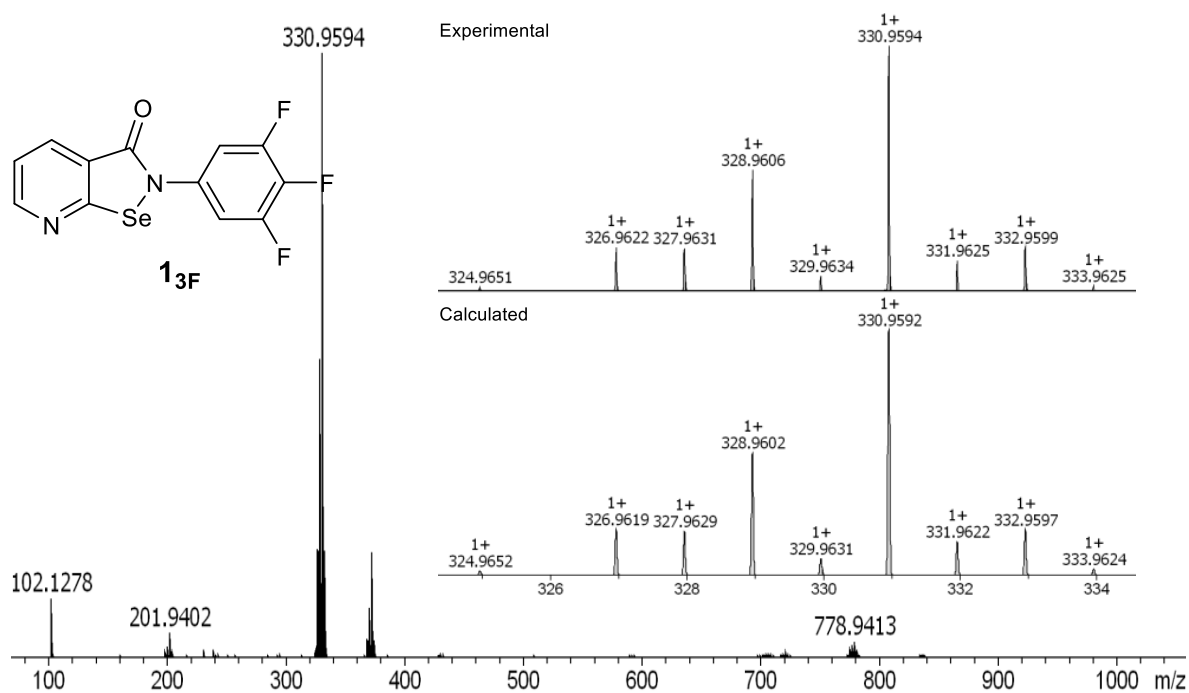


Figure S30: HRMS-ESI mass spectrum of molecule **1₃F** in the positive ion mode. The peak at 778 corresponds to the dimeric species.

3.10 Characterization of **1₃Met**

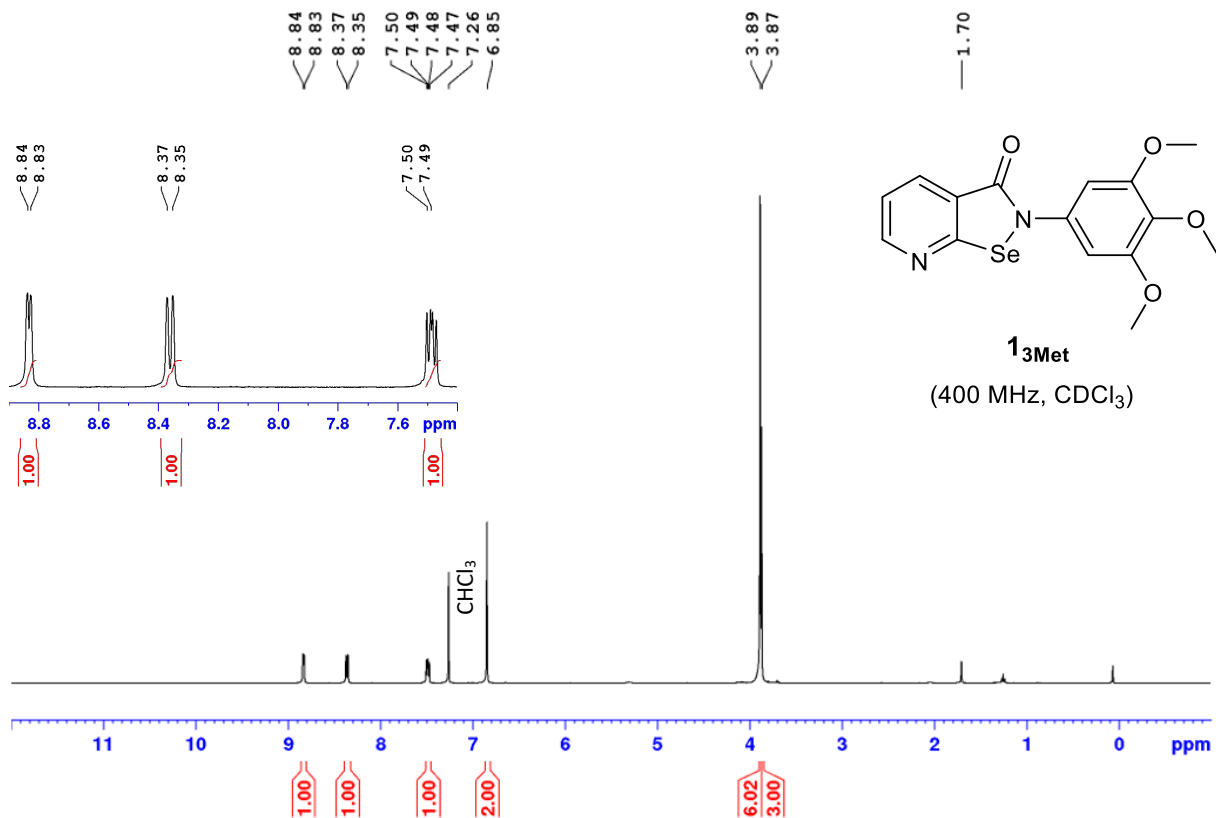


Figure S31: 400 MHz ¹H NMR in CDCl₃ of molecule **13Met**.

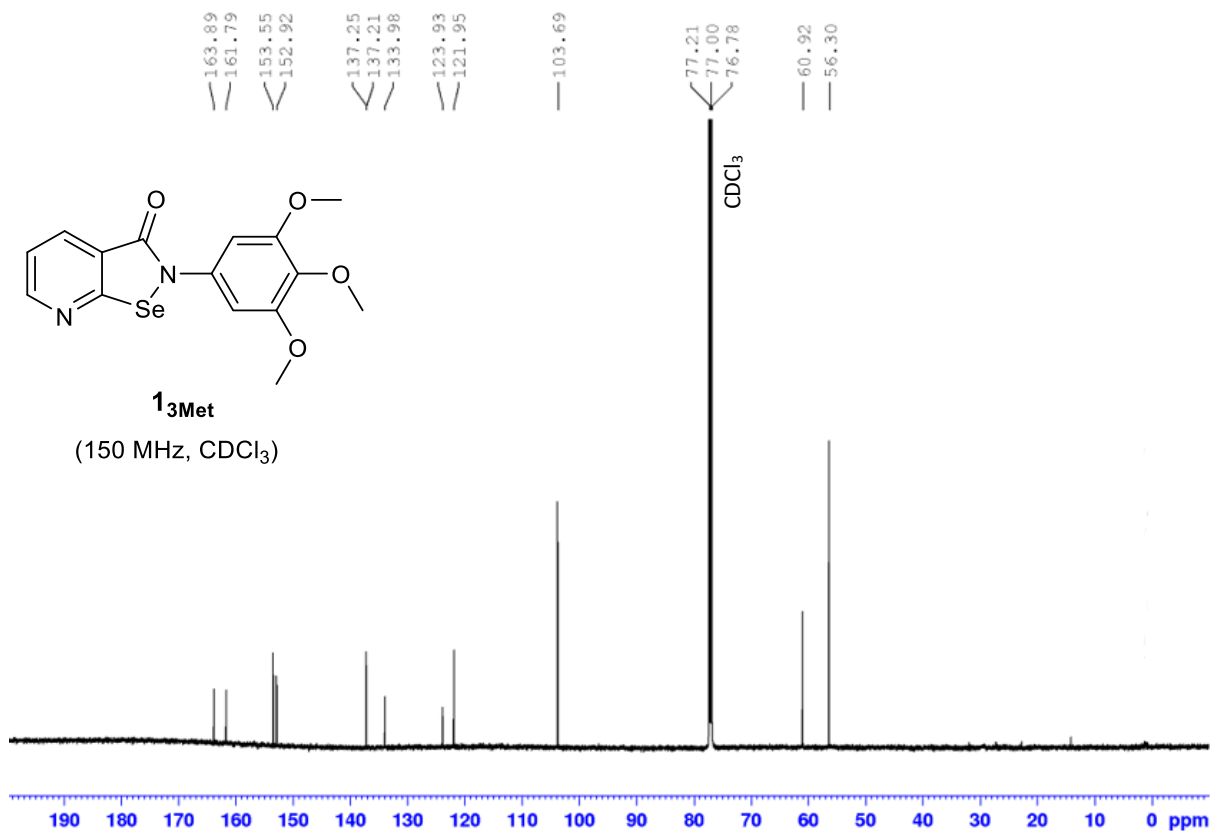


Figure S32: 150 MHz ¹³C NMR in CDCl₃ of molecule **13Met**.

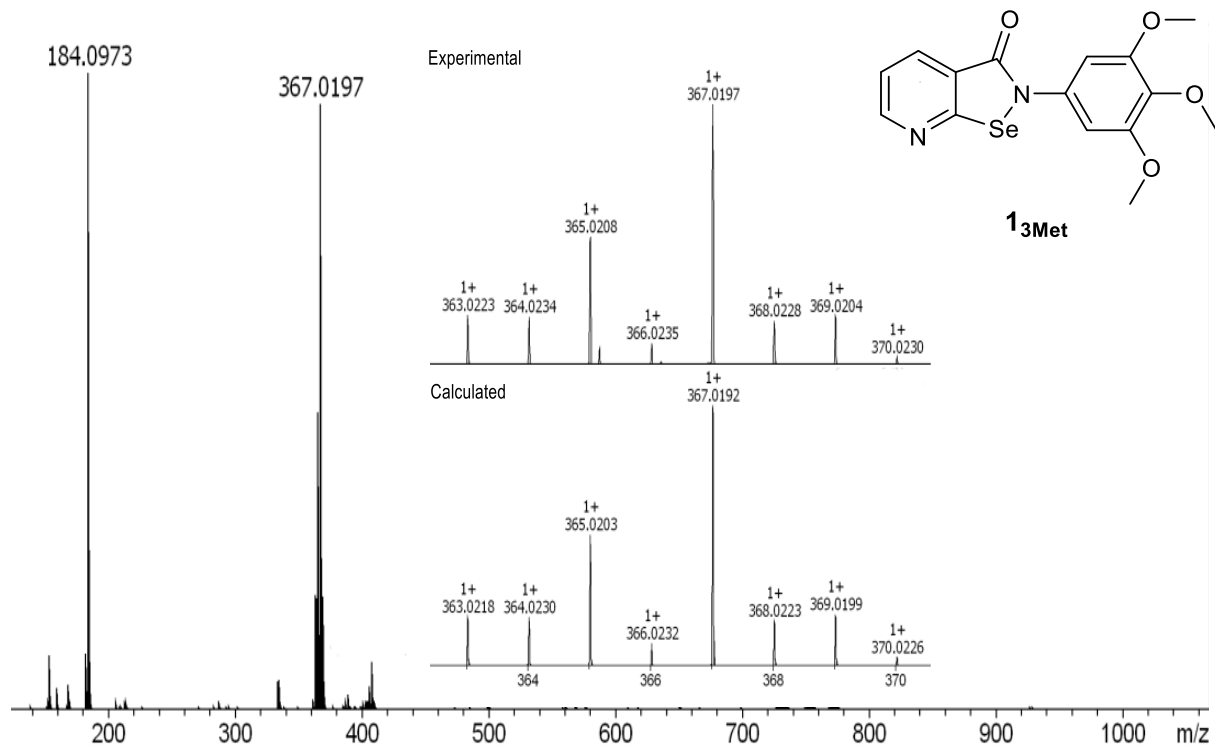
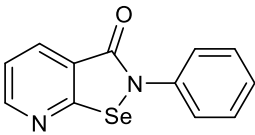


Figure S33: HRMS-ESI mass spectrum of molecule **13Met** in the positive ion mode.

4. Crystallographic data

Table S1. Crystal data and structure refinement for **1_{Ph}** (2333906).

Empirical formula	C ₁₂ H ₈ N ₂ OSe	
Formula weight	275.16	
Crystal system	Orthorhombic	1_{Ph}
Space group	Pca2 ₁	
Unit cell dimensions	a = 11.8989(10) Å b = 23.1512(18) Å c = 7.4136(6) Å	
Volume	2042.3(3) Å ³	
Z	8	
Density (calculated)	1.790 mg/m ³	
Absorption coefficient	3.653 mm ⁻¹	
F(000)	1088	
Crystal size	0.300 × 0.080 × 0.002 mm ³	

Data collection

Temperature	140(2) K
Wavelength	0.71073 Å
Theta range for data collection	2.455 to 33.078°.
Index ranges	-18 ≤ h ≤ 17, -35 ≤ k ≤ 35, -11 ≤ l ≤ 9
Reflections collected	7266
Independent reflections	5425 [R(int) = 0.0629]
Completeness to theta = 25.242°	94.8 %

Refinement

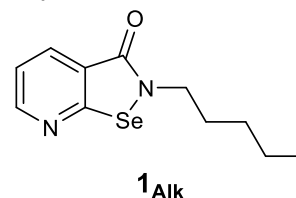
Absorption correction	multi-scan
Refinement method	Full-matrix least-squares on F ²
Data / restraints / parameters	7266 / 13 / 289
Goodness-of-fit on F ²	1.119
Final R indices [I > 2σ(I)]	R1 = 0.0476, wR2 = 0.1325
R indices (all data)	R1 = 0.0519, wR2 = 0.1444
Extinction coefficient	n/a
Largest diff. peak and hole	1.702 and -1.206 e ⁻ Å ⁻³

Table S2. Crystal data and structure refinement for **1_{Alk}** (2333763).

Empirical formula	C ₁₁ H ₁₄ N ₂ OSe
-------------------	--

Formula weight	269.20
Crystal system	Monoclinic
Space group	C 2/c
Unit cell dimensions	a = 25.268(7) Å b = 4.5670(12) Å c = 22.985(9) Å
Volume	2639.0(15) Å ³
Z	8
Density (calculated)	1.355 mg/m ³
Absorption coefficient	3.683 mm ⁻¹
F(000)	1088
Crystal size	0.100 × 0.057 × 0.020 mm ³

α = 90°.
β = 95.76(3)°.
γ = 90°.



Data collection

Temperature	100(2) K
Wavelength	1.54184 Å
Theta range for data collection	7.032 to 143.012°.
Index ranges	-18 ≤ h ≤ 30, -5 ≤ k ≤ 4, -26 ≤ l ≤ 28
Reflections collected	18255
Independent reflections	2238 [R(int) = 0.0476]
Completeness to theta = 25.242°	94.8 %

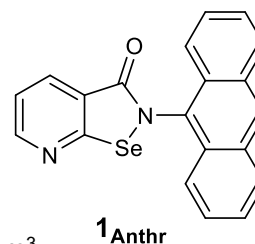
Refinement

Absorption correction	multi-scan
Refinement method	Full-matrix least-squares on F ²
Data / restraints / parameters	2433 / 0 / 137
Goodness-of-fit on F ²	1.191
Final R indices [I > 2σ(I)]	R1 = 0.0476, wR2 = 0.1113
R indices (all data)	R1 = 0.0519, wR2 = 0.1145
Extinction coefficient	n/a
Largest diff. peak and hole	0.776 and -0.698 e ⁻ Å ⁻³

Table S3. Crystal data and structure refinement for **1_{Anthr}** (2333913).

Empirical formula	C ₂₀ H ₁₂ N ₂ OSe
Formula weight	375.53
Crystal system	Triclinic

Space group	P-1	
Unit cell dimensions	a = 9.1044(2) Å	$\alpha = 70.8921(11)^\circ$.
	b = 9.4027(3) Å	$\beta = 83.9311(12)^\circ$.
	c = 12.5737(2) Å	$\gamma = 76.2805(12)^\circ$.
Volume	987.60(5) Å ³	
Z	2	
Density (calculated)	1.262 mg/m ³	
Absorption coefficient	1.907 mm ⁻¹	
F(000)	376	
Crystal size	0.080 × 0.080 × 0.060 mm ³	



Data collection

Temperature	100(2) K
Wavelength	0.71073 Å
Theta range for data collection	4.872 to 60.292°.
Index ranges	-12 ≤ h ≤ 12, -13 ≤ k ≤ 13, -17 ≤ l ≤ 17
Reflections collected	43351
Independent reflections	5049 [R(int) = 0.0257]
Completeness to theta = 25.242°	99.7 %

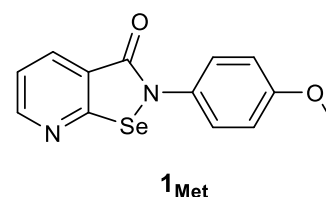
Refinement

Absorption correction	multi-scan
Refinement method	Full-matrix least-squares on F ²
Data / restraints / parameters	5822 / 0 / 217
Goodness-of-fit on F ²	1.088
Final R indices [I > 2σ(I)]	R1 = 0.0257, wR2 = 0.0690
R indices (all data)	R1 = 0.0305, wR2 = 0.0705
Extinction coefficient	n/a
Largest diff. peak and hole	0.593 and -0.797 e ⁻ Å ⁻³

Table S4. Crystal data and structure refinement for **1_{Met}** (2333910).

Empirical formula	C ₁₃ H ₁₀ N ₂ O ₂ Se	
Formula weight	305.19	
Crystal system	Monoclinic	
Space group	P2 ₁ /c	
Unit cell dimensions	a = 4.0279(4) Å	$\alpha = 90^\circ$.

	b = 13.8376(14) Å	$\beta = 94.648(8)^\circ$
	c = 20.631(2) Å	$\gamma = 90^\circ$
Volume	1146.1(2) Å ³	
Z	4	
Density (calculated)	1.769 mg/m ³	
Absorption coefficient	3.270 mm ⁻¹	
F(000)	608	
Crystal size	0.030 × 0.133 × 0.320 mm ³	



Data collection

Temperature	100(2) K
Wavelength	0.71073 Å
Theta range for data collection	1.774 to 31.373°
Index ranges	-5 ≤ h ≤ 5, -20 ≤ k ≤ 18, -29 ≤ l ≤ 29
Reflections collected	25886
Independent reflections	3652 [R(int) = 0.0364]
Completeness to theta = 25.242°	97.8 %

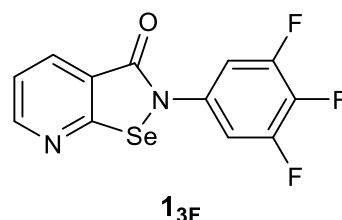
Refinement

Absorption correction	multi-scan
Max. and min. transmission	0.942 and 0.731
Refinement method	Full-matrix least-squares on F ²
Data / restraints / parameters	3680 / 0 / 164
Goodness-of-fit on F ²	1.324
Final R indices [I > 2σ(I)]	R1 = 0.0806, wR2 = 0.2052
R indices (all data)	R1 = 0.1070, wR2 = 0.2052
Extinction coefficient	n/a
Largest diff. peak and hole	0.575 and -0.819 e ⁻ Å ⁻³

Table S5. Crystal data and structure refinement for **1_{3F}** (2223676).

Empirical formula	C ₁₂ H ₅ N ₂ OSeF ₃	
Formula weight	329.14	
Crystal system	Triclinic	
Space group	P-1	
Unit cell dimensions	a = 3.8300(8) Å	$\alpha = 99.42(3)^\circ$
	b = 11.360(2) Å	$\beta = 96.01(3)^\circ$
	c = 12.780(3) Å	$\gamma = 94.80(3)^\circ$

Volume	542.6(2) Å ³
Z	2
Density (calculated)	2.015 mg/m ³
Absorption coefficient	3.338 mm ⁻¹
F(000)	320
Crystal size	0.020 × 0.050 × 0.100 mm ³



Data collection

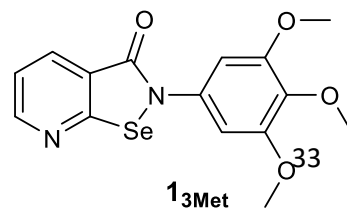
Temperature	100(2) K
Wavelength	0.700 Å
Theta range for data collection	0.981 to 25.949°.
Index ranges	-4 ≤ h ≤ 4, -14 ≤ k ≤ 14, -15 ≤ l ≤ 15
Reflections collected	2742
Completeness to theta = 25.242°	98.1 %

Refinement

Absorption correction	multi-scan
Max. and min. transmission	0.936 and 0.731
Refinement method	Full-matrix least-squares on F ²
Data / restraints / parameters	2182 / 0 / 173
Goodness-of-fit on F ²	1.113
Final R indices [I > 2σ(I)]	R1 = 0.1056, wR2 = 0.2555
R indices (all data)	R1 = 0.1519, wR2 = 0.2793
Extinction coefficient	n/a
Largest diff. peak and hole	1.860 and -1.566 e ⁻ Å ⁻³

Table S6. Crystal data and structure refinement for **1_{3Met}** (2333762).

Empirical formula	C ₁₅ H ₁₄ N ₂ O ₄ Se
Formula weight	365.24
Crystal system	Monoclinic
Space group	P2 ₁ /n
Unit cell dimensions	a = 4.2388(6) Å α = 90°. b = 14.2677(16) Å β = 91.498(13)°. c = 23.173(4) Å γ = 90°.
Volume	1401.0(4) Å ³
Z	4



Density (calculated)	1.732 mg/m ³
Absorption coefficient	2.701 mm ⁻¹
F(000)	736
Crystal size	0.010 × 0.067 × 0.180 mm ³

Data collection

Temperature	100(2) K
Wavelength	0.71073 Å
Theta range for data collection	2.26 to 27.50°.
Index ranges	-6<=h<=6, -20<=k<=21, -33<=l<=34
Reflections collected	4572
Completeness to theta = 25.242°	96.4 %

Refinement

Absorption correction	multi-scan
Max. and min. transmission	0.922 and 0.724
Refinement method	Full-matrix least-squares on F ²
Data / restraints / parameters	3302 / 0 / 203
Goodness-of-fit on F ²	1.117
Final R indices [I>2sigma(I)]	R1 = 0.0347, wR2 = 0.0212
R indices (all data)	R1 = 0.06500, wR2 = 0.0843
Extinction coefficient	n/a
Largest diff. peak and hole	0.925 and -1.277 e ⁻ Å ⁻³

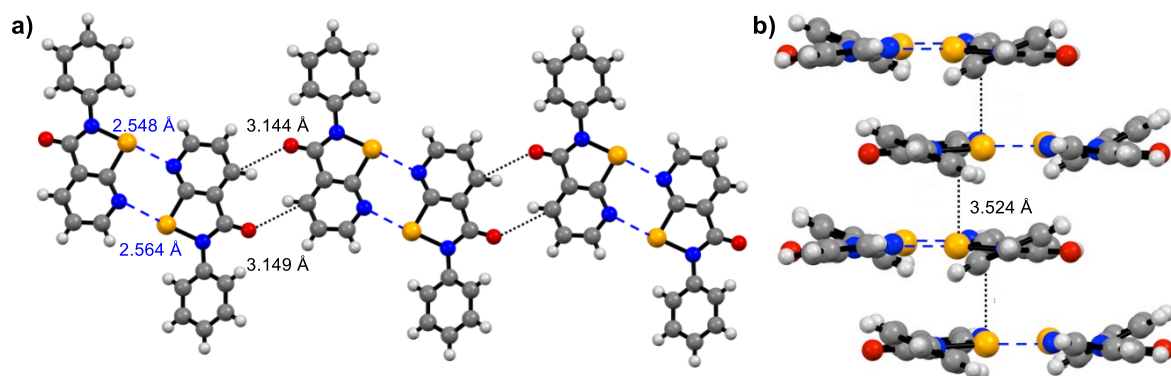


Figure S34: Molecular packing of **1_{Ph}**, held together by a) Se...N ChBs (pointed out with dashed blue lines) and HBs (highlighted with dotted black lines); b) crystal packing along *b* axis, expanded through Se... π vdW interactions. Crystallization solvent: THF. Space group: *Pca2*₁.

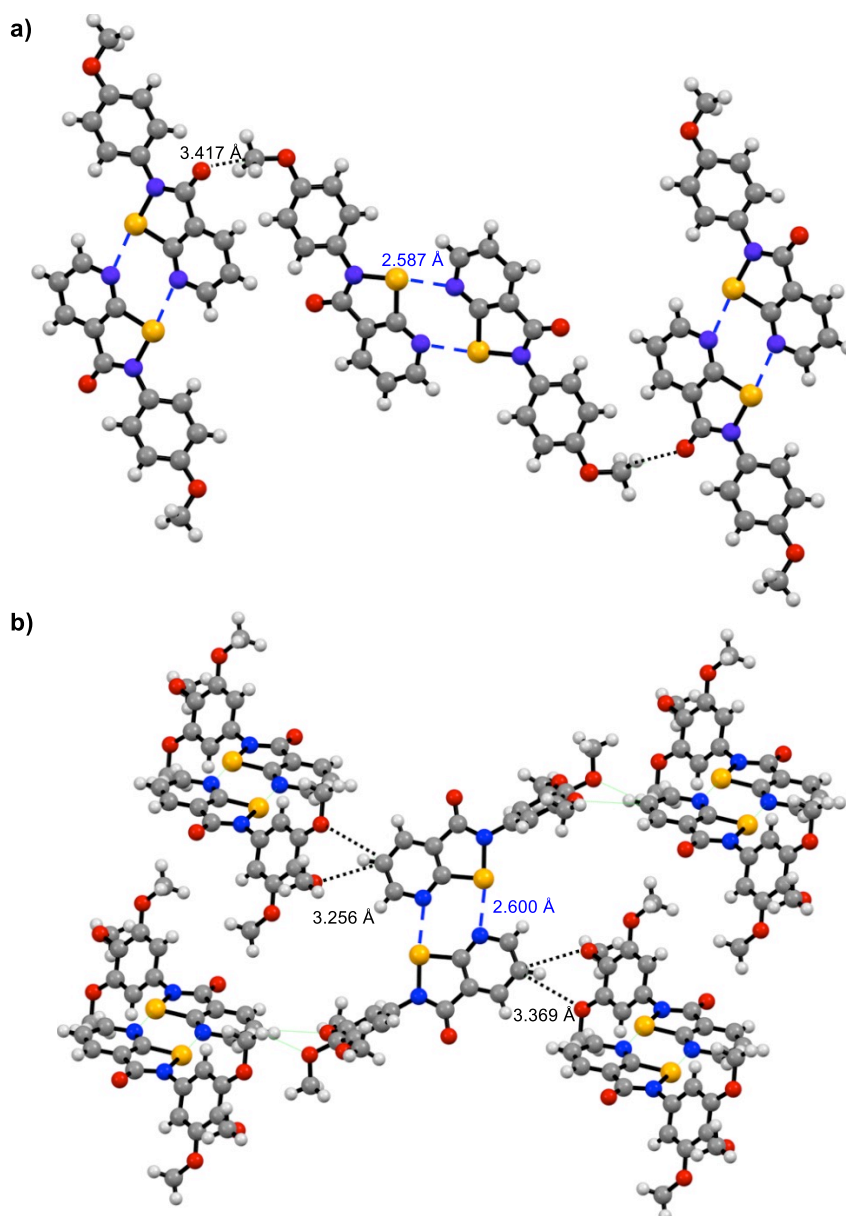


Figure S35: Molecular packing of a) **1_{Met}**, forming a 2D non-covalent polymer by means of double Se...N ChBs (pointed out with dashed blue lines) and HBs (highlighted with dotted black lines); crystal structure of b) **1_{3Met}**, developed through multiple HBs (highlighted with dotted black lines). Crystallization solvent: CHCl₃ for **1_{Met}**, THF for **1_{3Met}**. Space group: *Pca2*₁ for **1_{Met}**, *P2*₁/*n* for **1_{3Met}**.

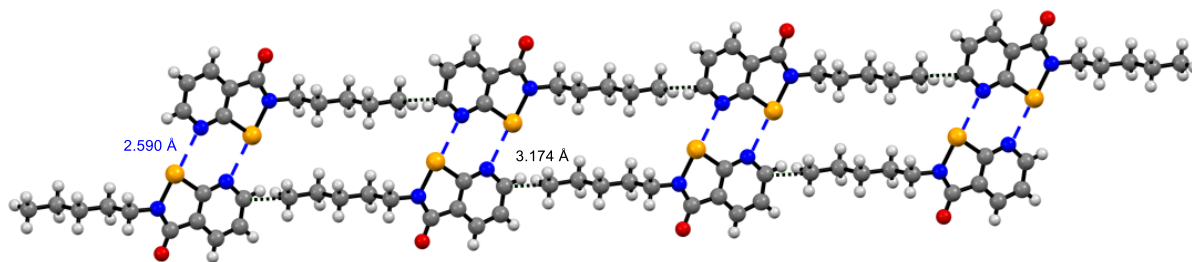


Figure S36: Double linear polymeric chain composing the molecular packing of **1_{AIK}**, driven by concurrent Se...N ChBs (highlighted with dashed blue lines) and C...C contacts (outlined with dotted black lines). Crystallization solvent: CHCl₃/EtOAc. Space group: C2/c.

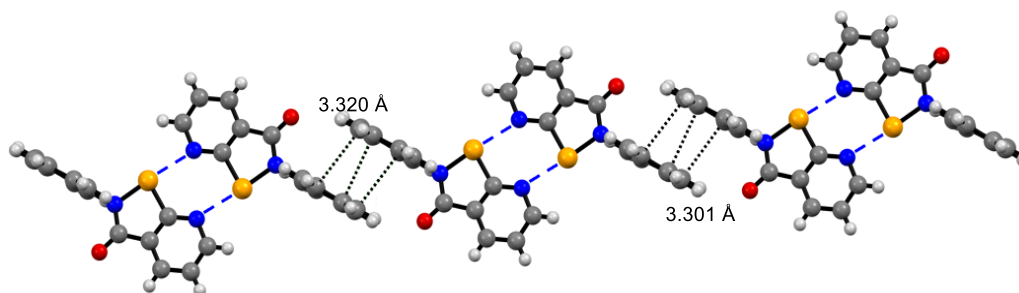


Figure S37: a) Self-assembly of **1_{Anthr}** in doubly Se...N chalcogen-bonded dimers and b) molecular packing developed through $\pi\cdots\pi$ stacking between the anthracene rings. Crystallization solvent: CHCl₃/toluene. Space group: P-1.

5. ^1H and ^{77}Se NMR measurements

5.1 Dilution experiments

Dimerization of compounds 1_i was investigated by dilution experiments in CDCl_3 at 298 K. The chemical shift data of the ^{77}Se resonance were fitted with Dynafit software packages^[42] using a 1:1 dimerization model and the obtained dimerization constants (K_d) are reported in the Figures below. The chemical shift data of the three pyridyl protons (H_a , H_b , and H_c) were fitted with Dynafit using a global fit approach in which the data of the three protons are fitted contemporaneously to the 1:1 dimerization model. The global fit approach increases the accuracy of the fitting results and it is particularly useful in this case where the chemical shift variations upon dilution are really small. The Figures below reports the obtained dimerization constants (K_d) and the fitting curve relative to proton H_a which is the one that shows the highest chemical shift variation upon dilution. In general, the dimerization constants obtained from the fitting of the ^{77}Se resonance and those from the pyridyl protons are in good agreement, with the latter being slightly higher in some cases. However, due to the larger chemical shift variation, the readout errors on the ^{77}Se signals are less prone to affect the fitting results, allowing the collection of a more consistent and wide set of results. Accordingly, this set of data is reported in the manuscript. In any case, the same trend in the K_d values is obtained from the ^1H titrations.

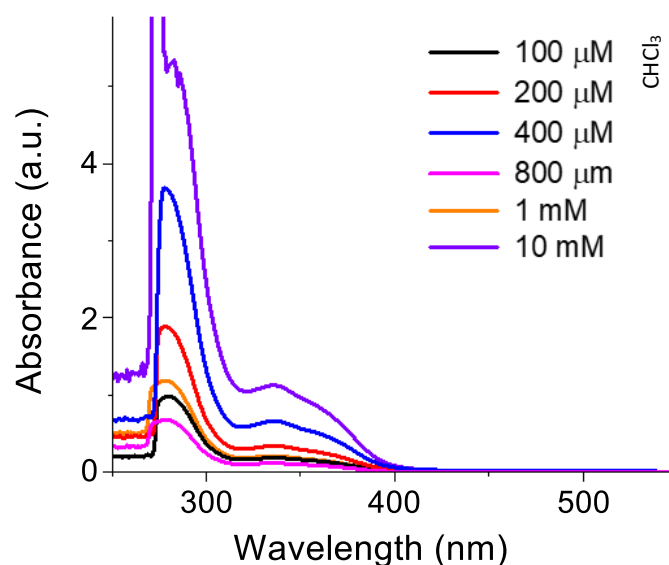


Figure S38: Absorption spectra of 1_{Ph} upon decreasing concentration, recorded in benzene at 298 K.

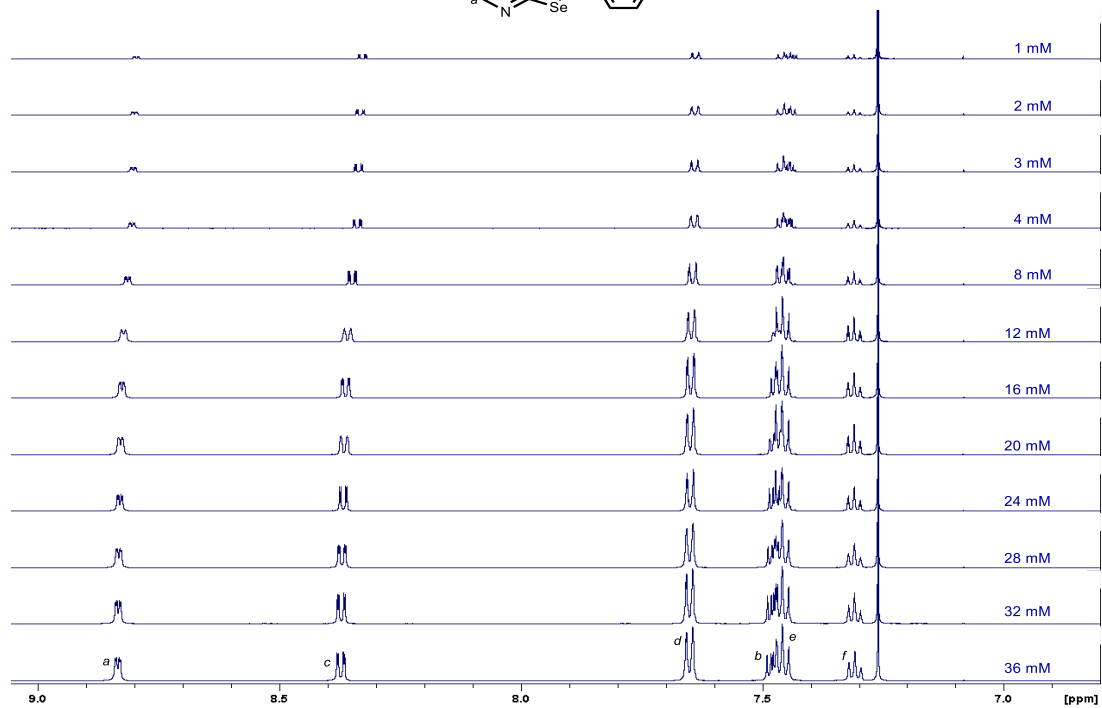
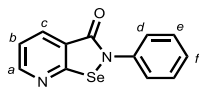


Figure S39: 600 MHz ¹H NMR overlapped spectra of 1_{Ph} diluted solutions in CDCl₃ at 298 K.

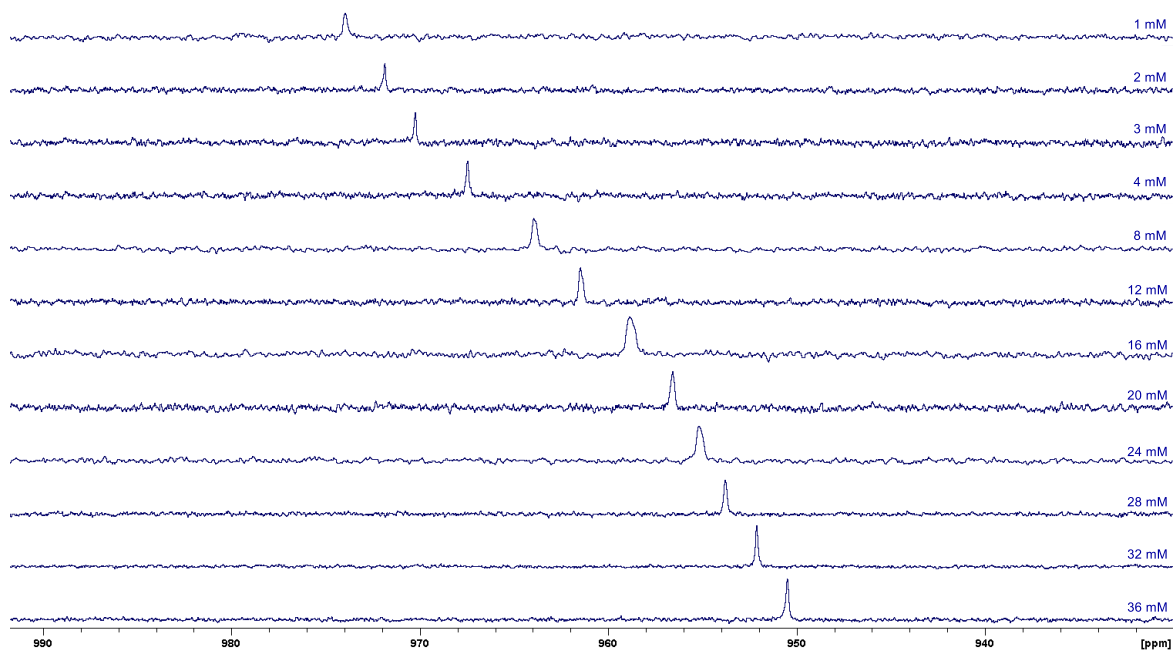


Figure S40: 115 MHz ^{77}Se NMR overlapped spectra of 1_{Ph} diluted solutions in CDCl_3 at 298 K.

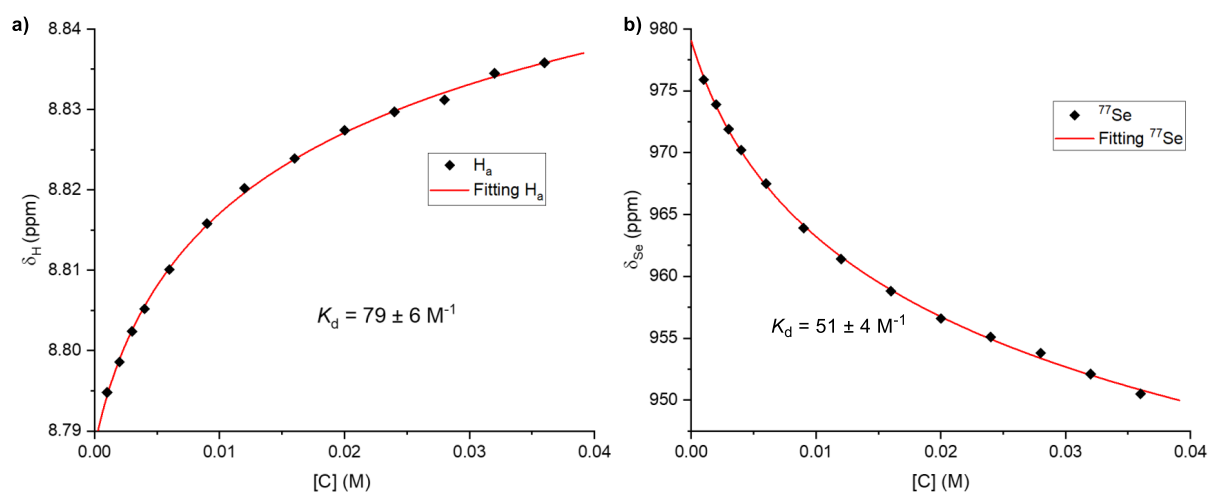


Figure S41: Experimental chemical shift from a) ^1H NMR and b) ^{77}Se NMR dilution experiments in CDCl_3 vs concentration of 1_{Ph} , fitted to a 1:1 dimerization equilibrium.

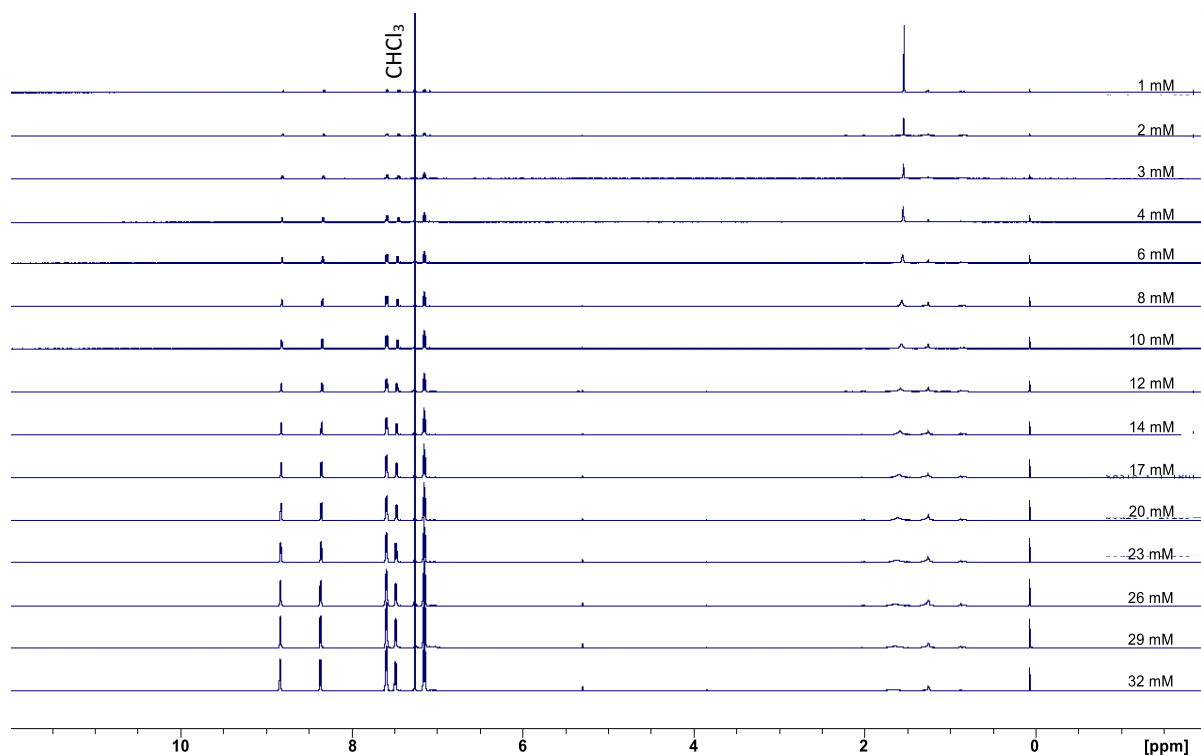


Figure S42: 600 MHz ^1H NMR overlapped spectra of 1_F diluted solutions in CDCl_3 at 298 K.

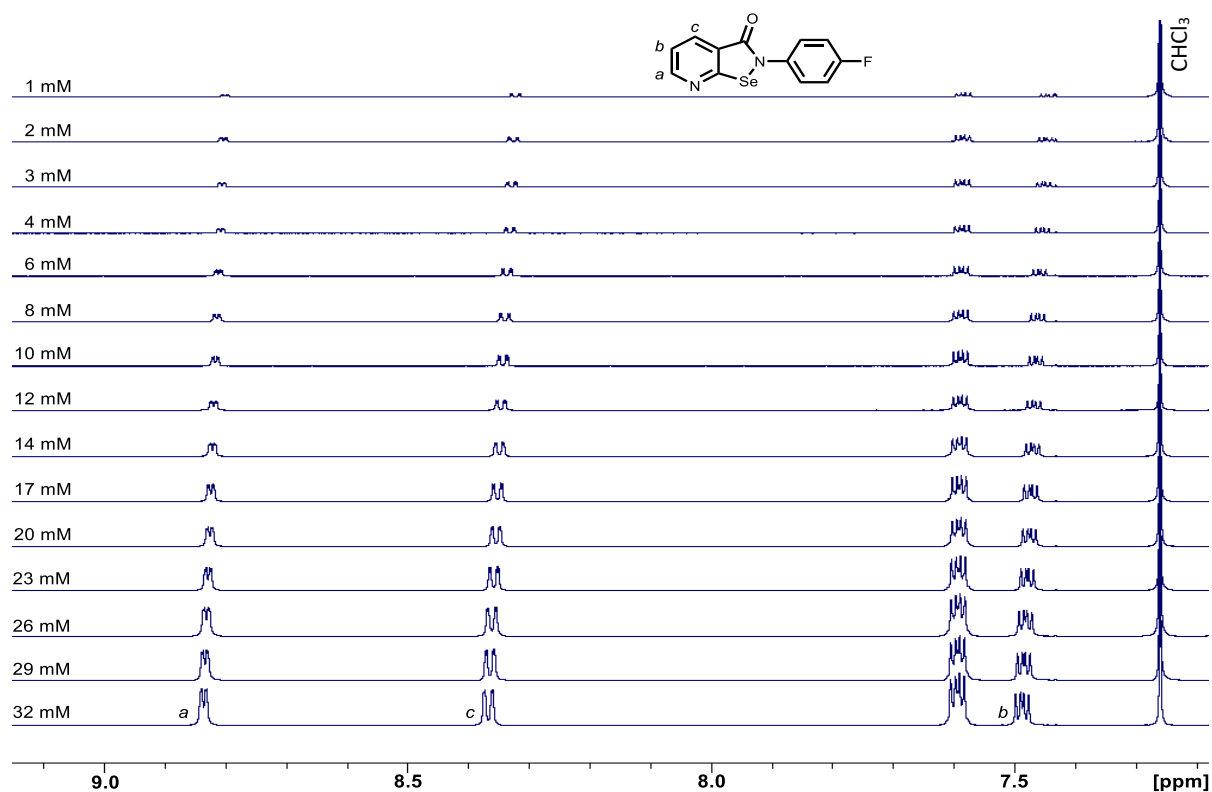


Figure S43: 600 MHz ^1H NMR zoomed overlapped spectra of 1_F diluted solutions in CDCl_3 at 298 K.

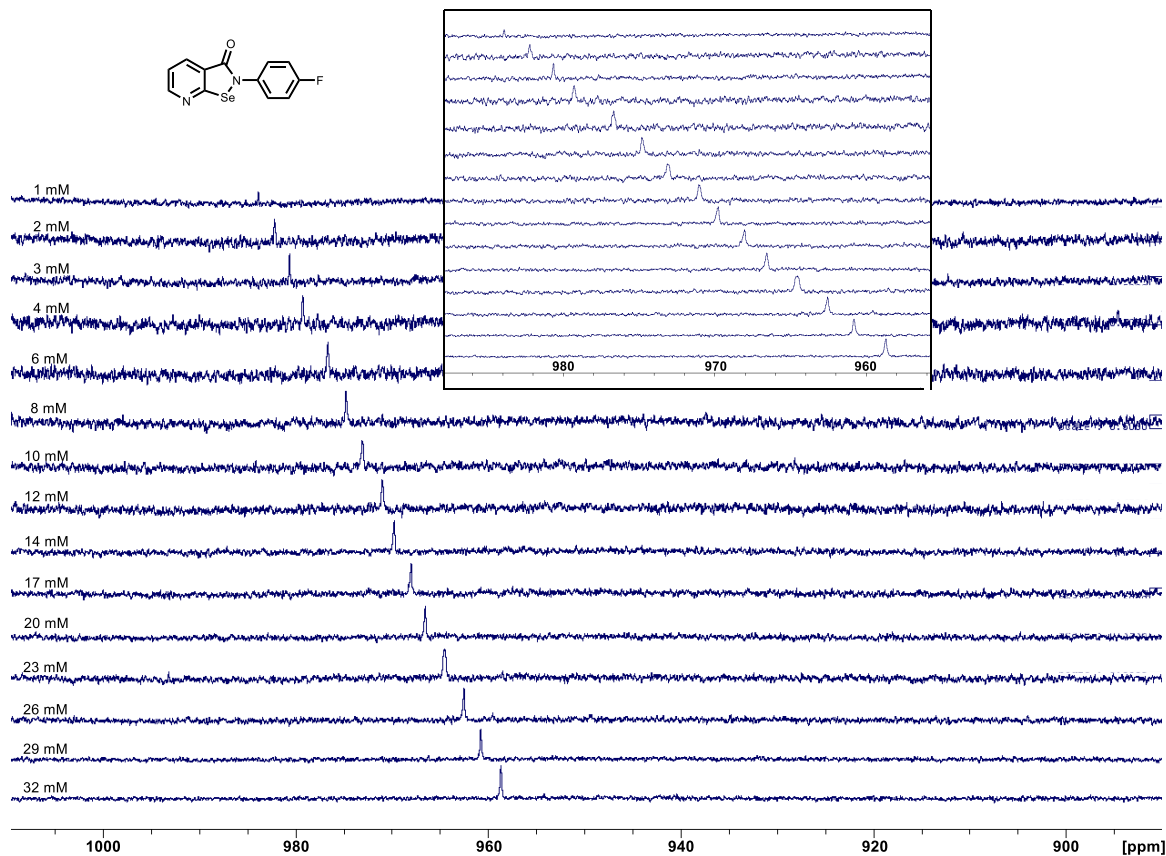


Figure S44: 115 MHz ^{77}Se NMR overlapped spectra of **1F** diluted solutions in CDCl_3 at 298 K.

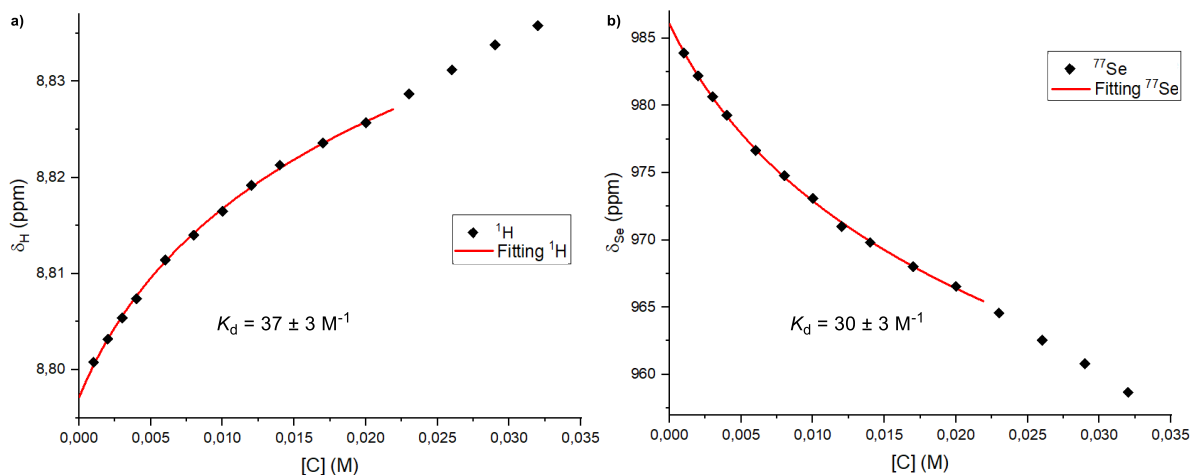


Figure S45: Experimental chemical shift from a) ^1H NMR and b) ^{77}Se NMR dilution experiments in CDCl_3 vs concentration of **1F**, fitted to a 1:1 dimerization equilibrium. The four points at higher concentrations were not included in the fitting process because they largely deviate from the binding isotherm. This is likely due to the low solubility of **1F** in CDCl_3 .

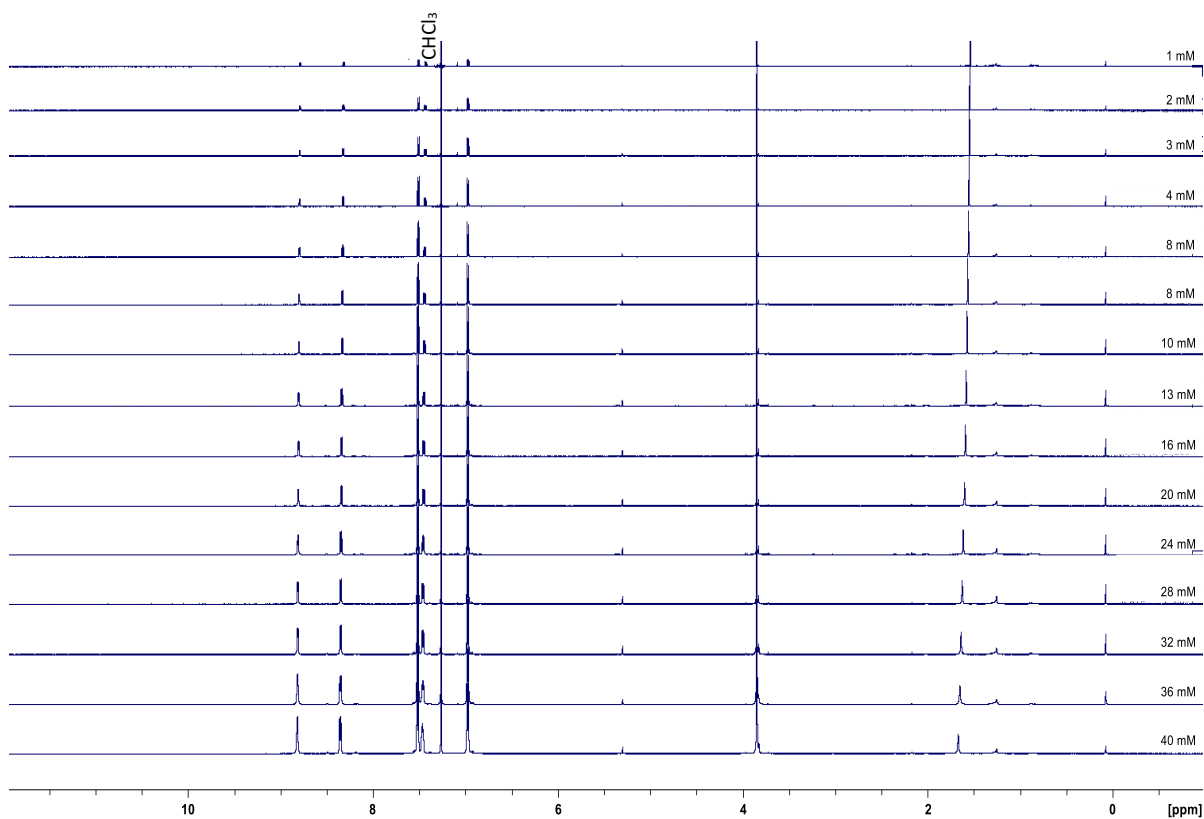


Figure S46: 600 MHz ^1H NMR overlapped spectra of 1_{Met} diluted solutions in CDCl_3 at 298 K.

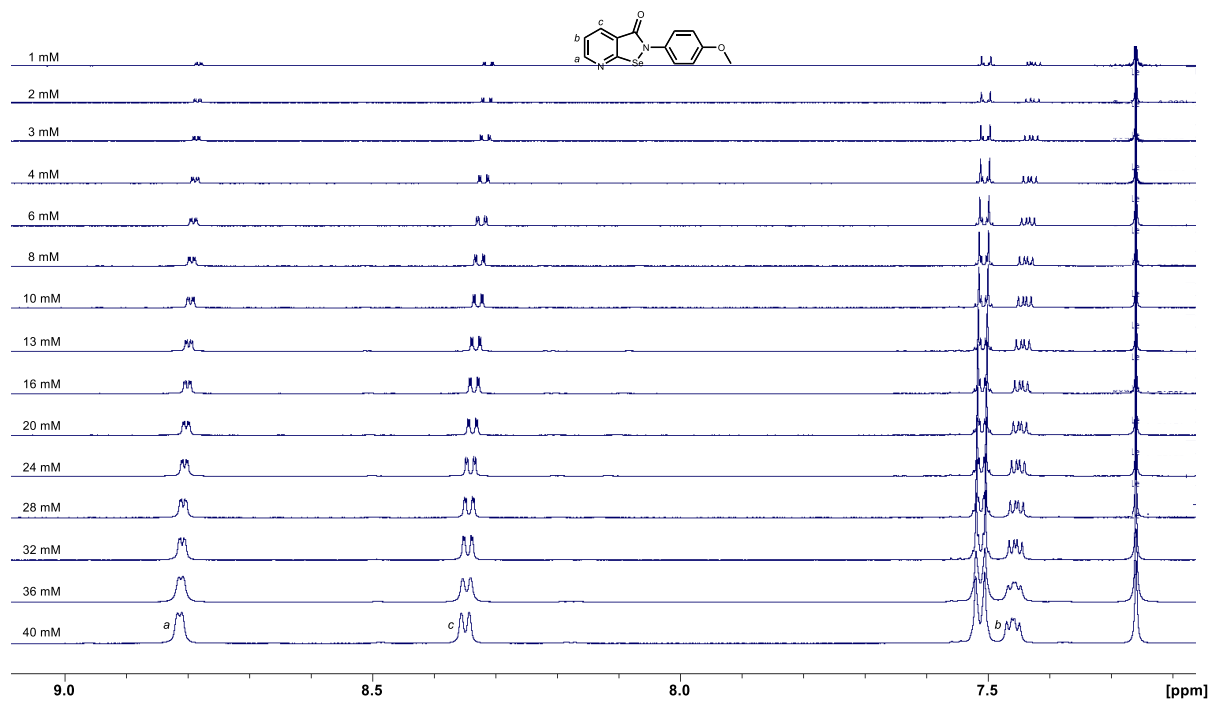


Figure S47: 600 MHz ^1H NMR zoomed overlapped spectra of 1_{Met} diluted solutions in CDCl_3 at 298 K.

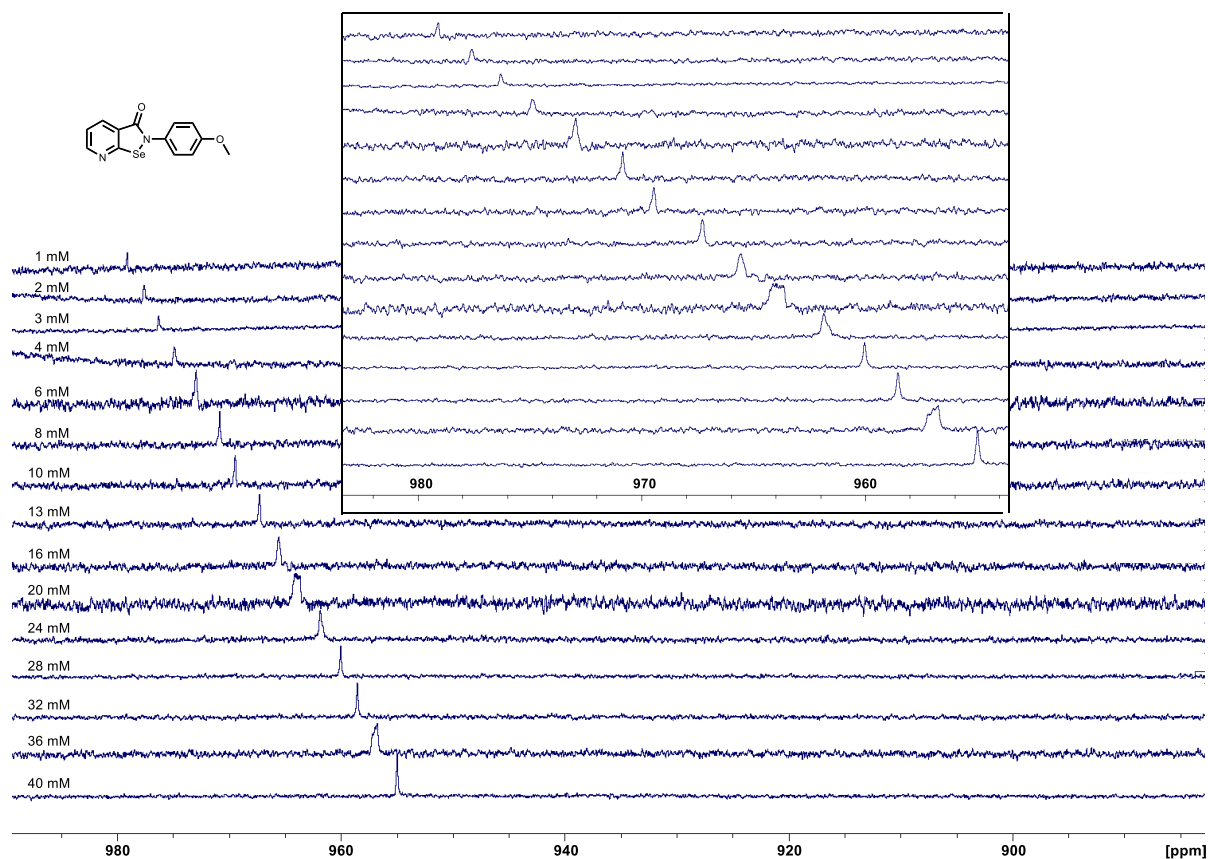


Figure S48: 115 MHz ^{77}Se NMR overlapped spectra of $\mathbf{1}_{\text{Met}}$ diluted solutions in CDCl_3 at 298 K.

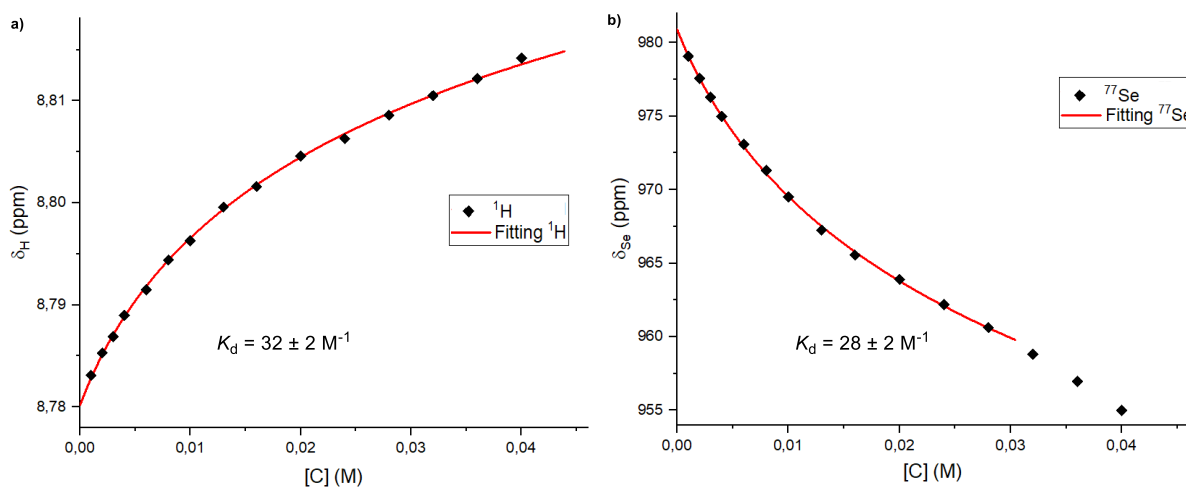


Figure S49: Experimental chemical shift from a) ^1H NMR and b) ^{77}Se NMR dilution experiments in CDCl_3 vs concentration of $\mathbf{1}_{\text{Met}}$, fitted to a 1:1 dimerization equilibrium. In the case of the ^{77}Se NMR dilution experiment, the three points at higher concentrations were not included in the fitting process because they largely deviate from the binding isotherm. This is not observed in the case of the ^1H NMR experiments and, therefore, it is likely due to scattering in the measurements of the ^{77}Se chemical shifts.

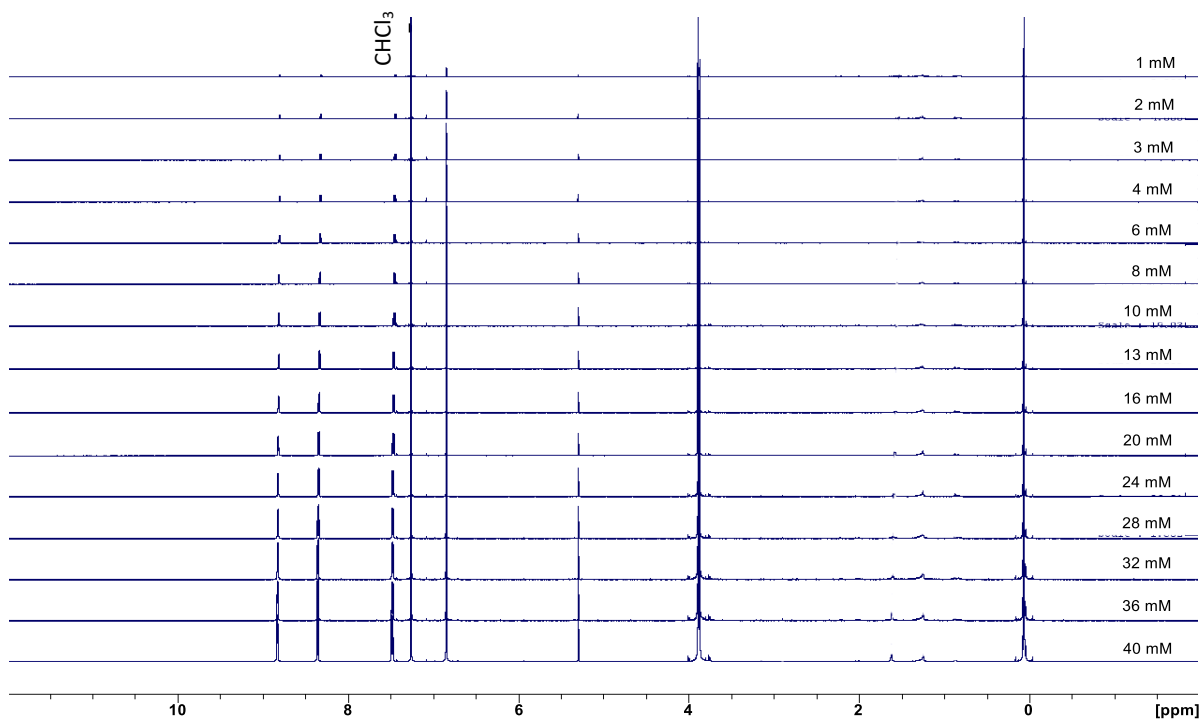


Figure S50: 600 MHz ^1H NMR overlapped spectra of $1_{3\text{Met}}$ diluted solutions in CDCl_3 at 298 K.

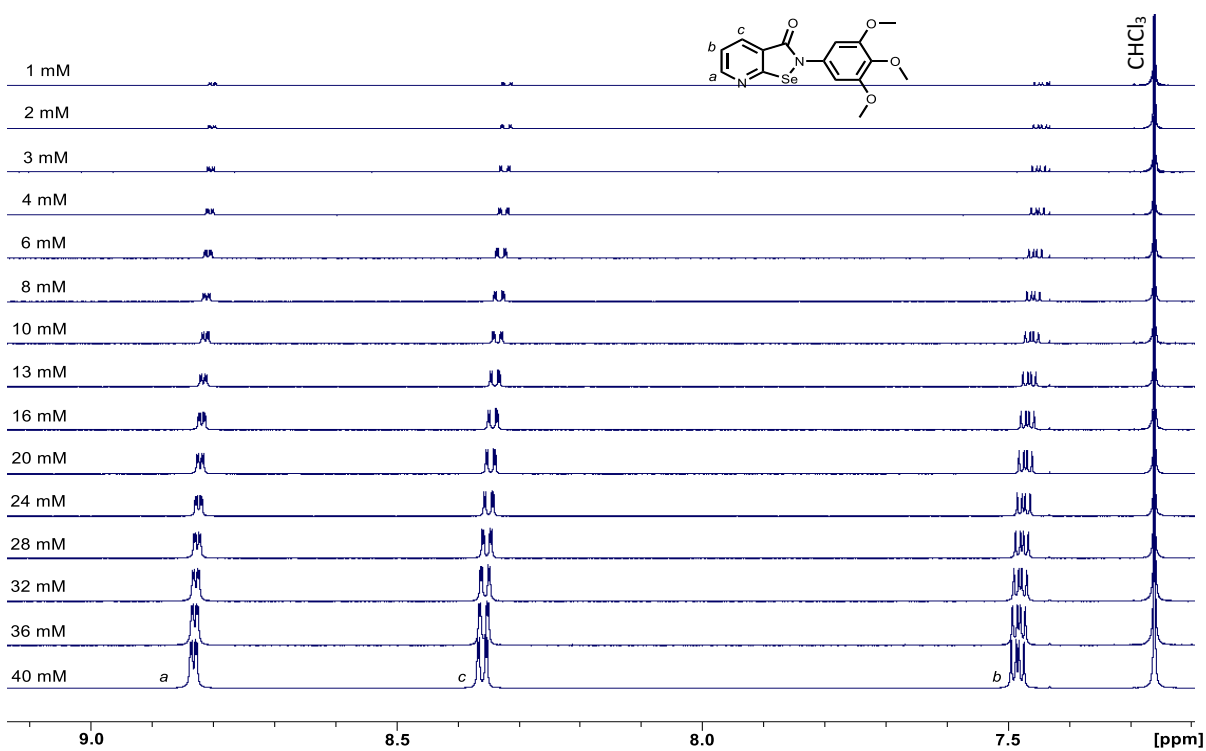


Figure S51: 600 MHz ^1H NMR zoomed overlapped spectra of $1_{3\text{Met}}$ diluted solutions in CDCl_3 at 298 K.

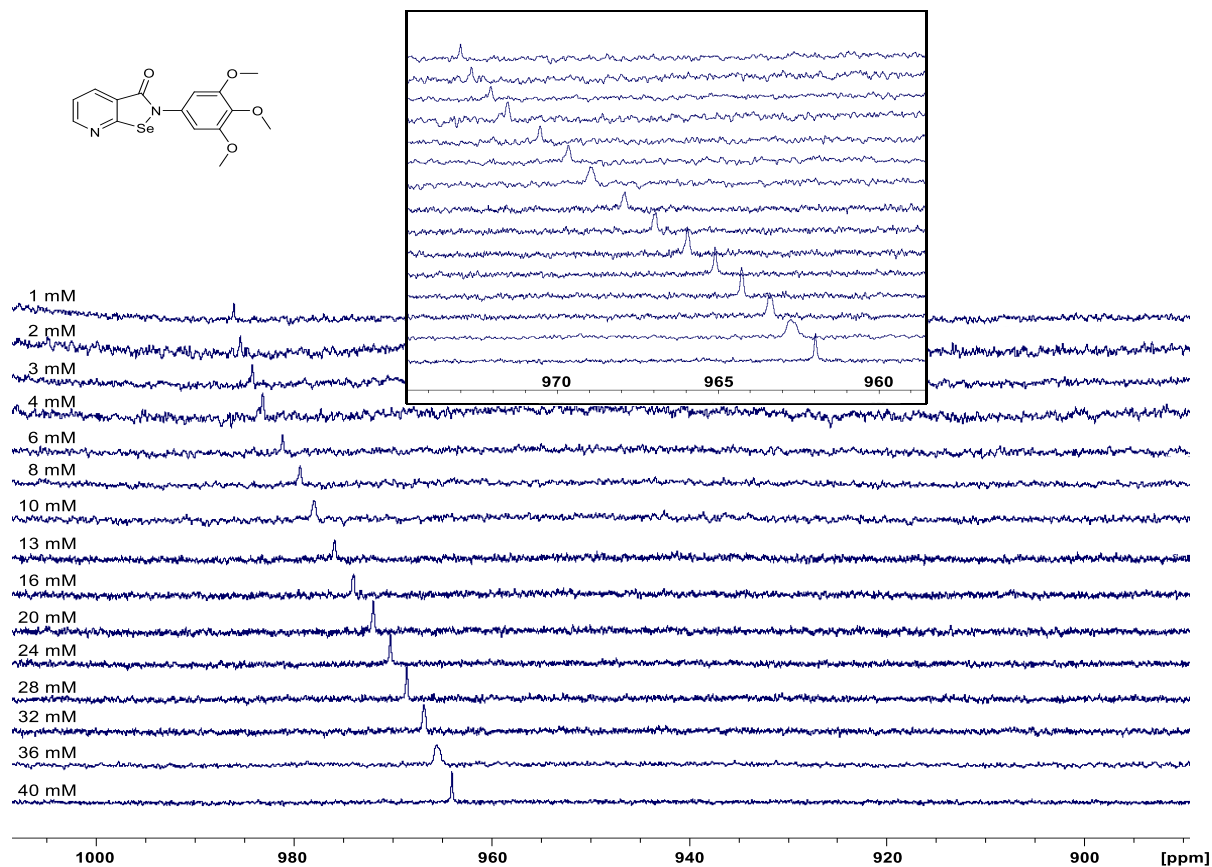


Figure S52: 115 MHz ^{77}Se NMR overlapped spectra of 13Met diluted solutions in CDCl_3 at 298 K.

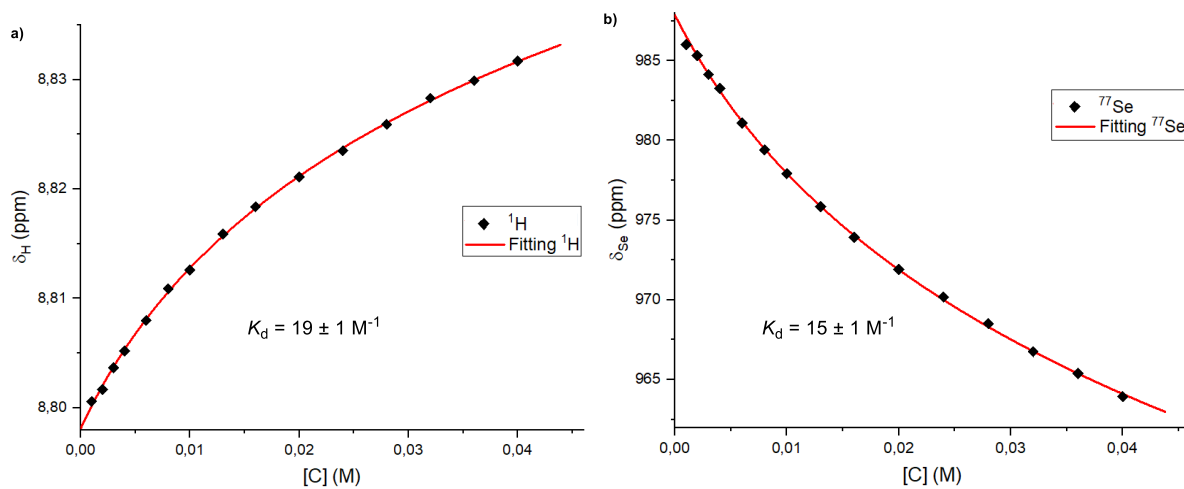


Figure S53: Experimental chemical shift from a) ^1H NMR and b) ^{77}Se NMR dilution experiments in CDCl_3 vs concentration of 13Met , fitted to a 1:1 dimerization equilibrium.

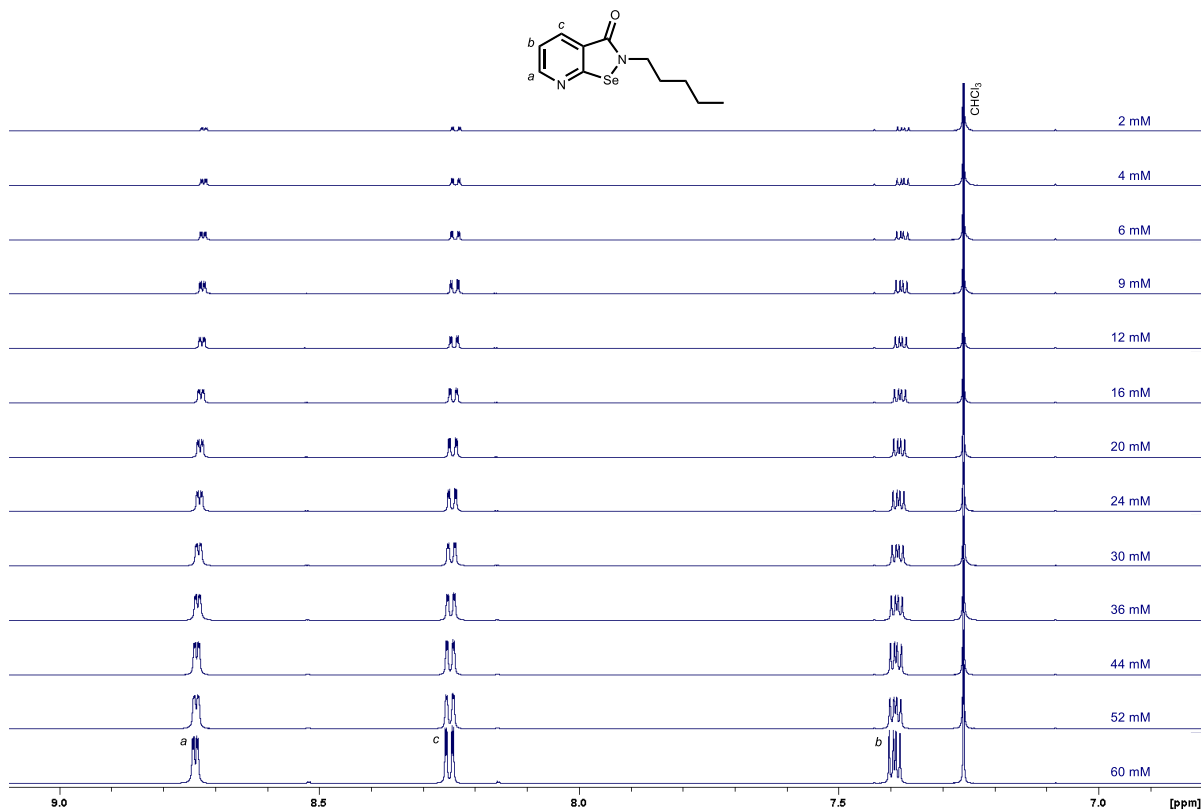


Figure S54: 600 MHz ¹H NMR overlapped spectra of **1_{AIK}** diluted solutions in CDCl₃ at 298 K.

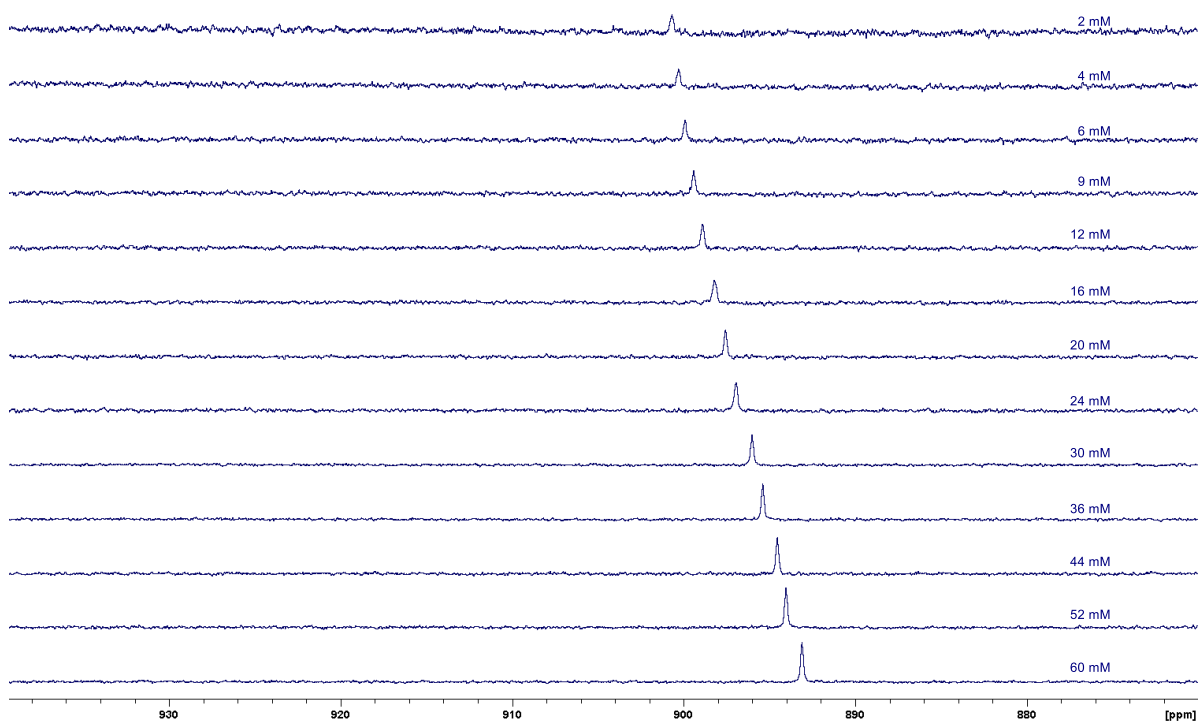


Figure S55: 115 MHz ⁷⁷Se NMR overlapped spectra of **1_{AIK}** diluted solutions in CDCl₃ at 298 K.

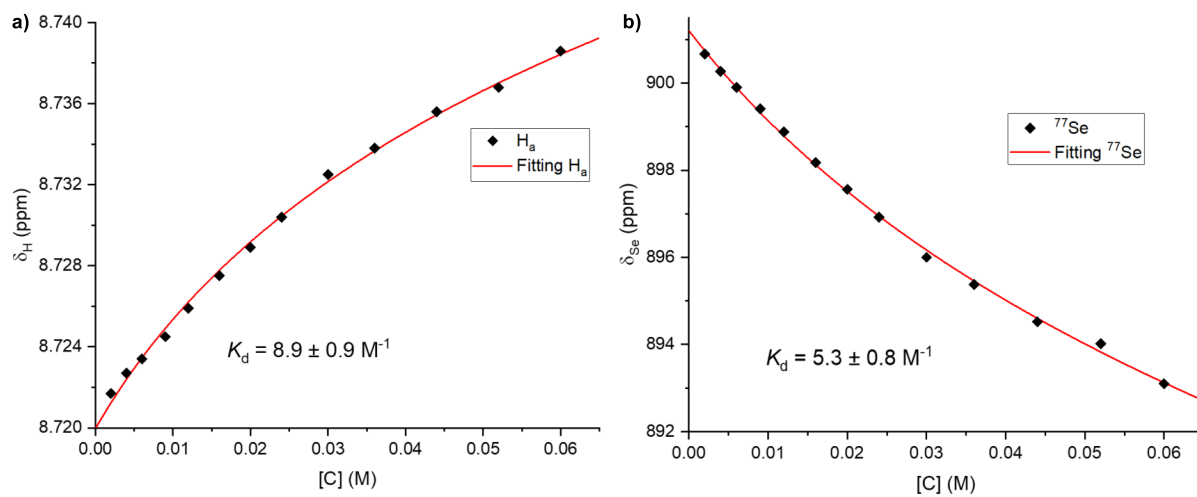


Figure S56: Experimental chemical shift from a) ^1H NMR and b) ^{77}Se NMR dilution experiments in CDCl_3 vs concentration of 1_{Alk} , fitted to a 1:1 dimerization equilibrium.

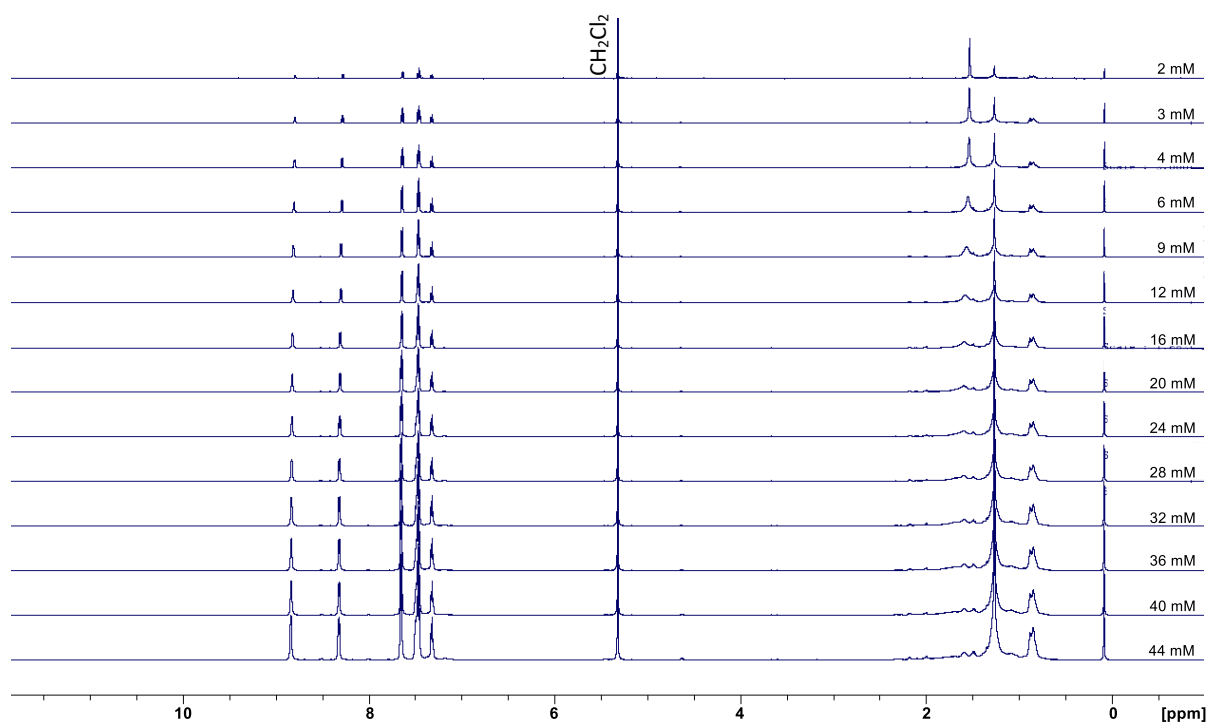


Figure S57: 600 MHz ^1H NMR overlapped spectra of 1_{Ph} diluted solutions in CD_2Cl_2 at 298 K.

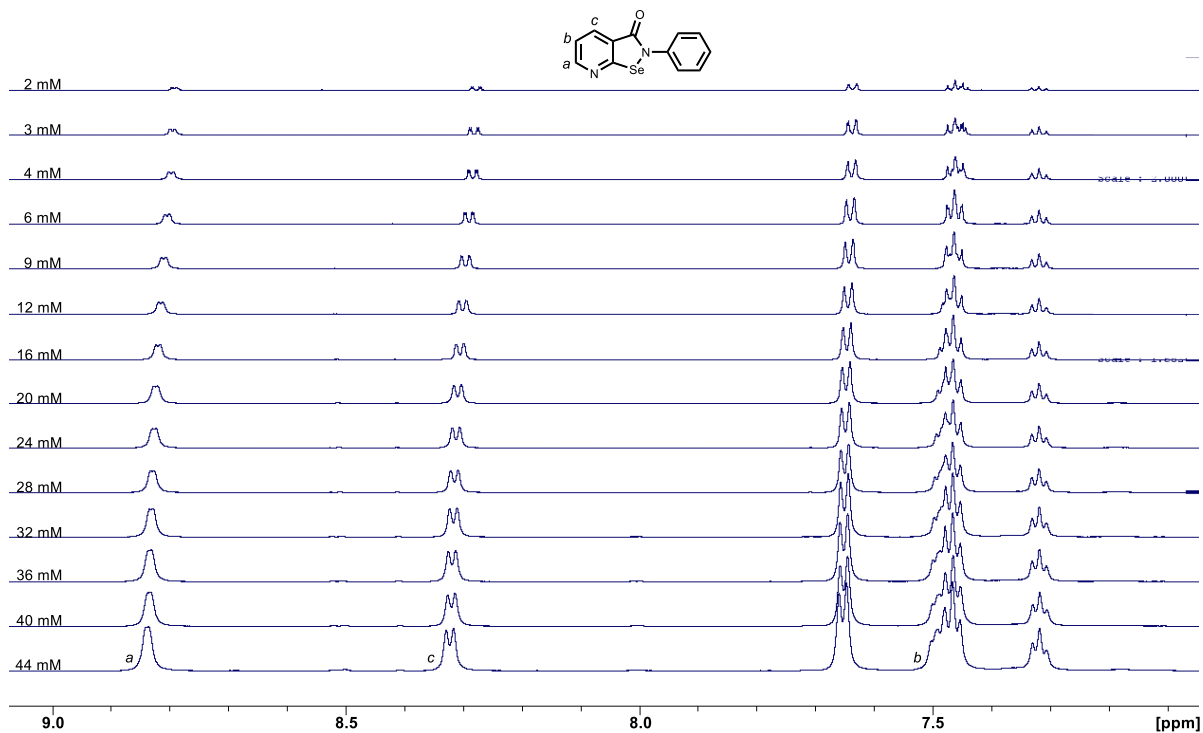


Figure S58: 600 MHz ¹H NMR zoomed overlapped spectra of **1_{Ph}** diluted solutions in CD₂Cl₂ at 298 K.

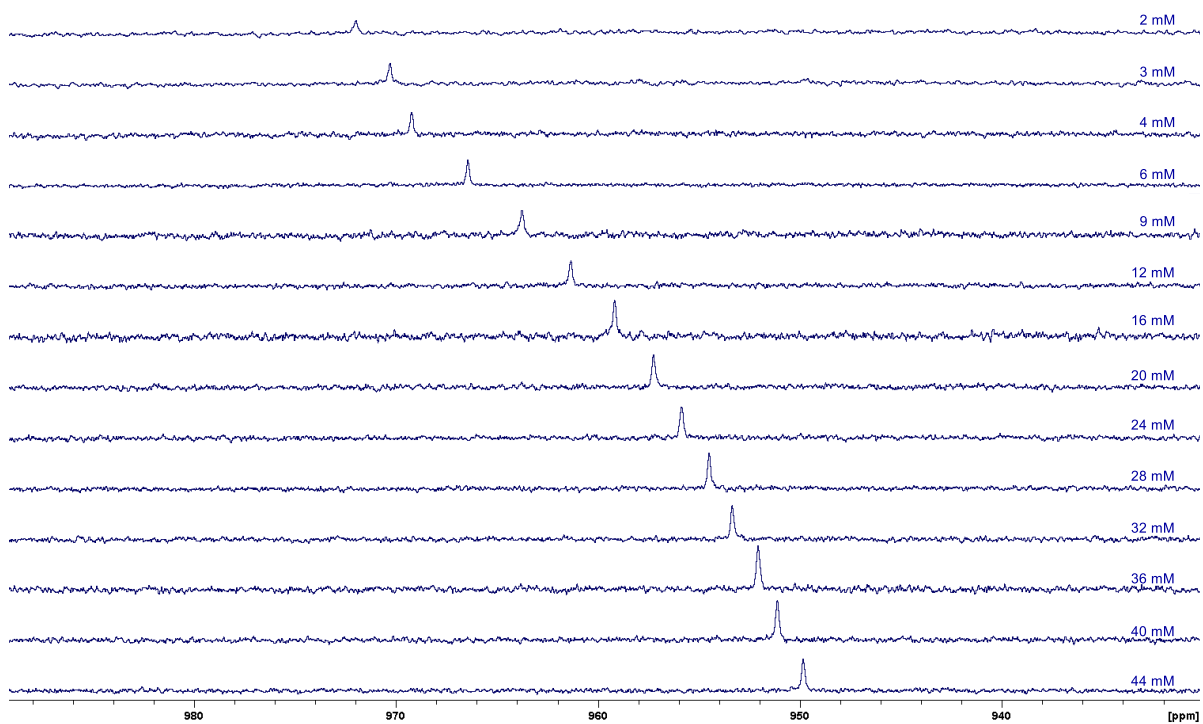


Figure S59: 115 MHz ⁷⁷Se NMR overlapped spectra of **1_{Ph}** diluted solutions in CD₂Cl₂ at 298 K.

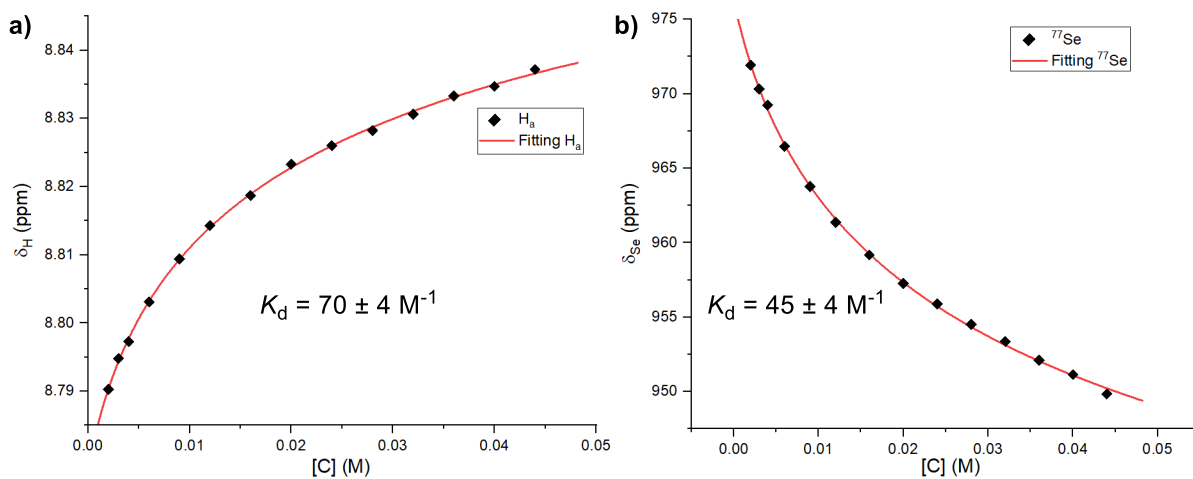


Figure S60: Experimental chemical shift from a) 1H NMR and b) ^{77}Se NMR dilution experiments in CD_2Cl_2 vs concentration of 1_{Ph} at 298 K, fitted to a 1:1 dimerization equilibrium.

Note for the reader: For the screening of 1_{Ph} in CD_2Cl_2 /toluene 1:1, to avoid the overlapping of the signals of the solvent with those of the molecule in the 1H NMR, only ^{77}Se NMR measurements were performed.

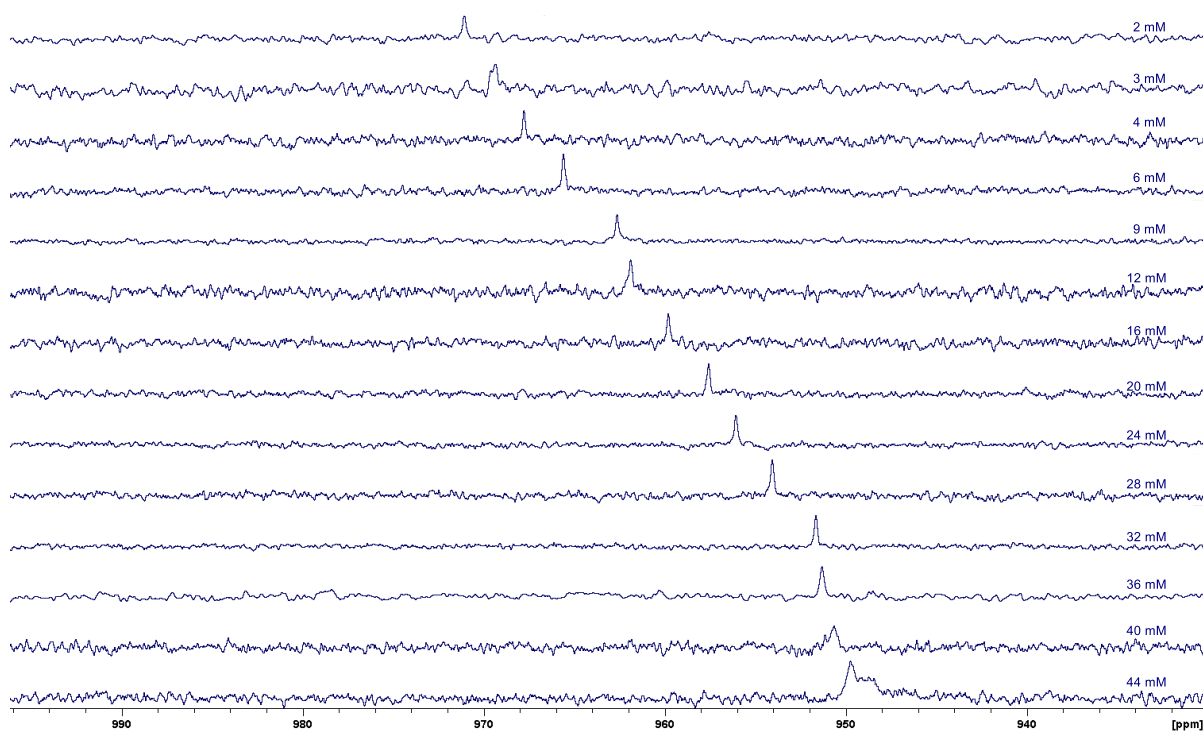


Figure S61: 115 MHz ^{77}Se NMR overlapped spectra of 1_{Ph} diluted solutions in CD_2Cl_2 /toluene at 298 K.

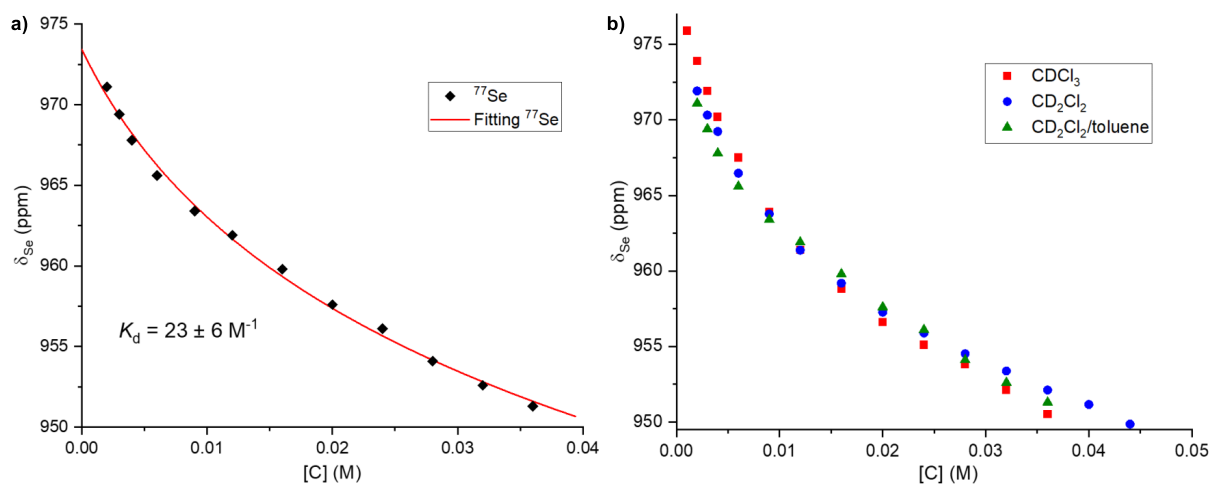


Figure S62: Experimental chemical shift from a) ^{77}Se NMR dilution experiments in $\text{CD}_2\text{Cl}_2/\text{toluene}$ vs concentration of 1_{Ph} at 298 K, fitted to a 1:1 dimerization equilibrium; b) plotted ^{77}Se NMR recorded in CDCl_3 , CD_2Cl_2 and $\text{CD}_2\text{Cl}_2/\text{toluene}$ solutions as function of concentration.

While the K_d values obtained in CDCl_3 and in CD_2Cl_2 are very similar ($51 \pm 4 \text{ M}^{-1}$ and $45 \pm 4 \text{ M}^{-1}$, respectively) the K_d measured in the $\text{CD}_2\text{Cl}_2/\text{toluene}$ is slightly lower ($23 \pm 4 \text{ M}^{-1}$). However, this is likely due to some deviation of the experimental points due to the limited solubility of 1_{Ph} in this solvent mixture. As a matter of fact, simply excluding the three points measured at the highest concentrations of 1_{Ph} a K_d value of $51 \pm 16 \text{ M}^{-1}$ is obtained. Moreover, plotting all the ^{77}Se chemical shift recorded from dilution experiments in the different solvents reveals their almost complete overlap, globally excluding a solvent effect in the ChB-driven dimerization of 1_{Ph} (Fig. S62b).

5.2 Variable Temperature (VT) experiments

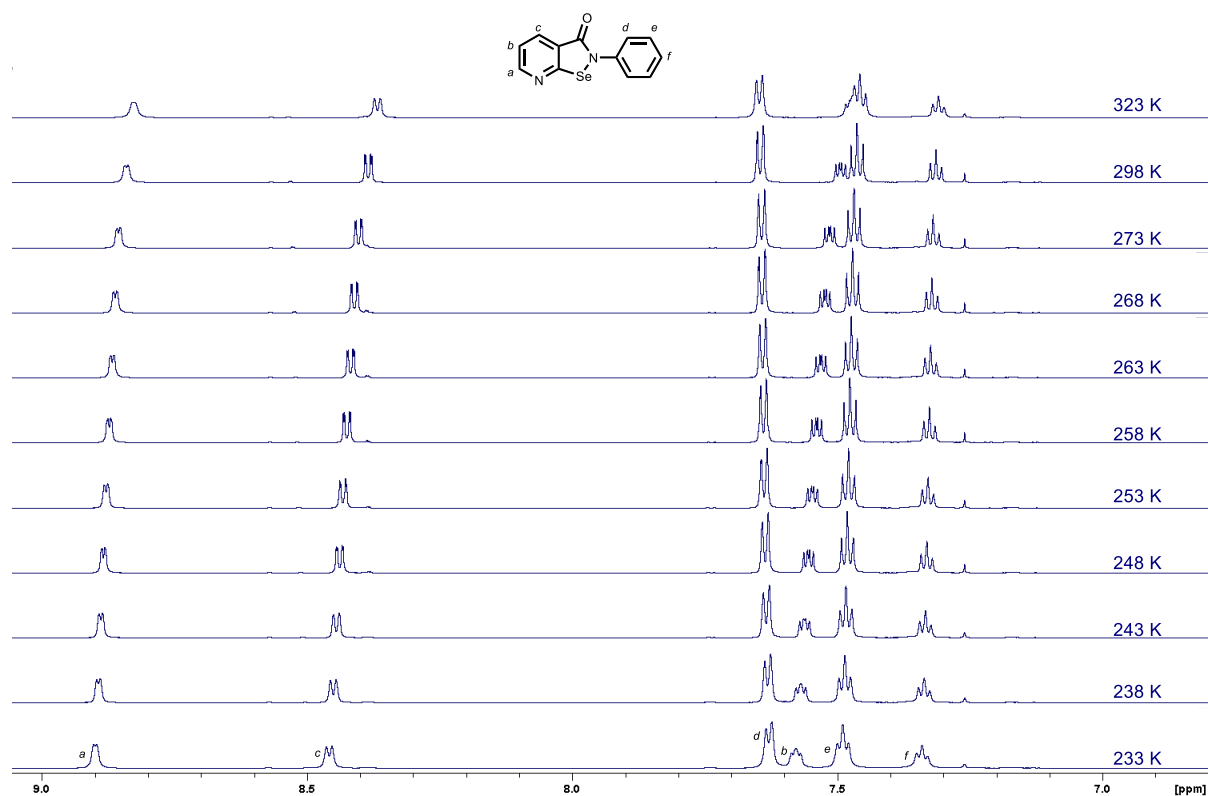


Figure S63: 600 MHz variable temperature (VT) ^1H NMR overlapped spectra of 20 mM 1_{Ph} solutions in CDCl_3 .

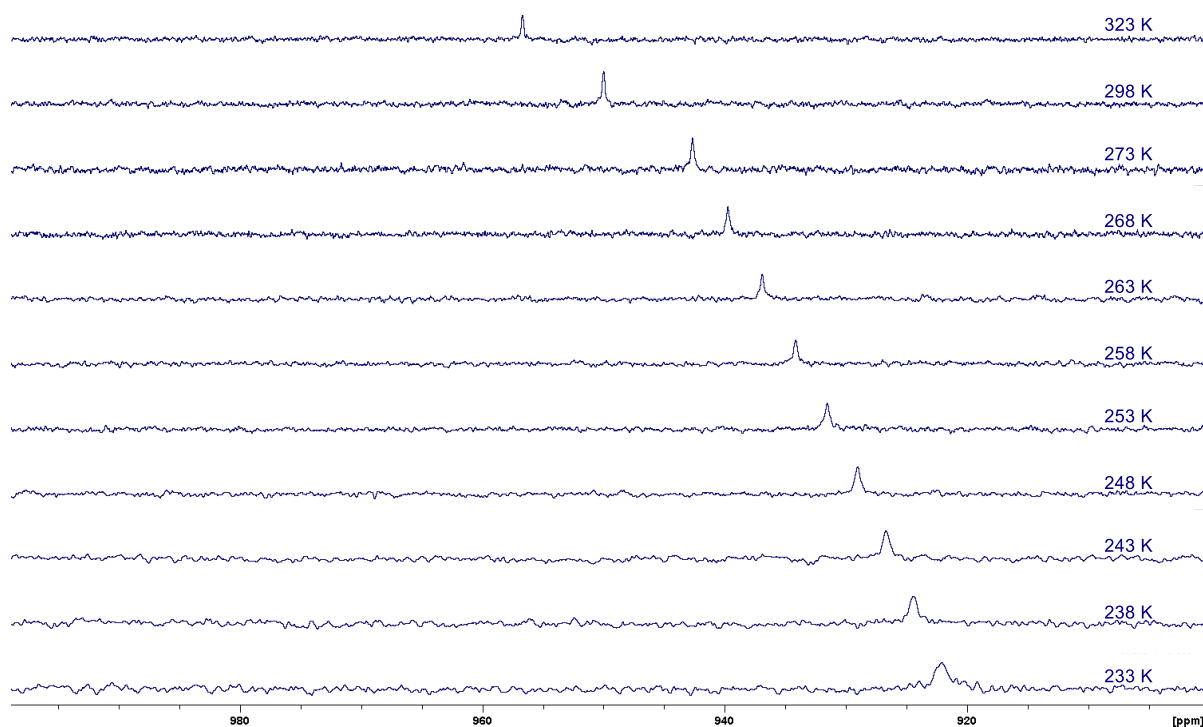


Figure S64: 115 MHz variable temperature (VT) ^{77}Se NMR overlapped spectra of 20 mM 1_{Ph} solutions in CDCl_3 .

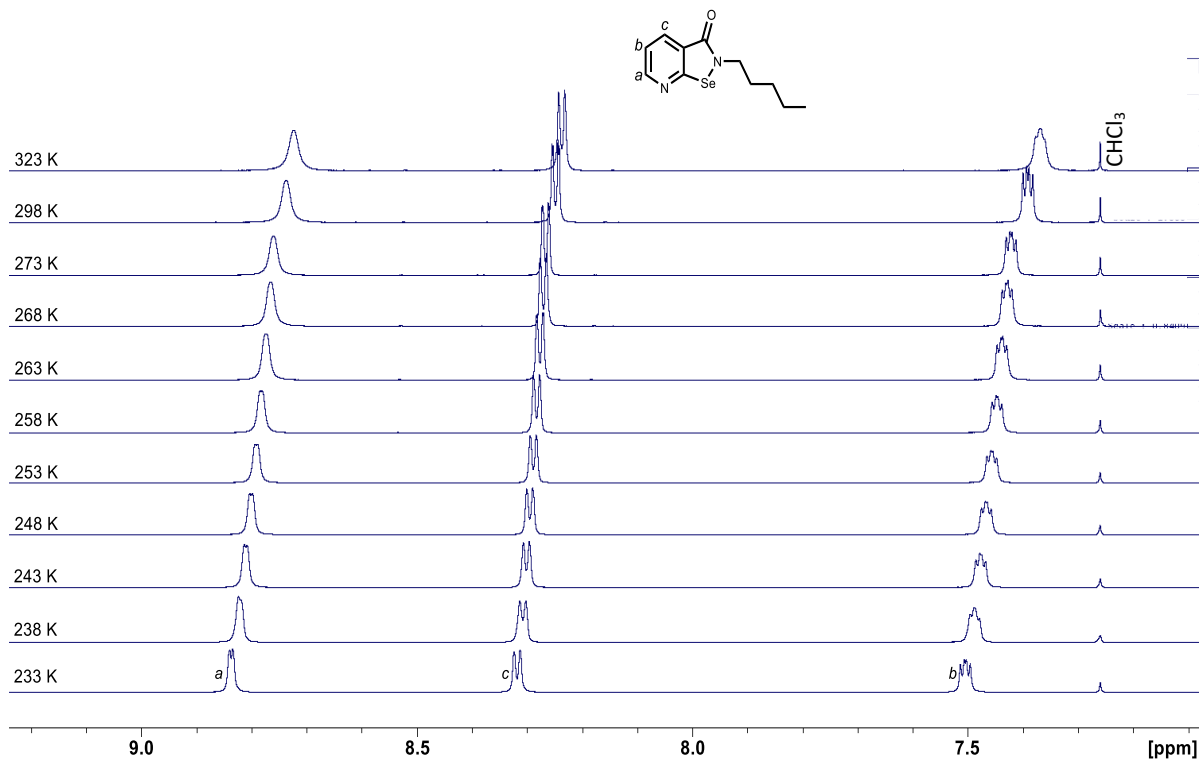


Figure S65: 600 MHz variable temperature (VT) ^1H NMR zoomed overlapped spectra of 20 mM **1AIk** solutions in CDCl_3 .

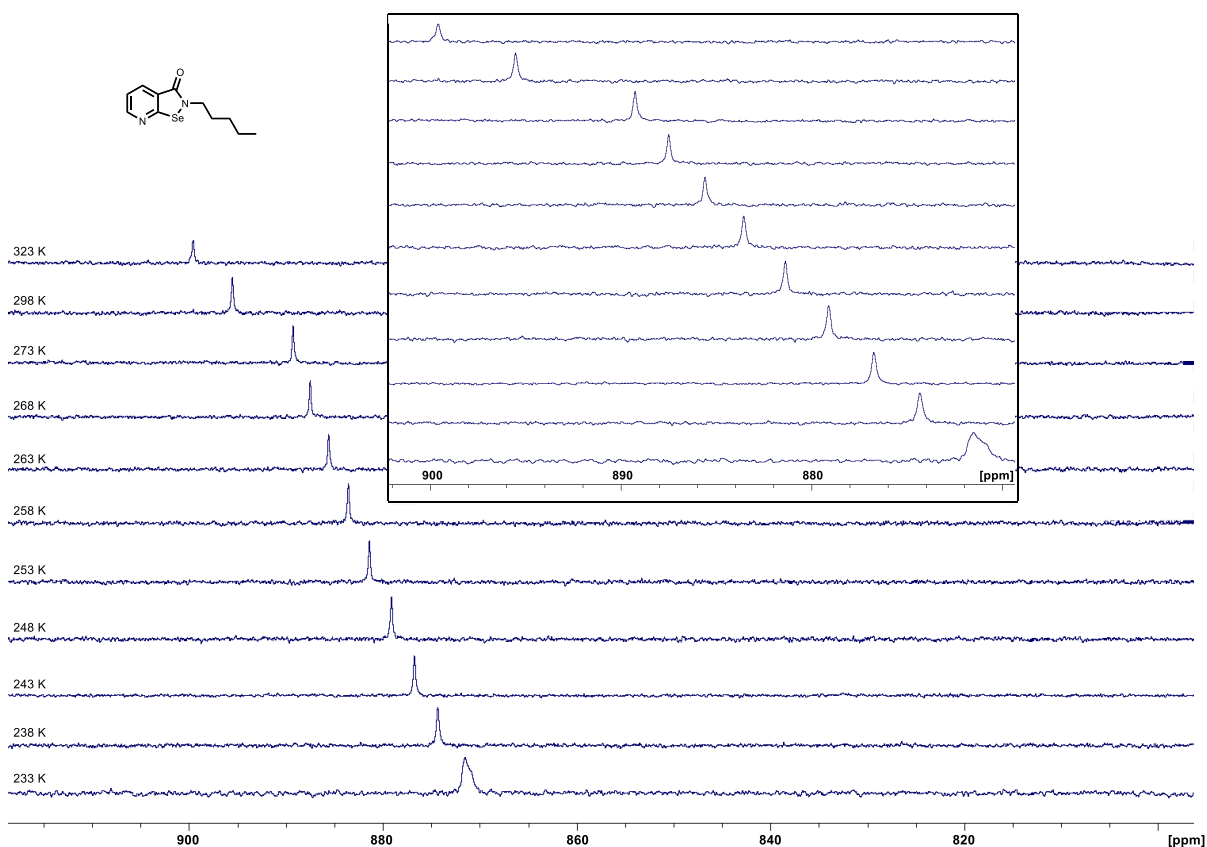


Figure S66: 115 MHz variable temperature (VT) ^{77}Se NMR overlapped spectra of 20 mM **1AIk** solutions in CDCl_3 .

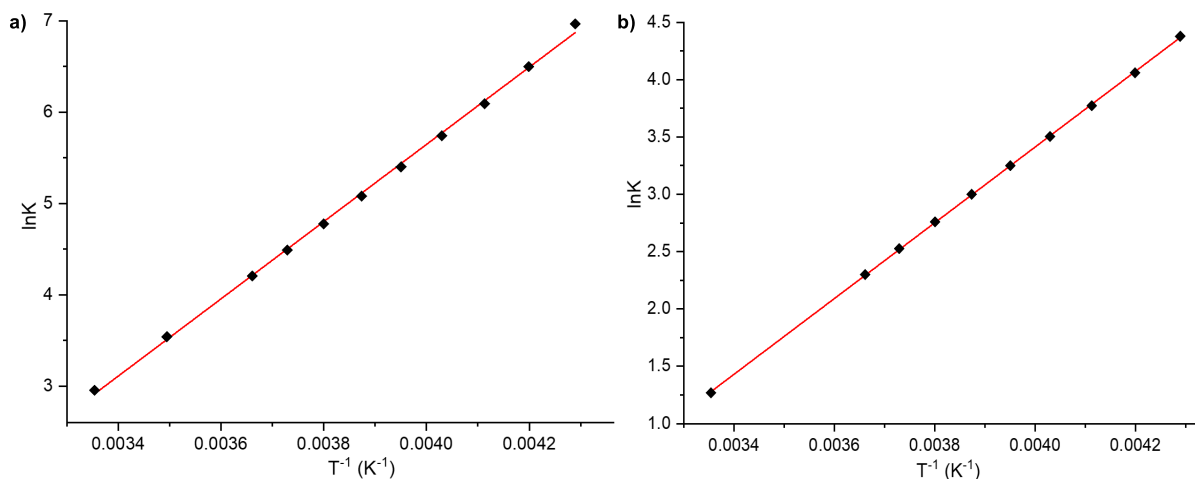


Figure S67: van't Hoff plot for the dimerization equilibrium of 20 mM solutions of a) **1_{Ph}** and b) **1_{Alk}** in CDCl_3 , determined in relation to ^{77}Se NMR spectra. Fitting parameters: $r^2 = 0.9993$ for **1_{Ph}**; $r^2 = 0.9989$ for **1_{Alk}**.

Table S7: Thermodynamic parameters obtained from ^{77}Se NMR investigations of **1_{Ph}** and **1_{Alk}**.

	From VT experiments				From dilutions	
	ΔH (KJ·mol ⁻¹)	ΔS (J·K ⁻¹ ·mol ⁻¹)	ΔG (KJ·mol ⁻¹)	K (M ⁻¹)	ΔG (KJ·mol ⁻¹)	K (M ⁻¹)
1_{Ph}	-35.18	-93.78	-7.22	18	-9.88	51
1_{Alk}	-27.45	-81.46	-3.16	3.6	-3.89	4.8

6. Computational studies

6.1. Density Functional Theory (DFT) calculations

The DFT calculations reported in this work have been performed via the mixed Gaussian and plane waves (GPW) method implemented in the CP2K package.^[43]

The choice of the exchange-correlation (XC) functional, which is always an important consideration when investigating molecular interactions, is especially controversial when it comes to the description of chalcogenide bonds. For instance, the work of *Bickelhaupt*^[44] recommends the usage of hybrid functionals, particularly B3LYP, as opposed to the addition of dispersion corrections to non-hybrid functionals – which might lead to overestimate the strength of chalcogen bonds. On the other hand, *Goerigk* argues against the usage of B3LYP and recommends instead dispersion-corrected functionals such as the PW6B95-D3.^[45] To address this conundrum, we have simply chosen to explore different XC functionals, namely PBE,^[46] PBE-D3,^[47] which feature a dispersion correction; vdW-DF69,^[48] which is a fully self-consistent, nonlocal XC functional and HSE06,^[49] which is a hybrid functional. Goedecker-type pseudopotentials^[50] with four, one, six, five and six valence electrons for C, H, O, N and Se respectively have been employed. The Kohn-Sham orbitals were expanded in a triple-zeta valence plus two sets of polarisation functions (TZV2P) Gaussian-type basis set. The plane wave cutoff for the finest level of the multi-grid^[43] has been set to 400 Ry to

efficiently solve the Poisson equation within periodic boundary conditions using the Quickstep scheme.^[43] Brillouin zone integration was restricted to the supercell Gamma point. We have found that a cubic simulation box (edge = 40 Å), introduces ~ 20 Å of vacuum between the periodic replica of the dimers in each direction, which is sufficient to converge the total energy to 2 meV/atom.

6.2 ALMO-EDA calculations

The Absolutely Localized Molecular Orbitals Energy Decomposition Analysis (ALMO-EDA) is a computational framework that can be used to investigate the different contributions to the total interaction energies we have discussed in the previous section. This framework has been extensively reviewed elsewhere^[51] and it is readily available within the CP2K package. For the purposes of this work, it suffices to say that within the ALMO-EDA formalism the total interaction energy E_{Tot} between two molecules can be written as:

$$E_{Tot} = E_{Frz} + E_{Pol} + E_{Cov}.$$

The frozen density term (E_{Frz}) is defined as the energy change that corresponds to bringing infinitely separated molecules into the dimer geometry without any relaxation of the molecular orbitals (MOs) on the monomers. The polarization energy (E_{Pol}) is defined as the energy lowering due to the *intramolecular* relaxation of each molecule's ALMOs within the field of all other molecules in the system. The remaining portion of the total interaction energy is the electron delocalization or charge-transfer energy term (E_{Cov}), which is calculated as the energy difference between the state formed from the polarized ALMOs and the state constructed from the fully optimized delocalized MOs. This framework also gives access to the actual charge transfer (CT) contribution, which is computed as the degree of electron relaxation from the polarized state to the delocalized state. By contrast, population analysis methods include not only the "true" CT, but also the separate effect of partitioning the charge distribution of the polarized pre-CT state. Thus, the key advantage of the ALMO approach is that it shows the electron transfer associated with the energy lowering due to dative interactions exclusively.

Crucial to the correct assessment of the interaction energy is an estimate of the BSSE, which is not introduced when calculating the frozen density and the polarization energy contributions (i.e., E_{Frz} and E_{Pol}) because constrained ALMO optimization prevents electrons on one molecule from borrowing the atomic orbitals (AOs) of other molecules to compensate for the incompleteness of their own AOs. However, the BSSE does enter the charge transfer terms (i.e., E_{Cov}) since both the BSSE and charge transfer result from the same physical phenomenon of delocalization of fragment MOs. Therefore, these terms are inseparable from each other when finite Gaussian basis sets are used to describe fragments at finite spatial separation.

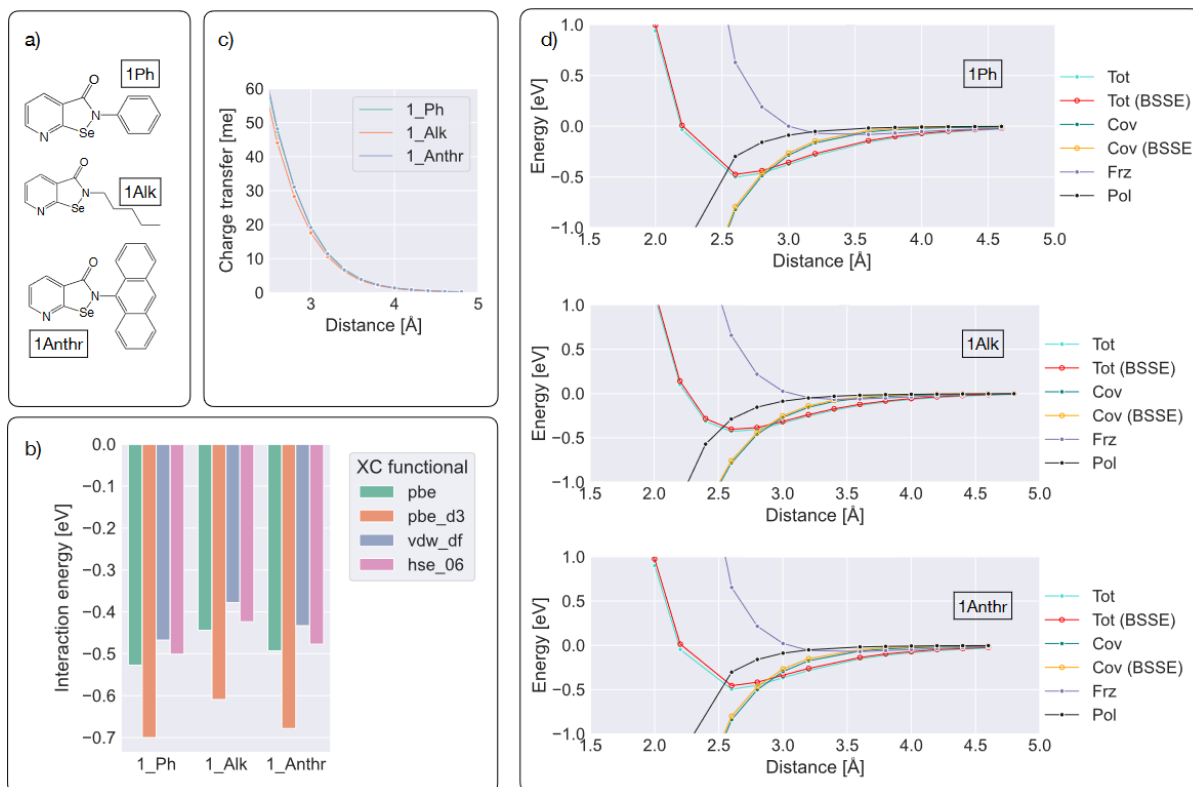


Figure S68: a) Molecular structures of the three Pyrselen derivatives we have considered for our DFT calculations; b) Interaction energies for the different dimers, computed via different XC functionals (see text); c) Charge transfer (CT) for the different dimers, as a function of the intermolecular distance (units of milli electrons, me); d) Contributions to the total interaction energy (Tot) for the different dimers as a function of the intermolecular distance; Frz, Pol and Cov refer to the frozen density, polarization, and covalent contribution terms, respectively (see text); the (BSSE) results include the basis set superposition error (see ESI) as well.

References

- [28] R. K. Harris, E. D. Becker, S. M. Cabral De Menezes, P. Granger, R. E. Hoffman, K. W. Zilm, *eMagRes* **2007**.
- [29] Bruker SAINT v8.38B Copyright © 2005-2019 Bruker AXS.
- [30] G. M. Sheldrick, *University of Göttingen, Germany* **1996**.
- [31] O. V. Dolomanov, L. J. Bourhis, R. J. Gildea, J. A. Howard, H. Puschmann, *J. Appl. Cryst.* **2009**, *42*, 339-341.
- [32] C. B. Hübschle, G. M. Sheldrick, B. Dittrich, *J. Appl. Cryst.* **2011**, *44*, 1281-1284.
- [33] G. M. Sheldrick, *SHELXS v 2016/4 University of Göttingen, Germany* **2015**.
- [34] A. L. Spek, *Acta Cryst.* **2009**, *D65*, 148-155.
- [35] A. Lausi, M. Polentarutti, S. Onesti, J. Plaisier, E. Busetto, G. Bais, L. Barba, A. Cassetta, G. Campi, D. Lamba, *The European Physical Journal Plus* **2015**, *130*, 1-8.
- [36] W. Kabsch, *Acta Crystallogr. Sect. D* **2010**, *66*, 125-132.
- [37] O. V. Dolomanov, L. J. Bourhis, R. J. Gildea, J. A. Howard, H. Puschmann, *J. Appl. Crystallogr.* **2009**, *42*, 339-341.
- [38] G. M. Sheldrick, *Acta Crystallogr. Sect. A Found. Adv.* **2015**, *71*, 3-8.
- [39] G. M. Sheldrick, *Acta Crystallogr. Sect. C Struct. Chem.* **2015**, *71*, 3-8.
- [40] W. Lin, L. Chen, P. Knochel, *Tetrahedron* **2007**, *63*, 2787-2797.
- [41] H.-S. Lin, L. A. Paquette, *Synth. Commun.* **1994**, *24*, 2503-2506.
- [42] P. Kuzmič, *Anal. Biochem.* **1996**, *237*, 260-273.
- [43] J. VandeVondele, M. Krack, F. Mohamed, M. Parrinello, T. Chassaing, J. Hutter, *Comput. Phys. Commun.* **2005**, *167*, 103-128.

- [44] L. de Azevedo Santos, T. C. Ramalho, T. A. Hamlin, F. M. Bickelhaupt, *J. Comput. Chem.* **2021**, *42*, 688-698.
- [45] N. Mehta, T. Fellowes, J. M. White, L. Goerigk, *J. Chem. Theory Comput.* **2021**, *17*, 2783-2806.
- [46] J. P. Perdew, K. Burke, M. Ernzerhof, *Phys. Rev. Lett.* **1996**, *77*, 3865.
- [47] S. Grimme, J. Antony, S. Ehrlich, H. Krieg, *J. Chem. Phys.* **2010**, *132*, 154104.
- [48] M. Dion, H. Rydberg, E. Schröder, D. C. Langreth, B. I. Lundqvist, *Phys. Rev. Lett.* **2004**, *92*, 246401.
- [49] A. V. Krukau, O. A. Vydrov, A. F. Izmaylov, G. E. Scuseria, *J. Chem. Phys.* **2006**, *125*, 224106.
- [50] S. Goedecker, M. Teter, J. Hutter, *Phys. Rev. B.* **1996**, *54*, 1703.
- [51] R. Z. Khaliullin, E. A. Cobar, R. C. Lochan, A. T. Bell, M. Head-Gordon, *J. Phys. Chem. A* **2007**, *111*, 8753-8765.